Hochschule für Angewandte Wissenschaften Hamburg
Hamburg University of Applied Sciences

Bachelorarbeit

Nils Napiwotzki

Influence of different 3D printer designs on the mechanical properties of polyamide compounds in Fused Filament Fabrication

Fakultät Technik und Informatik
Department Maschinenbau und Produktion

Faculty of Engineering and Computer Science
Department of Mechanical Engineering and Production Management

Nils Napiwotzki

Influence of different 3D printer designs on the mechanical properties of polyamide compounds in Fused Filament Fabrication

Bachelorarbeit eingereicht im Rahmen der Bachelorprüfung

im Studiengang Produktionstechnik und -management BA
am Department Maschinenbau und Produktion
der Fakultät Technik und Informatik
der Hochschule für Angewandte Wissenschaften Hamburg

in Zusammenarbeit mit:
LEHVOSS Group
Market Development 3D-printing
Alsterufer 19
20354 Hamburg

Erstprüfer/in: Prof. Dr. Jens Telgkamp
Zweitprüfer/in: Dr. Thiago Medeiros Araujo

Abgabedatum: 17.11.2020

Zusammenfassung

Name des Studierenden
Nils Napiwotzki

Thema der Bachelorthesis
Thema der Bachelorarbeit

Stichworte
3D Druck, FFF, Polyamid, tempern, mechanische Eigenschaften, thermische Eigenschaften, additive Fertigung

Kurzzusammenfassung
Das Ziel dieser Forschung ist es zu bestimmen, inwiefern sich das Design eines FFF Desktop 3D Druckers auf die thermischen und mechanischen Eigenschaften eines Polyamid-Compounds auswirkt. Dafür werden vier unterschiedliche Geräte ausgewählt und mehrere Prüfkörper mit festgelegten Ausgangsbedingungen gedruckt. Anschließend wird ein Teil dieser Prüfkörper thermisch nachbehandelt. Zur Bestimmung der Eigenschaften, wurden genormte Prüfverfahren durchgeführt, um die Materialeigenschaften der Prüfkörper zu bestimmen. Es zeigt sich, dass durch das Design der Anteil des kristallinen Gefüges beeinflusst wird. Es zeigt sich jedoch auch, dass ein Großteil der Eigenschaften durch die Nachbehandlung erzielt werden kann.

Auf dieser Grundlage lässt sich nicht sagen, dass ein aufwendig gestalteter Desktop 3D Drucker zwangsläufig bessere Ergebnisse erzielt.

Name of Student
Nils Napiwotzki

Title of the paper
Influence of different 3D printer designs on the mechanical properties of polyamide compounds in Fused Filament Fabrication

Keywords
3D-printing, FFF, Polyamide, Annealing, mechanical properties, thermal properties, Polyamide compound, additive manufacturing

Abstract
The goal of this research is to determine how the design of a FFF desktop 3D printer, especially its shielding from the environment, affects the thermal and mechanical properties of a polyamide compound. For this purpose, four different machines are selected, and several test specimens are printed with fixed start conditions. Subsequently, a part of these test specimens is thermally post-treated. To determine the properties, standardized test procedures were performed to determine the material properties of the test specimens. It is shown that the design influences the proportion of the crystalline structure. However, it is also shown that a large part of the properties is achieved by the after-treatment.

On this basis, it cannot be said that an elaborately designed desktop 3D printer necessarily achieves better results.

Table of Contents

List of Figures

List of Tables

List of Abbreviations

CAD ... *Computer-Aided Design*
CNC ... *Computerized Numerical Control*
DSC ... *Differential Scanning Calorimetry*
FFF ... *Fused Filament Fabrication*
HDT ... *Heat Deflection Temperature*
PA6 ... *Polyamide 6*
PTFE ... *Polytetrafluorethylen*

1 Introduction

Additive manufacturing or often called 3D printing is a valid option when it comes to the selection of a manufacturing process. It offers companies the possibility to integrate complex geometries into their manufacturing processes and drastically reduces the time to manufacture. Fused Filament Fabrication (FFF), is one of the key technologies at an industrial scale. This technology has developed in recent years from a technology for hobbyists to a serious production basis. At the forefront are the numerous desktop 3D printers. This thesis investigates the influence of different 3D-printing machines have on printed parts [1–3].

In the FFF, polymers are melted and deposited along a defined travel path. A software called slicer generates a machine path, called G-Code, from the CAD data. The slicing software adds printer-specific process parameters to the geometric CAD data and stores them in the G-code. This file will be transmitted to the machine. Thereby, a three-dimensional object can be created layer by layer [4–7].

The materials used in FFF all have one thing in common, they are all thermoplastic polymers. Apart from this common property, however, they can differ greatly from each other. The various polymers are divided into three main groups. The standard polymers, engineering polymers and high-performance polymers. In addition, a distinction is made between polymers and polymer compounds. In the case of compounds, additives are added to the base polymer to improve the properties or even add new properties to the basic polymer. The basis of the investigation in this work is a polyamide 6 based compound or PA6 for short. PA6 belongs to the group of technical polymers and is characterized by high heat resistance and excellent mechanical properties. Polyamides offer the special feature that their properties are largely determined by the subsequent water absorption of the components. For this reason, these components are often specified as conditioned, i.e. as parts in which water absorption from the environment has already taken place. A further factor for the properties is the crystallization of the polymer. For this reason, parts, especially parts that have been produced in the FFF process are post-treated. The post-treatment takes place in an oven, in which the added heat completes the crystallization of the part [8–11].

The industry around FFF is very broadly diversified and addresses to the most different customers. This applies to the materials used, which offer the best possible properties for the respective application, but also for the machines, which can be desktop devices or highly productive production machines. The differentiation between a machine as an industrial machine or a desktop device is mainly based on the dimensions of the machine as well as on the specifications and features found in common production facilities. An industrial 3D printer is also often more expensive than a desktop device. A price difference of the factor 10 or higher is not unusual. This does not mean that desktop devices are not suitable for production. In recent years, desktop 3D printers have increasingly evolved into efficient and productive machine tools [12]. It is possible to use these machines to produce prototypes, tools or even consumer products. These machines are aimed at hobbyists as well as research laboratories or production facilities and vary greatly in price and features. As a center of research, a selection of the printers currently available on the market was taken.

The printers used, are each common printer in their field of application. They differ primarily in price, in their basic design and as well as in their shielding from the environment.

The aim of this bachelor thesis is to show what influence the actions and efforts that the respective manufacturers invest in their machines have on the mechanical properties of the processed material. By that it is very interesting to see which factor is affected by the different printers. A distinction is to be made between functions that effect the user experience, functions that offer an advantage during the printing process, and functions that even have an impact on the printed part itself. It must be shown whether and how the machine design itself affects the mechanical and thermal properties of the printed part if all other process parameters are equated. The same process parameters are added to the G-code by the slicing software, and the external environmental factors are also monitored throughout the test. Thus, the input parameters are identical for each of the specimens to be tested and the printer itself will be considered as a black box. The output values of the black box however are determined from the mechanical properties of the specimens. For this purpose, the same number of test specimens are produced in each machine under controlled conditions. For this reason, it is important to investigate how this effort and the integration of new designs affect the mechanical properties of the final component.

The investigated mechanical properties are defined by means of a tensile test according to DIN EN ISO 527, an impact test according to DIN EN ISO 179-1 as well as the testing of the heat resistance HDT-A according to DIN EN ISO 75-1. These values are recorded for all machines after conditioning the test specimens. Additionally, the test specimens are examined with and without previous annealing.

2 State of art

The following chapter describes the current state of the art on important technical terms and technologies, which is intended to support the understanding of the subject matter covered in this work.

2.1 FFF

Fused Filament Fabrication (FFF) is often also known under the name Fused Deposition Modeling short FDM®. This is a manufacturing process from the field of additive manufacturing. Mainly thermoplastic polymers are being used in this technology. The process was developed in the late 1980s by Scott Crump and commercialized ten years later by the company Stratasys, founded by Scott Crump himself [7].

In this extrusion-based process, a plastic wire, also called filament, serves as the starting material. The filament is fed into the FFF machine by an extruder, which often consists of two counter-rotating gears (

Figure 1).There, the filament is guided through a hot chamber, the HotEnd, and then exits from a printing nozzle in liquid form. The HotEnd is usually a steel block with three holes. The main bore is used to connect the extruder with the nozzle. This connection creates a channel for the filament. Along this channel the filament changes from solid to liquid state. A second hole is used to fix a heating element to introduce thermal energy into the steel block. The third hole is used to fix a temperature sensor to control the temperature of the hot end. The nozzle in the heating block is available in different diameters and materials. The diameter is decisive for the quality and resolution of the printed component. A larger nozzle allows a higher extrusion volume and thus higher speeds, since fewer layers are required. The different materials of the nozzle are needed for different filaments. Brass nozzles are suitable due to their good thermal conductivity. If abrasive materials are printed, e.g. filaments with a carbon fiber content, a hardened nozzle material is preferred to counteract the wear of the nozzle. This can be for example a ruby nozzle or a nozzle of hardened steel.

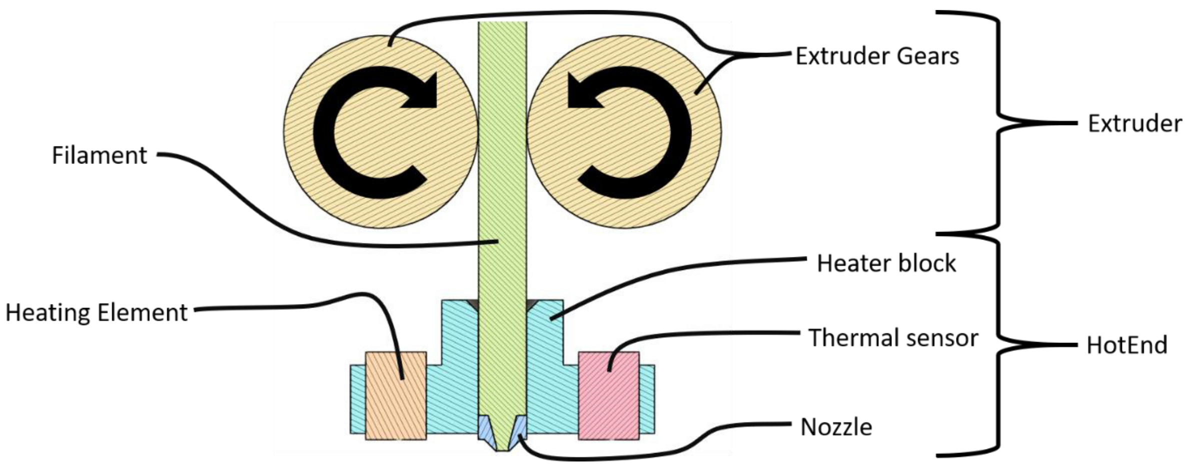

Figure 1: Extruder and HotEnd combination. Source: based on [13]

This entire device is mounted on a frame, which allows CNC controlled movement of the x-, y- and z- axes.
The printing part is created by dividing the geometry into layers. These layers are generally between 0.1 mm and 0.4 mm in height. The layers are first applied by the machine onto a printing bed and then onto each other. Due to the high exit temperature of the molten polymer, each layer bonds with the one below. Layer by layer, a three-dimensional object is thus created from the two-dimensional single layers.
The starting point for each 3D print is the CAD geometry data. The CAD object is then exported as a .stl-file. In this file format, the geometry of the component is described as an outer surface consisting of a triangles (mesh). This file can be processed in the next step with a so-called slicer. The slicer is a software which divides the three-dimensional object into two-dimensional layers to control the axis movements of the machine. In addition to the geometry data, the slicer also has other tasks. It adds all process-relevant information to the model. This includes material-specific data such as temperature and density. The slicer also processes machine parameters such as speeds and build space.
These information are then saved in another file format. This file, also known as G-Code, contains all the necessary information line by line, which is processed as a build job by the firmware installed on the printer.

At the early stages of the technology's dissemination, the technology was initially used to create prototypes or tools. This is because it offers the advantage of almost complete design freedom in the development process. Time to Market can be reduced significantly with this technology [12]. The costs for tools or assembly aids can also be drastically reduced by manufacturing with FFF.
In the meantime, the quality of the components produced in this way has matured to such an extent that entire small series can be produced by additive manufacturing. The freedom of design and the low machine and tool costs open new markets. Adaptability and batch size 0 are no longer a problem in production planning[12].

2.2 Printer Designs

Filament based 3D printers can be found on the market in many different designs. These FFF machines can be categorized as industrial and desktop machines. While the industrial machines have all criteria to fit within the classical industrial environment, the desktop 3D printers are rather small and simpler. In addition to the external dimensions, these machines differ in handling, maintenance, safety features, price as well as in the connection and integration into industrial processes. Desktop devices, on the other hand, have a consumer-friendly appearance and can be visually integrated into offices and technical labs. Apart from their external appearance, desktop devices are no longer inferior to their major counterparts. Most of the features that until recently were reserved for industrial machines have now made it into desktop printers.

Firstly, the differences of an FFF 3D printer can be described by its kinematics. There are printers that work with a "Delta" motion system (Figure 2). This type of motion control is characterized by the fact that the hot end is attached to three arms. These three arms can perform a vertical movement. None of these movements is responsible for a specific axis. The relative movement is a result of the interaction of all three movements.The more common movement design, which can also be found in all printers in this work, is the "Cartesian" (Figure 2). Here each axis of the printer is responsible for the respective x, y or z axis. Which component moves on which axis can be different [14].

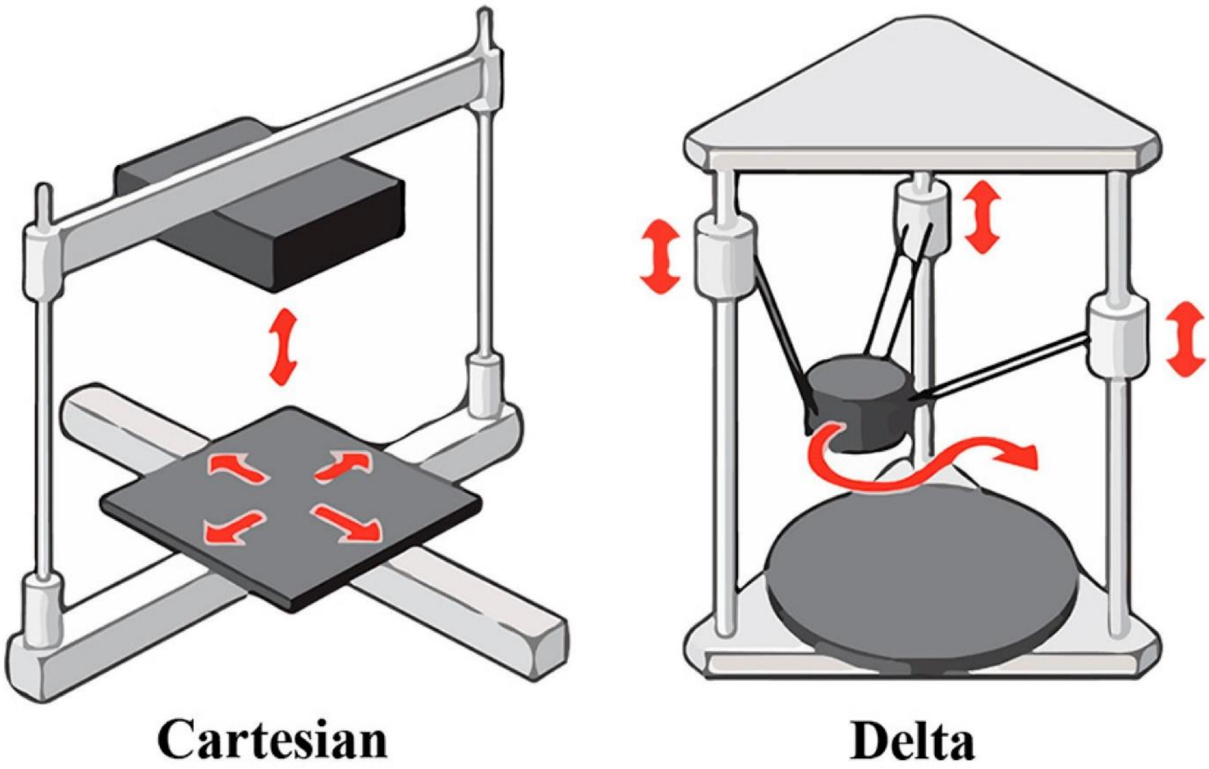

Figure 2: Schematic of cartesian printer (right) and delta printer (left). Source: [14]

Besides the differences in the type of drive, there is another major difference between the machines available on the market. The arrangement of HotEnd and extruder. Machines where the extruder is located directly above the hot end on the moving part of the machine are called direct drive. Here the material is pulled into the HotEnd. This type of drive makes it possible to print especially flexible materials because the distance between hot end and extruder is short and flexible filaments can be pulled rather than pushed. This has the disadvantage that more mass must be moved by the motion system of the printer. In contrast to this design is the Bowden design. Here the extruder is located at a fixed position on the printer and the material is pushed to the hopper by a tube. This pressing of the material over a long distance is often inaccurate and sluggish when changes occur. This is not only due to the long distance but also to the friction that occurs. An advantage, however, is that the moving parts of the printer are faster and more precise due to the lower mass.

The design aspect of particular interest in this thesis is the printer casing. Ambient temperature and humidity can have a decisive influence on the properties of the component. 3D printers on the market today differ in how open the build space is exposed to the environment. This shielding involves a great deal of effort, so it can be said that the degree of shielding is proportional to the price of the machine.
The fact that the shielding influences the processability of the materials has already been shown in many works. ABS is a prominent example of this. [15] This material can only be processed in FFF under controlled conditions. Whether and how strongly this controlled condition affects the mechanical properties has only been investigated to a limited extent. Which printers are examined and how they differ from each other is described in the following subchapters.

2.2.1 Prusa i3Mk3

One of the printers used in this work is the Prusa i3Mk3s from Prusa Research (Figure 3). This device is an open source printer, which was developed from the RepRap project. The idea of RepRap goes back to Adrian Bowyer, it consists of the idea to create a 3D printer that can create its own components and thus replicate itself. The abbreviation RepRap stands for Replicating rapid-prototyper. These open source plans are under a GNU Gerneral Public Licence. From this idea the Prusa i3 was developed in May 2012. The frame of the printer consists of aluminum profiles and 26 printed plastic components [12].

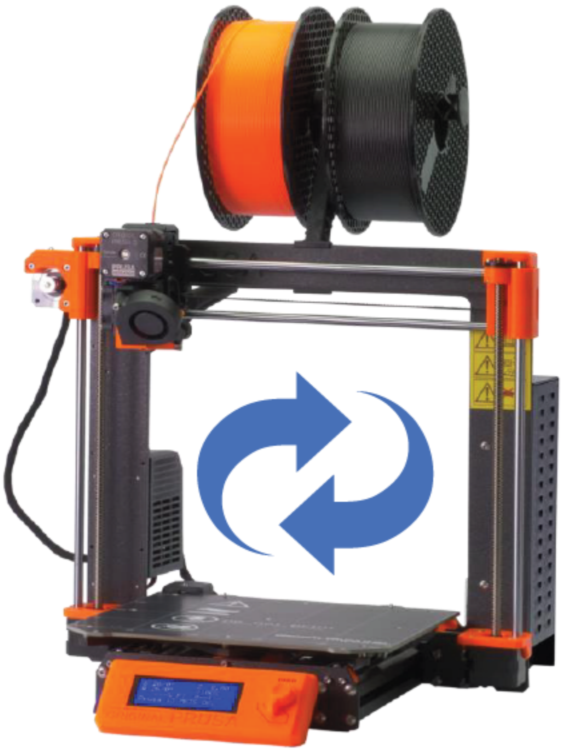

Figure 3: Schematic representation of the effect of the environment on the Prusa i3Mk3s. Source: Based on [16]

It has a heated printing bed and a printing surface made of PEI-coated spring steel. It has a hot end, which can reach temperatures of up to 300°C. The printer processes filament with a diameter of 1.75 mm. A steel heating block for heating a brass nozzle with an outlet diameter of 0.4mm is provided. The temperature of the HotEnd is measured with a thermistor. The extruder consists of two toothed gears for feeding the filament. The extruder and the HotEnd are installed in a direct drive configuration.

The printer was selected for this test series because the printing platform is completely unprotected from the environment on all sides. The simplicity of the design makes it a good test object for the effects and investigations in this thesis.

2.2.2 Ultimaker S3

Another 3D printer in this test series is the Ultimaker S3 from Ultimaker (Figure 4). According to the company, this printer is the entry into industrial and professional filament 3D printing. The housing of this machine is closed at the sides, so that the printing area is only open to the environment from above.

Figure 4: Schematic representation of the Ultimaker S3 shielding. Source: Based on [17]

The printer has a heated printing bed and a printing area made of coated glass. The maximum printing area of the printing plate is 230 x 190 x 200 mm (H*W*D): It also has a dual HotEnd so that different materials can be processed simultaneously. The HotEnds can be heated to temperatures of up to 320°C. The filament processed in this device has a diameter of 2.85 mm. The Ultimaker has exchangeable print heads, the so-called printcore. In the test, the printer is equipped with a 0.4 AA printcore. AA refers to the nozzle material, here brass. The addition 0.4 describes the diameter of the nozzle with 0.4 mm. The Ultimaker's extruder consists of two toothed gears and is mounted on the back of the device. The filament is guided into the printcore via a PTFE tube in a bowden configuration.

The design of this printer is the next step in shielding the printing area from the environment and thus a further step towards a controlled processing atmosphere.

2.2.3 Ultimaker S5

In addition to the Ultimaker S3, the Ultimaker company also offers the Ultimaker S5 (Figure 5). This printer is another step towards industrial 3D printing. The housing of this machine is closed not only on the sides, but also on the top, so that the printing area is completely isolated from the environment.

Figure 5: Schematic representation of the Ultimaker S5 shielding. Source: based on [18]

S5 has all the features and technology of the S3, except for a larger build volume. The build volume is 330 x 240 x 300 mm (H*W*D): Like the Ultimaker S3, the S5 also has exchangeable print cores. In the test, the printer is equipped with a 0.4 AA printcore. The extruder of the Ultimaker S5 is also located on the back of the device. Here, again, the filament is fed into the printcore via a PTFE tube in a bowden style setup.

This printer offers complete shielding of the printing area from its surroundings.

2.2.4 Makerbot MethodX

Like the Ultimaker S5, the Makerbot MethodX also offers a closed housing (Figure 6). In this case, however, the housing is additionally insulated. This insulation is necessary because this device does not have a heated bed. Instead, hot air is used to bring the entire printing chamber to the desired ambient temperature. This heated chamber provides a more uniform ambient.

Figure 6: Schematic representation of the Makerbot MethodX shielding. Source: based on [19]

A plastic-coated spring steel plate serves as a printing base of the Makerbot MethodX. The temperature of the print chamber can reach up to 100°C. The printer has two extruders. Like the Prusa, the Makerbot uses filaments with a diameter of 1.75mm. The Makerbot MethodX is equipped with completely exchangeable print heads, which include the HotEnd and the extruder. In the test the printer is equipped with a LABS extruder which includes a 0.4 mm nozzle. The extruder is located directly above the HotEnd, therefore it concerns as a direct drive configuration.

This machine offers the advantage that it is not only isolated from the environment, but that the environment within the machine itself is controllable and uniform. The printer also differs in that the printing bed is not heated and the environment is brought to the operating temperature by a hot air fan.

2.3 Polyamide Compound

Many polymers and polymer compounds are used in plastics extrusion and many of them are specially adapted and modified for 3D printing. Each material serves a different application. These polymers can be depicted and classified in the so-called polymer pyramid. (Figure 7)

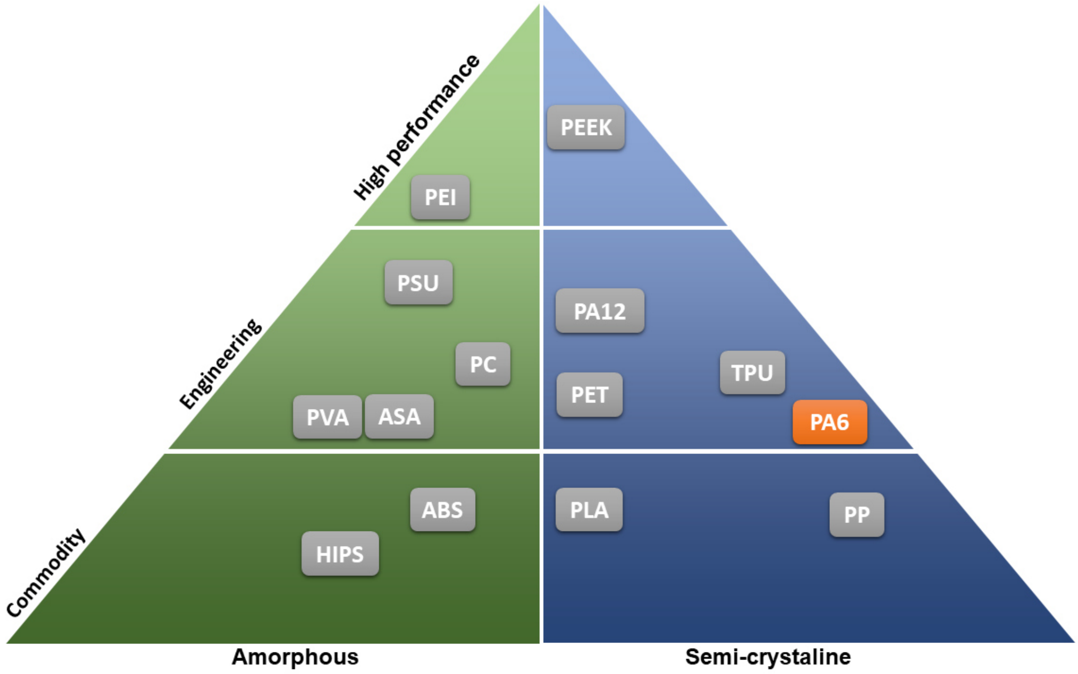

Figure 7: Polymer pyramid. Source: based on [16]

Polyamides, or PA for short, are technical plastics that are characterized by good heat and chemical resistance. They are semi-crystalline materials and are one of the oldest engineering polymers available. There are many different types of PA with PA6 and PA66 being the most common. [20] Polyamide was invented in the mid-1930s and is known to many as nylon[21]. PA has excellent mechanical properties and is used in a variety of products. Polyamides have the special property that their mechanical properties are strongly determined by the absorption of water. Especially with polyamide it is necessary to use a dry starting material. The moisture absorption of polyamide is between 2 % - 4 % relative humidity[22–24].

In this work a polyamide compound produced be the company LEHVOSS Group is used. The product “LUVOCOM® PA^{HT} 9825 NT” is based on a PA6 and it was specially developed to address the complications in 3D printing, e.g. moisture absorption and the warping that occurs during printing, has been greatly reduced. warping results from the crystallization of the structure in the layers close to the printing bed due to the thermal energy of the bed. The crystallization creates a stress gradient within the component, which bends the component upwards.

The material can be processed without side effects under uncontrolled environmental conditions. The LUVOCOM $\mathrm{PA}^{\mathrm{HT}}$® 9825 NT is optimized to store less moisture. The moisture absorption is only half that of conventional PA6 and the time to complete saturation is four times longer. These properties make this material particularly suitable for use in this work. Many problems have already been solved on the material side, so the focus of the printers is on achieving the best possible mechanical properties. An extract of the technical datasheet of the tested material is shown in Figure 8 .

LUVOCOM® 3F PAHT 9825 NT

LUVOCOM® 3F
Additive manufacturing solutions

High-temperature polyamide
unreinforced, natural color

Physical properties		Test method	Specimen	Units	Typical value
Specific gravity		ISO 1183-3		g/cm³	1,20
Water absorption	23°C / 24h	ISO 62	MPTS ISO 3167 A	%	<0,3
Melt flow rates (MFR)	250°C / 2,16kg	ISO 1133	pellet	g/10 min	3,6
Melt volume rate (MVR)	250°C / 2,16kg	ISO 1133	pellet	cm³/10 min	3,47
Linear mould shrinkage		DIN 16742	MPTS ISO 3167 A	%	0,3-0,5
Mechanical properties at 23°C / 50% rh					
Tensile strength	dry, @50 mm/min	ISO 527	MPTS ISO 3167 A	MPa	85
Elongation at maximum force	dry, @50 mm/min	ISO 527	MPTS ISO 3167 A	%	3,6
Modulus of elasticity	dry, @1 mm/min	ISO 527	MPTS ISO 3167 A	GPa	3,4
Charpy impact strength	dry	ISO 179 1eU	80x10x4mm	kJ/m²	NB
Thermal properties					
Heat distortion temperature	HDT A	ISO 75	molded sample	°C	90
Continuous service temperature	20.000 h	IEC 60216	MPTS ISO 3167 A	°C	120
Service temperature	during lifetime max. 200h		MPTS ISO 3167 A	°C	160
Coefficient of thermal expansion		ISO 11359	10x8x4 mm	10^{-5}/K	0,5
Thermal conductivity in plane	hot disk	ISO 22007	‖ 60x60x3 mm	W/mK	0,3
Electrical properties					
Insulation resistance strip electrode	R25	DIN IEC 60167	MPTS ISO 3167 A	Ω	$>10^{12}$
Surface resistance	ROB	DIN IEC 60093	Ronde 60x4mm	Ω	$>10^{12}$

Main features

Low influence from moisture and temperature on dimensional stability and electrical properties, compared with PA66

Figure 8: Extract of the technical datasheet of LUVOCOM® PA^{HT} 9825 NT.

2.4 Annealing

Polymers contains of long repeating molecule chains. These chains have two types of molecular structures: crystalline and amorphous. The crystalline structures are partially ordered. The amorphous part has a disordered or chaotic form. While the crystalline parts are stiff, amorphous polymers behave elastically and flexibly. By liquefying the plastic in the nozzle of the 3D printer, the plastic is mostly amorphous [25]. In this state, the material solidifies when exposed to the air. Due to the rapid cooling of the layers on top of each other, additional stresses are created within the component due to the temperature gradient. In addition, more heat is supplied to the lower layers due to the heated printing bed than to the layers further up [26].

The post-treatment of plastic components from the FFF printer offers the possibility to optimize the components afterwards. One of these processes is called annealing. This process serves to complete the maximum crystallization in the component. The prerequisite for this is an amorphous or partially crystalline material. For this purpose, the crystal chains are energetically re-arranging to create a solid structure (Figure 9). To achieve this, the material must be brought above the so-called glass transition temperature (Tg). At this temperature, the amorphous components of the polymer change into the glassy or rubbery state. The glass transition temperature is therefore often called the softening temperature. This soft amorphous phase provides sufficient space for new organization in the microstructure. [27] This allows small structural defects to be compensated and repaired. Each polymer has its own specific glass transition temperature depending on its molecular structure. Polyamide 6 has a glass transition temperature of 60 °C. However, this value depends on the moisture contained in the material. For successful annealing, a temperature above Tg must be applied. The temperature must not exceed the maximum operating temperature. At this temperature, the material will soften to much and loose its shape. Heating the material further and above the degradation temperature, the material decomposes and is irreversibly damaged.

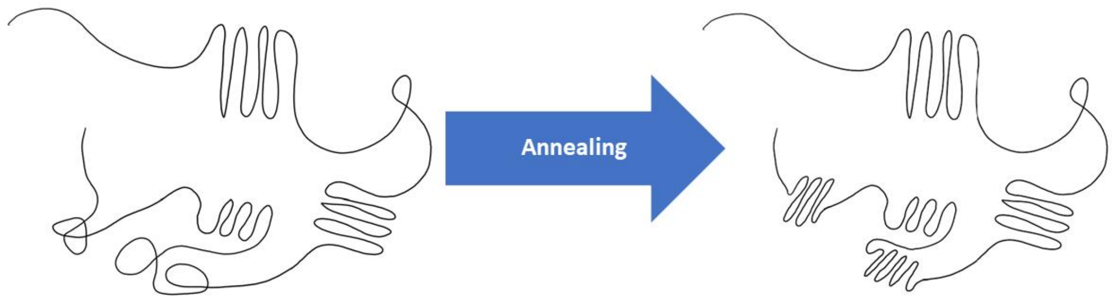

Figure 9: Polymerechain before (left) and polymerechain after annealing (right).

2.5 Conditioning

Another post-treatment for plastics, especially polyamides, is conditioning. Conditioned describes the state the polyamide is in when it is saturated with water. For this purpose, the material is stored in a special container until it reaches the conditioned state. Within this container there is a constant relative humidity and temperature. The strength and stiffness of the material decreases after conditioning. The elongation on the other hand is increased by conditioning. Furthermore, the glass transition temperature shifts to a lower value. Only through the storage of moisture does the polyamide acquire its characteristic strength and elasticity. In the data sheets of the material, the properties are usually specified as "conditioned", as this meets the requirements of the later application [23].

Water molecules diffuse through the material, searching for charged areas and forcing polymer chains apart. For this reason, polyamide parts swell up after being exposed to moisture. The separation of the polymer chains reduces the polar attraction between the bonds and enables increased chain mobility. This leads to reduced mechanical properties. Within the amorphous areas, the water binds to the polymer chain through hydrogen bonds. Fortunately, the crystalline regions show a high resistance against separation by the water because the bonds between the amide groups are stronger than the attraction to water [24]. (Figure 10)

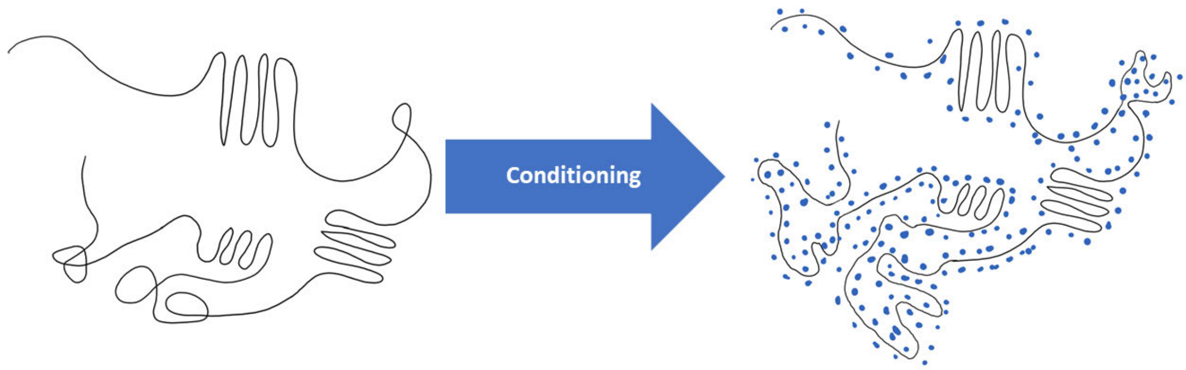

Figure 10: Effect of conditioning on a polymer chain.

3 Experimental Methodology

This chapter and its subsections describe the procedure of this test series.

3.1 Pretest

The main purpose of the pre-test is to find suitable settings for all the devices. For this purpose, the settings specified by the material manufacturer are used as the baseline setting. For the test, print profiles are created for all printers in the slicer software Cura. The process parameters are adopted for all machines, only printer-specific settings such as the homing routine or the size of the installation space are adjusted.

Small test cubes are printed to ensure that the machine firmware calculate the software values correctly. For this purpose, three builds with five cubes each are printed on each machine. These 10 mm^3 cubes are used to check whether the printers extruded the same amount of material. For this purpose, the cubes are measured and weighed to calculate the density of the cubes. The density is also measured with a pycnometer.

The Makerbot MethodX is treated separately here and in the whole further course. Compared to the other machines, it does not offer a connection to the software Cura and does not use a standard G-Code. The settings have been adjusted in the MakerbotPrint software to be like the profiles created in Cura in all important settings.

In addition, a set of tensile specimens is printed and tested on each printer by DIN EN ISO 527. This test serves as a pre-check, to ensure that the values are within the expected range before the whole test begins. These results are then compared with those of the technical data sheet to ensure that they are in line with expectations.

3.2 Preparation

The tests are performed one after the other under monitored conditions. For this purpose, the material is pre-dried for 48 hours in an oven at 100°C to ensure that there is no residual moisture in the material. The material is then stored in a filament dryer. From this dryer the material is loaded directly into the respective printers. The dryer ensures that no condensation occurs on the surface of the material at temperatures above 50°C and a humidity level of no more than 15%. The humidity and temperature of the room is recorded directly at the printer's workstation with the help of a data logger. The dry material is loaded through a tube directly into the extruder of the respective printer. Thus, the material is exposed to ambient conditions only after exiting the nozzle.

The environment is recorded with a testo Saveris 2 WLAN data logger system. This logger stores the relative room humidity and the ambient temperature. For the recording of the moisture content inside the filament dryer a self-built data logger consisting of an Arduino Nano and a DHT22 sensor is used.

3.3 Printing

Two types of test specimens must be printed to test the mechanical properties. On the one hand, these are tensile test specimen according to DIN EN ISO 527. Five of each of these test specimens are printed on one printing bed. These tension bars are printed in the “flat” position and the “edge” position as shown in Figure 11. From this point on, the orientation marked as "flat" refers to the orientation of the specimens in the XY plane. The "edge" orientation therefore refers to the orientation in the YZ plane.

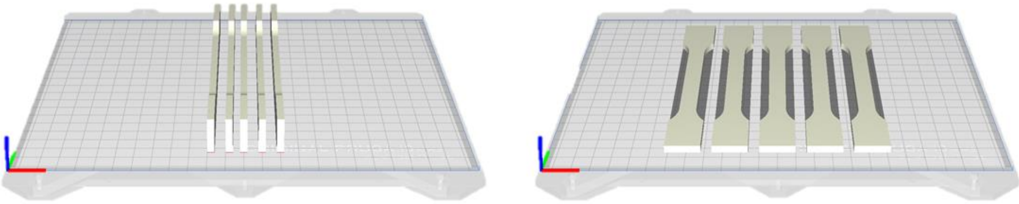

Figure 11: Layout of the tensile specimen edge (left) tensile specimen flat (right) and in the Cura Slicer.

Beside the tensile bars, cuboids with the dimensions 10 mm x 4 mm x 80 mm are printed according to DIN EN ISO 75-2, DIN EN ISO 179 1eU and DIN EN ISO 178. These test specimens are needed to determine the mechanical properties such as impact strength and flexural strength as well as the thermal properties of the HDT. These specimens are also printed in the “flat” and “edge” orientation as shown in Figure 12. There are 15 test specimens per printing bed.

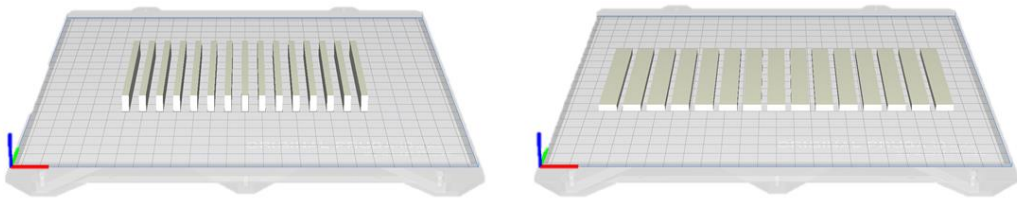

Figure 12: Layout of the Charpy specimen edge (left) Charpy specimen flat (right) in the Cura Slicer.

Since the properties are tested with and without subsequent annealing, the test specimens are required in a duplicate version.

When examining different machines from different manufacturers, it is essential to create a common basis. In this case the common basis is the G-Code. This must be identical in all settings relevant to printing. These basic settings are listed in the following (Table 1).

Slicer settings in Cura			
	Setting	**Value**	
Quality	Layer height	0,2	mm
	Layer width	0,6	mm
Material	Extruder temperature	265	°C
	First layer extruder temperature	265	°C
	Printbed temperature	80	°C
	First layer printbed temperature	80	°C
	Material flow	100	%
Speeds	First layer print speed	20	mm/s
	Infill print speed	40	mm/s
	Outline print speed	40	mm/s
Layers	Number of outlines	3	
	Number of bottom layers	3	
	Number of top layers	3	
Infill	Infill pattern	Lines	
	Infill percentage	100	%
	Infill overlap	30	%
Cooling	Cooling fan speed	0	%

Table 1: Slicer settings in Cura.

These G-Codes were generated with the open source software package Cura 4.5.0. The height and width of the layers shown in the table are common values which are often chosen to produce components in FFF. The material settings are taken from the manufacturer's printing guideline document. It describes how the material can best be processed. The speeds are slightly below the processing speeds of the material to ensure that a constant material volume flow is guaranteed. The number of layers is also based on a value normally used in production. To assess the effect of the environment more precisely, the fan for cooling the component is disabled. This also helps to keep the energy of the heat inside the component to achieve a better connection of the layers. In addition, the travel paths of the printers are examined to ensure that the structure of the individual layers is identical for each printer.

3.4 Post-treatment (Annealing)

After printing, the test specimens are sealed in a plastic bag. One part of the test specimens is annealed in an oven. In this oven, the material is first heated to 65 °C for one hour. Then the temperature is increased to 85 °C and the material is treated for another five hours (Figure 13). These two stages are chosen to allow crystallization to take place as slowly as possible. A slow crystallization prevents the geometrical change of the components. The stresses that were preserved in the component during the printing process can be released by sudden heating and deform the entire test specimen. This two-step method of annealing can reduce this deformation to a possible minimum. A completely deformation-free annealing process cannot be realized with polyamides due to their semi-crystallinity. [15] The degree of deformation depends on how much stress has been created in the component during the compression process.

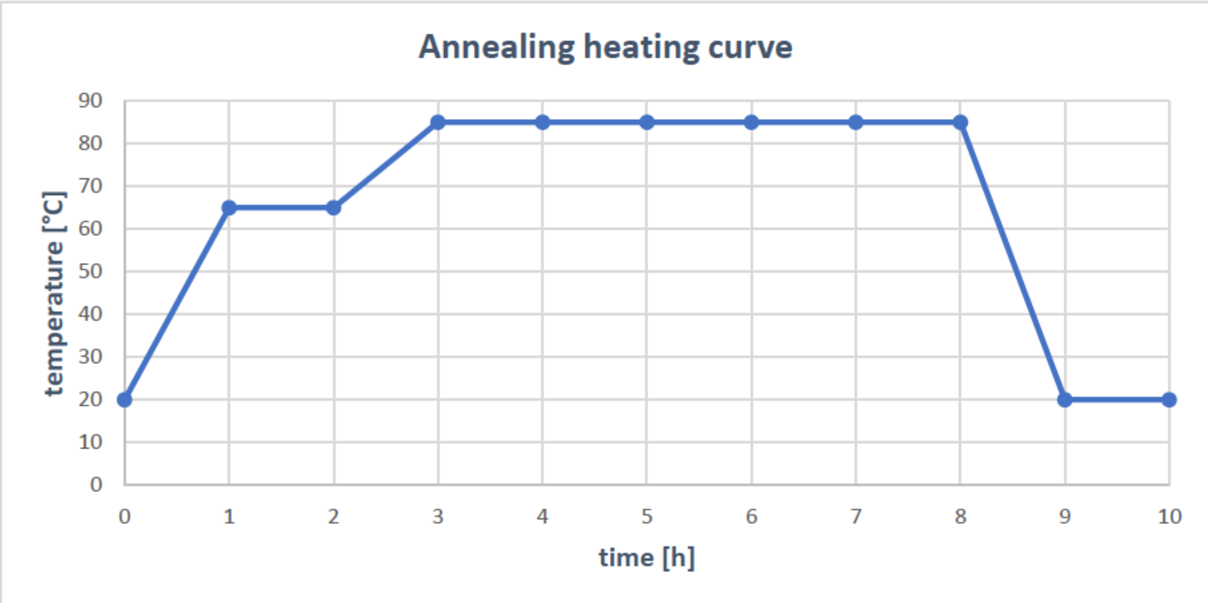

Figure 13: Annealing heating curve.

3.5 Testing

The following chapter describes which tests are necessary to collect the required comparative data. These include the execution of the pre-tests as well as those required for the determination of the mechanical and thermal properties.

3.5.1 Density determination

The density measurement is performed to see if a comparative value can be achieved. For this purpose, the 1 mm² cubes of the pre-test were first measured and weighed with a fine scale. The density of the cubes can then be determined from these values. The density is determined by the following formula:

$$\rho = \frac{m}{V} \tag{1}$$

Where ρ is the density, m the mass and V the measured volume.

Three print jobs with six cubes each were printed on each of the four printers. The Pycnometer tests is performed by “micromeritics AccuPyc II 1340”.

In addition to the manual determination of the density, the density was then determined with a pycnometer. The measurement with a pycnometer is based on the principle of volumetric displacement. For this, the vessel filled with liquid is first weighed. Then the solid to be measured is added and weighed again. From the difference in weight the density of the solid is calculated with:

$$\rho_{solid} = \frac{m_{solid} - m_{empty}}{(m_{liquid} - m_{empty}) - (m_{solid+liquid} - m_{solid})} * \rho_{liquid} \tag{2}$$

Where ρ_{solid} is the density of the material to be measured, m_{solid} the mass of the material, m_{empty} the mass of the empty vessel, m_{liquid} the mass of the added liquid and ρ_{liquid} the density of the added liquid.

Additionally, the density of the filaments was determined to provide a comparative value.

The measurements were taken with an analog caliper gauge. The mass was weighed with a "KERN PFB".

3.5.2 Tensile Test according to DIN EN ISO 527

One of the most important parameters of mechanical material properties is the tensile strength. This value describes the maximum tensile stress at which a material fails. To obtain this value, a tensile test is carried out according to DIN EN ISO 527. These specimens are tested with a “ZwickRoell ZMART.PRO”. The test speed of the tensile test is 50 mm/min. Other noteworthy characteristic values from this test are elongation at maximum force and the tensile modulus.

The specimen tested in this test is the test body 1A which is defined in DIN EN ISO 3167. The characteristic dimensions of the multipurpose test specimen are a length of 80 mm, a width of 10 mm and a thickness of 4 mm. Five test specimens are required for each measurement.

3.5.3 Charpy impact properties according to DIN EN ISO 179 1eU

Impact strength is another important parameter of the mechanical properties of the material. To obtain this value, a Charpy notched bar impact test is carried out according to DIN EN ISO 179 1eU, which is the preferred test according to ISO 10350-1. This test is preferred according to the single point values ISO 10350-1. At this dynamic bending of the test specimen, which occurs due to an impact-like stress, the test specimen breaks, and the absorbed kinetic energy can be measured.

The specimen tested in this test is the unnotched Charpy specimen. The characteristic dimension of the test specimen is a width of 10 mm, a thickness of 4 mm and a length of 80 mm. Five test specimens are required for each measurement. These specimens are tested with a "ZwickRoell HIT25P Pendulum Impact Tester" equipped with the “RoboTest H” for automation.

3.5.4 Flexural Strength according to DIN EN ISO 75-2

Flexural strength is a mechanical property that is determined with the three-point bending test according to DIN EN ISO 75-2. For this test, a Charpy test specimen is exposed to a load and the deflection is measured in parallel. This test can be used to determine the characteristic values of flexural strength, elongation, flexural modulus, and elongation at break.

The specimen tested in this test is the Charpy test specimen. The characteristic dimension of the test specimen is a width of 10 mm, a thickness of 4 mm and a length of 80 mm. Five test specimens are required for each measurement. These specimens are tested with a "ZwickRoell RetroLine". The test speed is 10 mm/min.

3.5.5 HDT according to DIN EN ISO 178

The Heat Deflection Temperature (HDT) is the temperature at which a test specimen deforms up to a standardized dimension. This is a thermal material property. For this test, a Charpy specimen is stressed with a load, the temperature is raised, and the deflection is measured at the same time. This test is standardized according to HDT ISO 75-2. The test method used is method A with a bending stress of 1.8 MPa and a linear heating rate of 120°C/h. The maximum allowed deflection is 0.34mm. This test can be used to determine the temperature at which the allowed final displacement is reached.

The specimen tested in this test is the Charpy test specimen. The characteristic dimension of the test specimen is a width of 10 mm, a thickness of 4 mm and a length of 80 mm. Three test specimens are required for the evaluation. These samples are tested with an "INSTRON HV500".

3.5.6 DSC According to DIN EN ISO 11357-1

Differential Scanning Calorimetry (DSC) is a technique that measures the heat flow into or out of a material as a function of time and temperature. The polymer crystallinity can be determined with DSC by quantification of the heat associated with the melting (fusion) of the polymer. The exact procedure is recorded in DIN EN ISO 11357-1. DSC is also a method for determining polymer crystallinity. The heat required to melt the polymer is measured and compared with a reference value of a 100% crystalline microstructure. This difference is directly proportional to the crystalline portion of the polymer structure. The percentage of crystallinity inside the polymer can be calculated as:

$$\Delta_m H = \int_{T1}^{T2} C_p dT \qquad (3)$$

$$w_{Cryst} = \frac{\Delta_m H_{Prob}}{\Delta_m H^0} \qquad (4)$$

With $\Delta_m H_{Prob}$ being the enthalpy of the probe, $\Delta_m H^0$ being the enthalpy of a fully crystalline structure and w_{Cryst} being the percentage of the crystalline structures.

The temperature spectrum in this test was a heating from 30 °C to 280 °C at a speed of 10 K/min. The DSC analysis was performed with a "METTLER TOLEDO DSC 1 STAR® System".

3.6 Scope and Limitation

Such a macroscopic view of a manufacturing process offers many variables and influencing factors. To evaluate the resulting properties of the produced parts requires a lot of tests and investigations.

The four different machines from different manufacturers are the basis for the investigations. All the differences in the construction, both mechanical, electrical, and thermal, must be considered as a black box. The specific influence of all these components cannot be differentiated. But it is not only the machines themselves that offer a diverse starting position. The material used also differs. These differences can be found in the different filament diameters and possible microscopic differences in the structure of the different batches. The moisture content of the material cannot be specified exactly either since inline measurement of the core moisture is not possible.

From these differences, both on the machine side and on the material side, further irregularities arise in the form of the extruded quantity of the material. This irregularity is mainly due to the different designs of extruders and HotEnds and is therefore the link between material and machine. All these variables can be evaluated very well as a black box. In detail, it is not possible to say which component is ultimately decisive for the result to be seen.

The most serious factor here is the lack of compatibility of the devices in a common software. The absence of this interface makes it impossible to compare the Makerbot with the other printers. However, the tests of the Makerbot can be compared with itself. The difference between treated and untreated specimen on the same machine provide important information about the degree of crystallization.

Limitations in the consideration of the results are additionally a test approach according to standards, which are all designed for samples created in injection molding. This is mitigated by the fact that the industry has agreed to accept these standards as a suitable means of comparison.

The tensile bars in the "edge" orientation are not an optimal exception. The fact that these specimens must be supported with support material in the test cross section and therefore notches and surface damage were left on the surface falsifies the test results. The degree of damage is not uniform across all machines up to the Makerbot, on which these samples could not be produced.

Another way of comparing would be to optimize for each individual printer. Then the best results of the various printers can be compared. However, this approach offers the same difficulties and only shifts the problem to other variables. The approach chosen here is therefore identical starting conditions for all machines up to the point where the printer control takes over.

4 Result and discussion

The results are presented using the different test methods on the specimens produced in the FFF process using the specific 3D-printers mentioned before.

4.1 Density determination

Before the main tests can be started on the individual machines, it must be ensured that the settings made can produce the same results. Whether the same amount of material is extruded from the machines. This comparison is made with the densities produced by the printers. For this analysis, test cubes were printed on each of the printers.

The density measured with the pycnometer, here shown in Figure 14, shows a uniform distribution. All the printers show densities that differ only slightly from the filaments. However, this deviation is identical for all the tested machines, which all produce a density of 1.16 g/cm³.

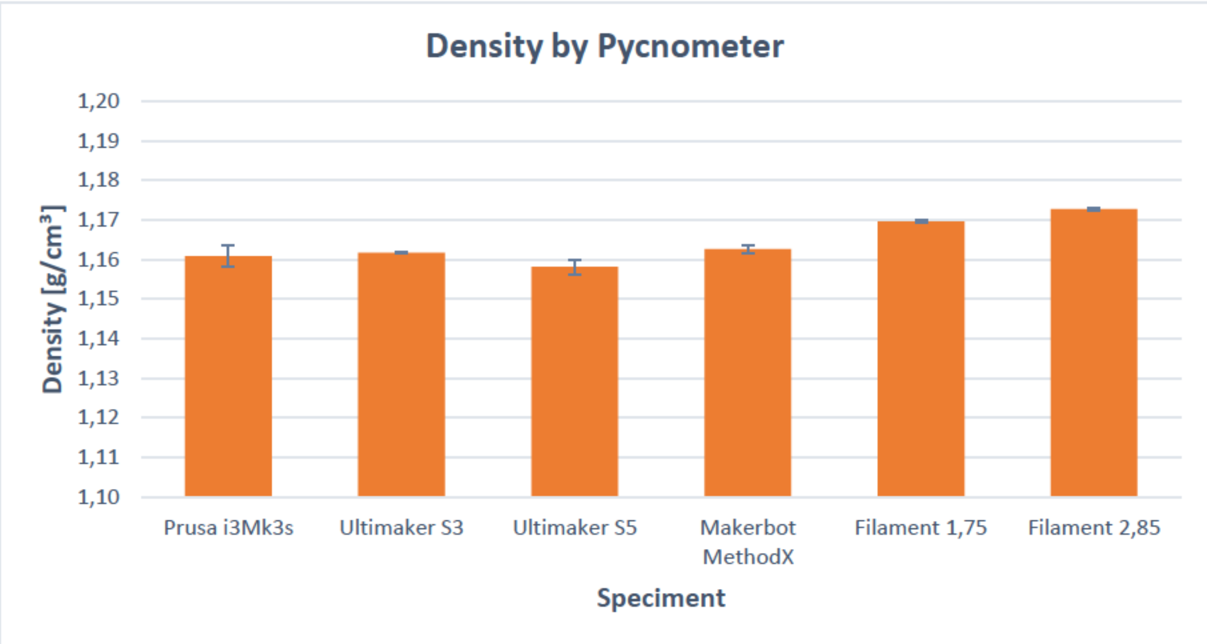

Figure 14: Part density measured by pyconometer.

This result is to be expected. The density of the material does not change due to the printing process. What should be determined is the porosity of the components. For this determination, a test with a pycnometer is unsuitable, because the defects of the layers are open, and displacement of the liquid is not measured.

The samples that were measured with a caliper gauge after printing and weighed on a fine balance show a different pattern, shown here in Figure 15.

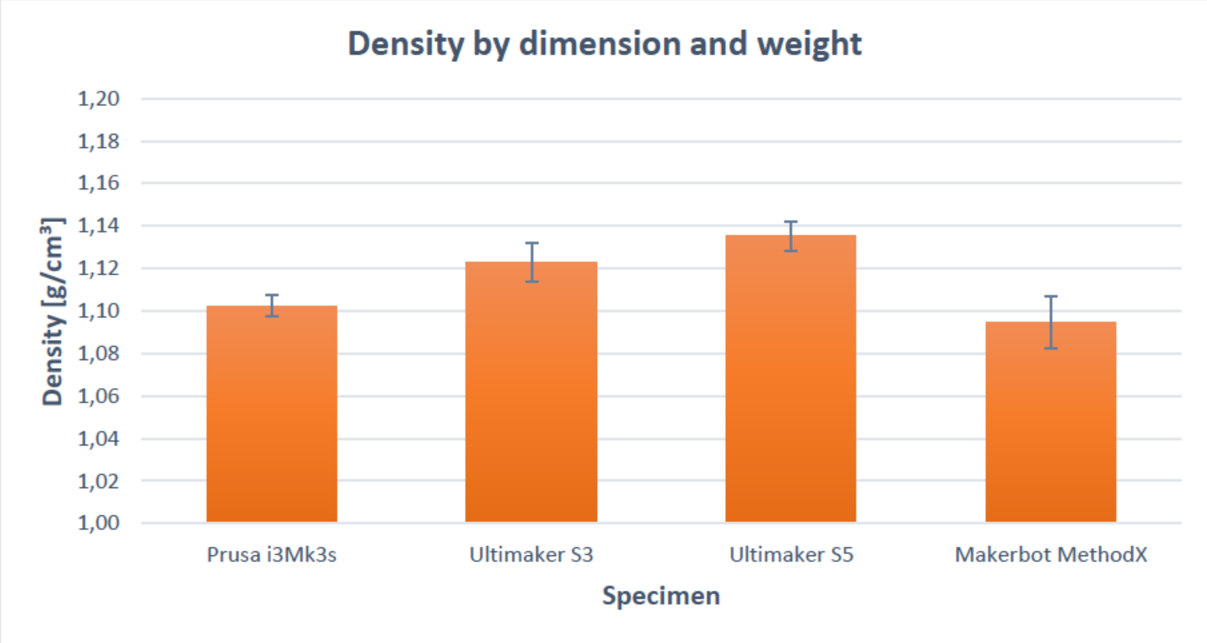

Figure 15: Part density measured by dimension and weight.

The scattering of the results is very large in this measurement. The G-Codes were developed with a focus on uniform dimensional accuracy, and it is the mass of the test specimens that shows the differences (Table 2). Especially the density of the Makerbot and Prusa seem to be low in comparison.

Machine	Mean weight [g]	Mean volume [mm³]	Mean density [g/cm³]
Prusa i3Mk3s	120,94	1097,12	1,10
Ultimaker S3	121,00	1077,75	1,12
Ultimaker S5	119,94	1056,65	1,14
Makerbot MethodX	116,39	1063,08	1,09

Table 2: Geometry and weight for density calculation

The density calculated here not only includes the material density, but also considers internal porosity. This result indicates that there are cavities or gaps between the layers.
Furthermore, this method of determination is inaccurate. The tactile measurement of the geometry also includes surface roughness and therefore produces an incorrect measurement of the geometry.

The fact that the values for the Makerbot are low is due to the limited adaptation possibilities of the G-code of the corresponding software.

4.2 Ambient Condition

To ensure that all test specimens were manufactured under the same conditions, the environmental parameters were monitored and measured during all tests (Figure 16).

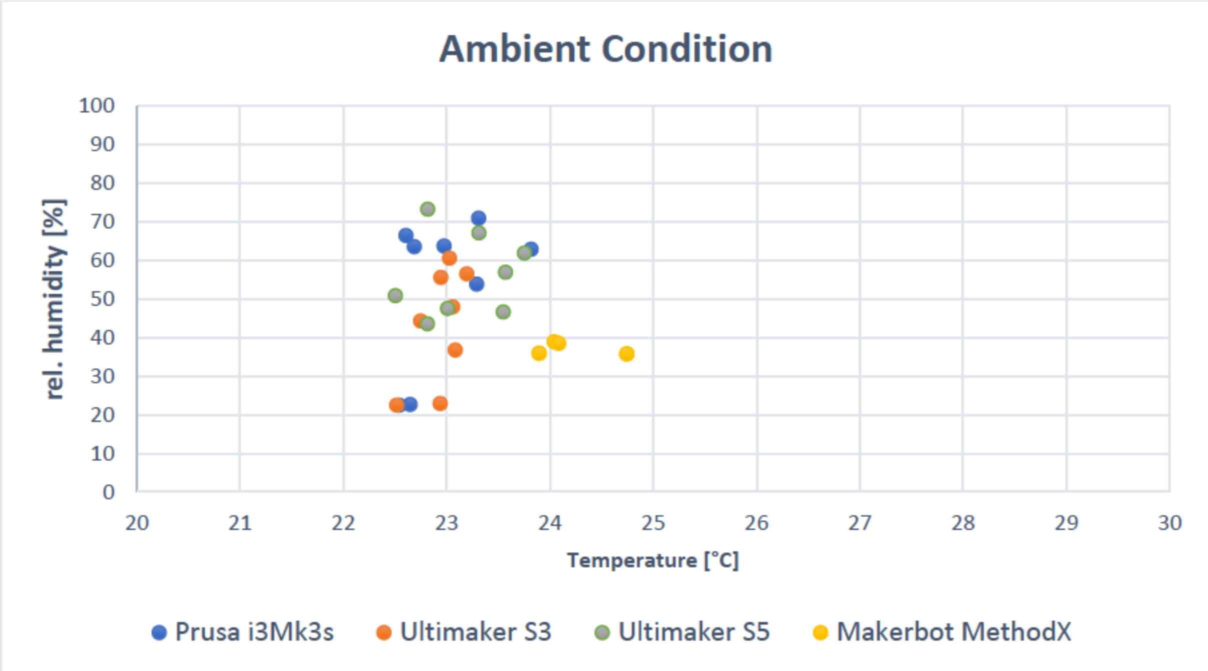

Figure 16: Ambient condition during the prints.

The room temperature shows insignificant differences during all tests. Differences of this small magnitude should not affect the comparability of the prints. These differences are therefore negligible.

The humidity, on the other hand, fluctuates significantly over the tests. To what extent this influences the properties of the test specimens produced during printing cannot be said. After printing, all test specimens are conditioned under the same conditions anyway.

Another key value is the moisture of the material. This has been pre-treated under the same conditions. However, storage during printing is just as important, as moisture absorption is very fast with polyamides. The filament dryer used had a constant value of 60 °C over the entire test period. The moisture inside was recorded during each print (Figure 17).

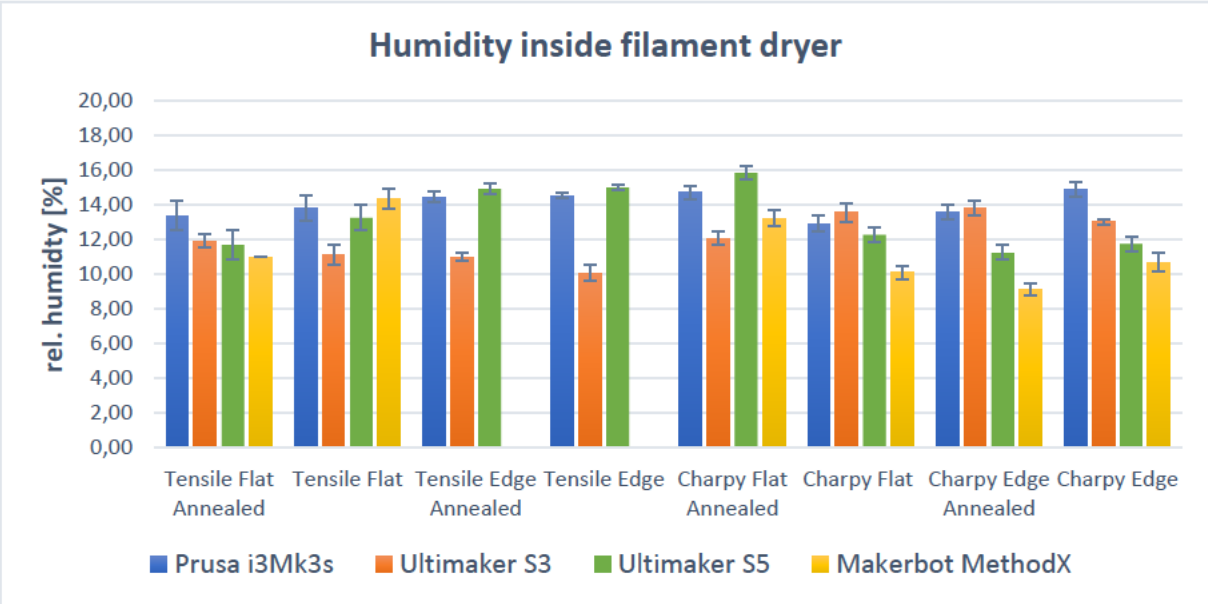

Figure 17: Humidity inside filament dryer.

The relative humidity inside the dryer can be seen for each printer and specimen. The decisive factor here is that the fluctuation of the humidity between the printers during a specimen print is as small as possible.

The largest deviation is seen in the printing of the tensile specimens at the "edge" position without annealing. Here the difference between the Ultimaker S3 and the Ultimaker S5 is about 4%. The sensor used to measure humidity, a DHT22, has an accuracy of +-2%. This inaccuracy therefore does not allow any statement to be made as to whether this could influence the condition of the base material.

4.3 Tensile Test according to DIN EN ISO 527

The data of the tensile test are generally shown in a stress-strain diagram. As an example, the diagrams from the Prusa i3Mk3s measurements (Figure 18).

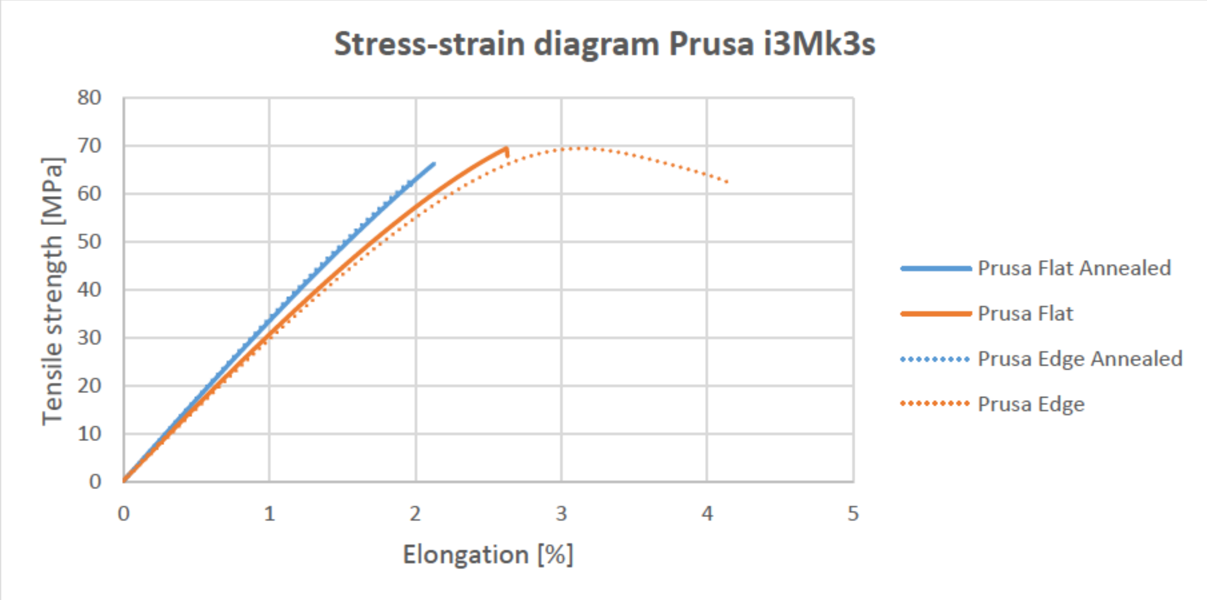

Figure 18: Stress-strain diagram of Prusa specimen.

In this diagram the stress is represented by the strain of the specimen. The diagrams shown here are those which best describe the average of the five measurements. In addition, the measurements of both orientations are shown, with and without annealing. This example shows that the two untreated samples have a higher elongation than those that were not treated. In order to investigate these properties in more detail, these values are considered separately in the following and compared with the other printers.

The results of the tensile test are one of the key results when it comes to considering mechanical properties. First, the tensile stress of the printed as “flat” specimen, which is shown in the Figure 19.

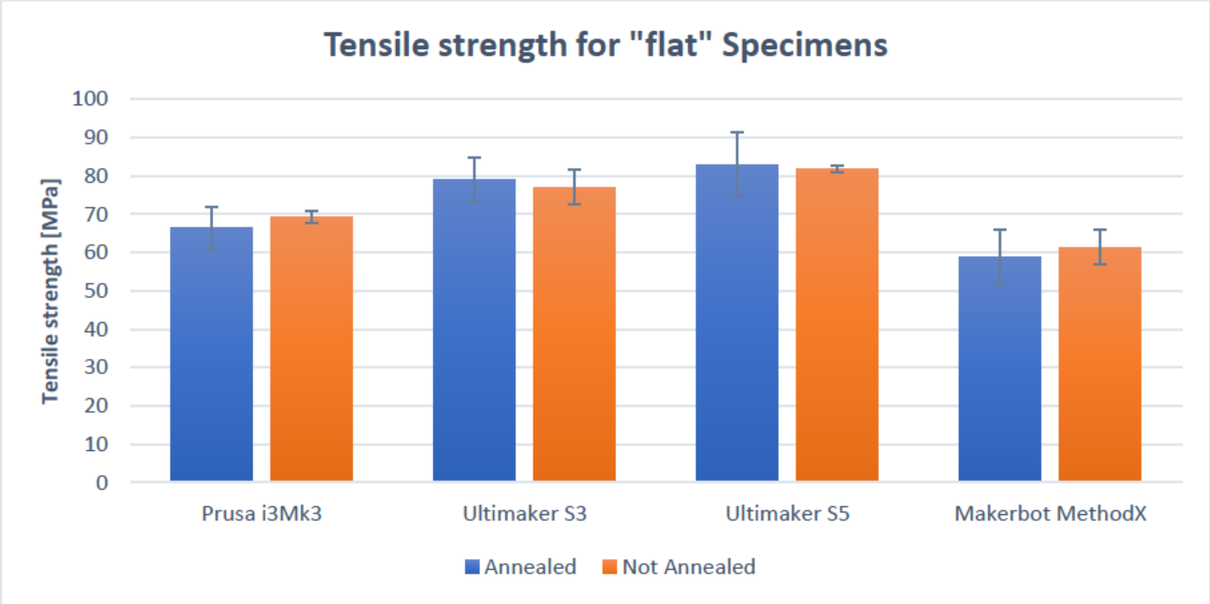

Figure 19: Tensile strength for "flat" specimens.

Here it can be seen that the peak values of the machines are different. The Ultimaker S5 performes best with a tensile strength of 83 MPa. The lowest result is achieved by the Makerbot MethodX with only 61 MPa. However, there is no difference in the tensile strength between the annealed samples and the samples directly from the printer. This suggests that the post-treatment has no influence on the tensile strength itself.

The visible decrease in tensile stress is a consequence of the standard deviation. There is no recognizable effect of annealing. The low value of the Makerbot can be explained by looking at the specimen (Figure 20).

Figure 20: Example of tensile test specimen printed on the Makerbot MethodX.

Here visible gaps between the lines of the first layer can be seen. This is due to limited settings in the software of the Makerbot. These gaps weaken the component due to the lack of material and the notch forces generated at the edges.

The tensile strength of the "edge" specimens is shown below (Figure 21).

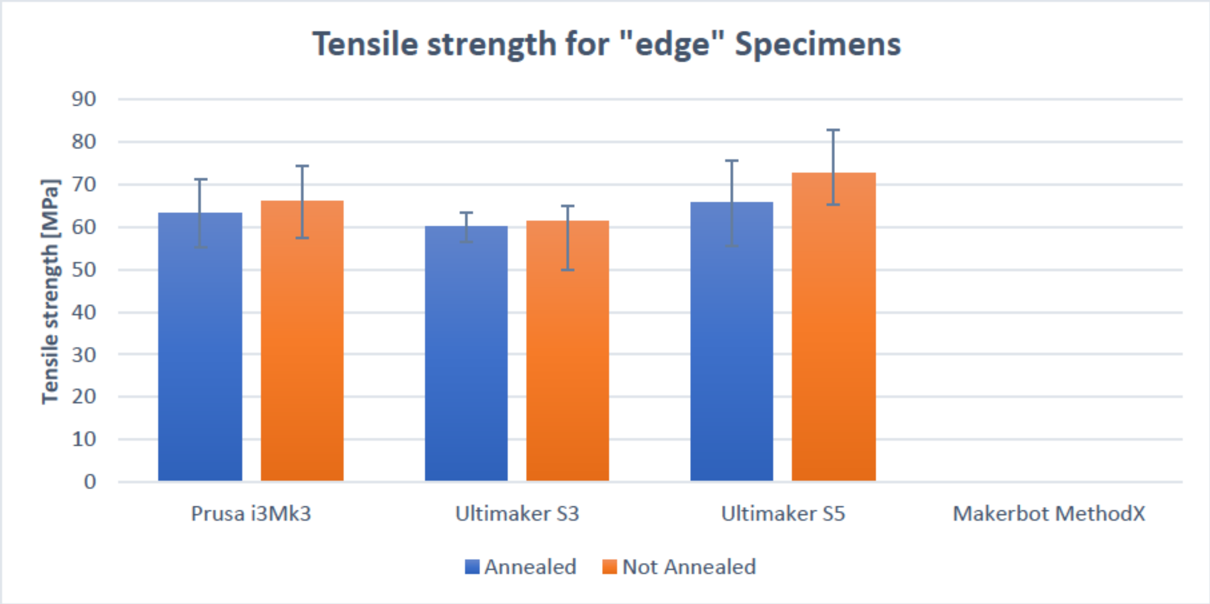

Figure 21: Tensile strength for "edge" specimens.

For those printed as "edge" samples, the difference between the values produced by the different printers is smaller. Within the deviation, there is even no difference to be seen.

The reason that differences in the "edge" tension rods are smaller could be that these tension rods have a low infill and most of the specimen consist of outer layers. In contrast, in the case of the "flat" specimens, the infill makes up a smaller proportion of the total part. The outer shells seem to differ less between the machines than the infill. So, the outer layers seemed to be able to achieve the same tensile strength.

The tensile bars of the Makerbot again cannot achieve the results of the other machines. There is no data of the Makerbot available for the tensile stresses of the samples printed in the "edge" orientation, because any support setting in the software of the Makerbot could not provide acceptable results.

In contrast, the effect of annealing on tensile specimen elongation can be seen. As shown in Figure 22.

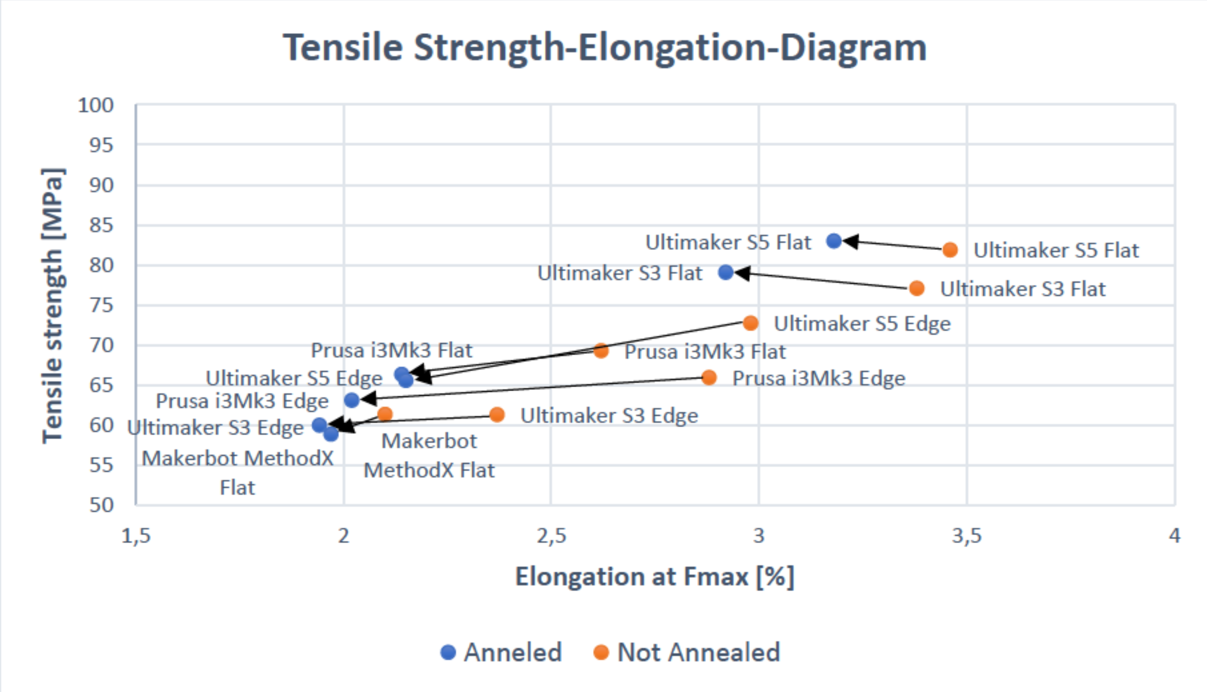

Figure 22: Tensile strength-elongation-diagram.

The elongation decreases significantly. The decrease in strain is not uniform. The Prusa i3Mk3s benefits more from the subsequent annealing than, for example, the Ultimaker S5 or the Makerbot. This suggests that the design of the printer has an impact on the effectiveness of the post-treatment. The post-treatment makes the components stiffer. This can be expected due to the characteristic properties of a crystalline structure.

This effect can be seen in the vectors shown here, but it becomes even clearer when looking at the tensile modules. As an example, the values for the "flat" tensile bars are shown in Figure 23.

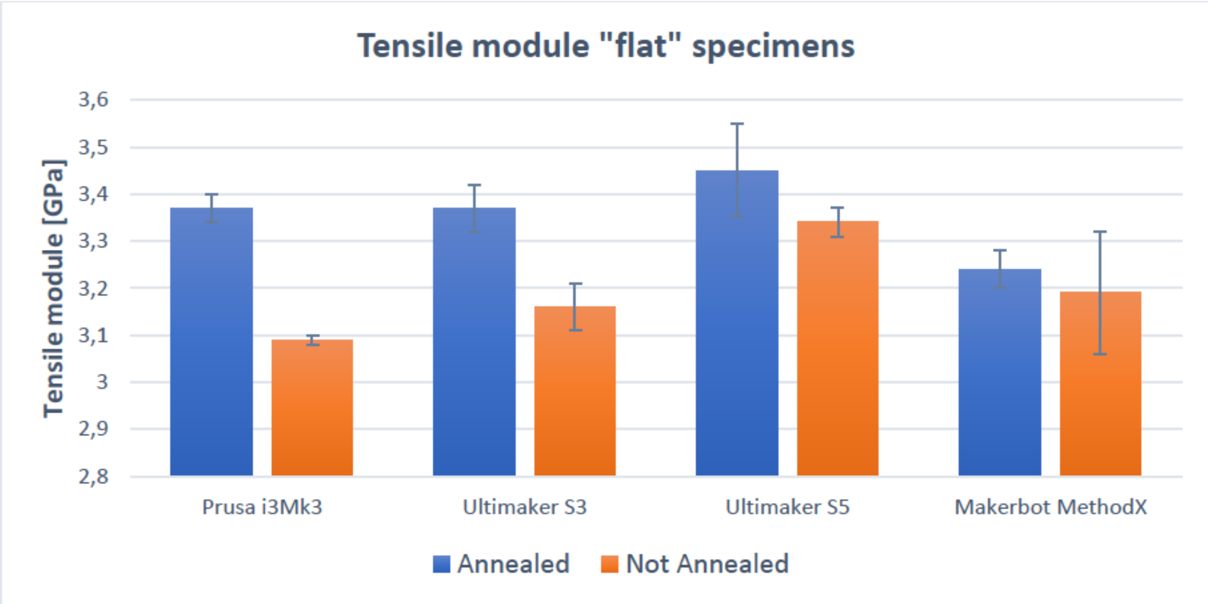

Figure 23: Tensile module for "flat" specimens.

On the Prusa i3Mk3s the tensile modulus increases by 8%. With the Ultimaker S3 it is 6%, with the Ultimaker S5 it is 3% and the difference with the Makerbot is 2%.

This observation is consistent with the assumption that the design of the printer influences the mechanical properties. The order in which the printers are protected from the environment is the same as the order in which the annealing process influences the manufactured parts. The better the build volume is protected, the lower the effect of the annealing process. This is since, in a well-insulated build space, the component can already form crystalline structures during printing. The better the component is shielded, the higher the percentage of crystalline structures. These structures are created by the heat of the printing bed. This thermal energy penetrates the component and thus promotes the formation of crystals. In Makerbot MethodX it is not the printing bed, but the entire environment that provides the thermal energy. Therefore, the effect of annealing is particularly low with this printer. The crystal structure is already almost completely formed. Here it can be seen that the difference between untreated and treated state of the samples decreases with the shielding to environment.

4.4 Impact Strength according to DIN EN ISO 179 1eU

The eU notched bar impact test provides the impact strength as well as the impact energy. The impact strength and the impact energy show qualitatively the same result. Looking at the results of the impact energy in Figure 24 and Figure 25.

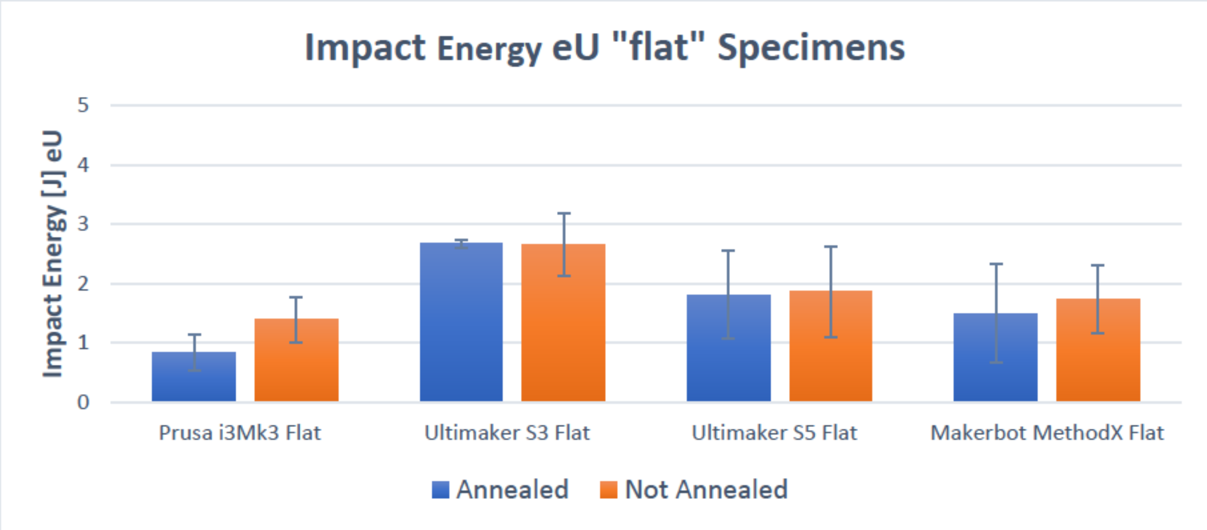

Figure 24: Impact energy for "flat" specimens.

The notched impact energy is shown here for the specimens printed as "flat". Here the Ultimaker S3 shows the best result. Followed by the Ultimaker S5 and the Makerbot MethodX with the Prusa as last. With Prusa, the value after annealing is lower than before treatment. This is not observed with the other machines.

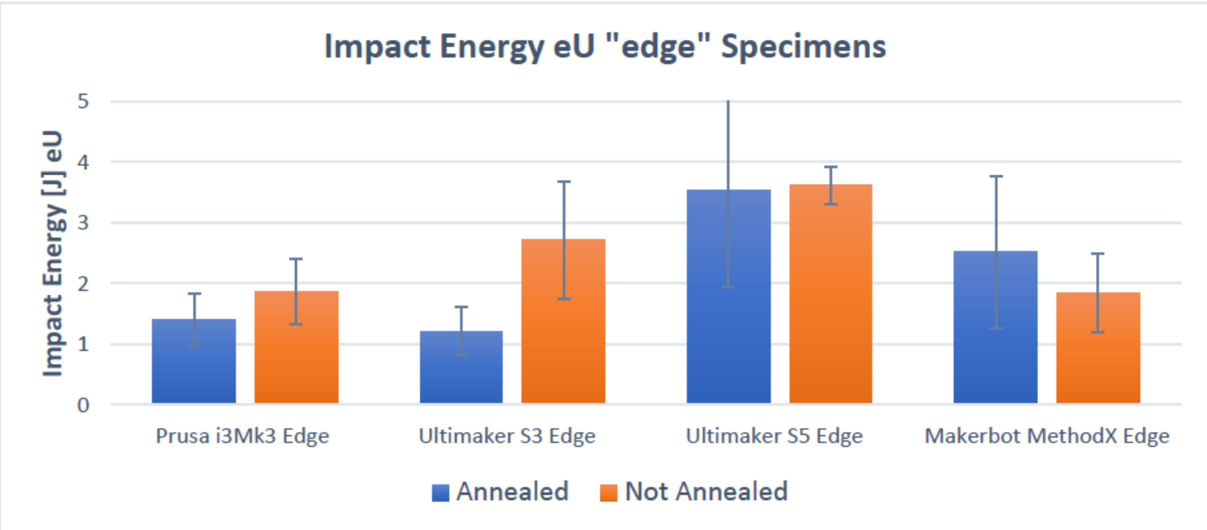

Figure 25: Impact energy for "edge" specimens.

It is noticeable that the specimens of the "edge" orientation show higher values than those in the "flat" orientation. Here the Ultimaker S5 shows the best result.

With the "edge" samples, there are differences between the annealed and untreated samples on the Prusa i3Mk3s and the Ultimaker S3. The Ultimaker S5, on the other hand, shows no visible changes due to the post-treatment. With the Makerbot, on the other hand, an increase in impact energy can be seen.

Looking at the impact strengths of all samples in Figure 26, it can be said that the two Ultimaker machines deliver the peak values.

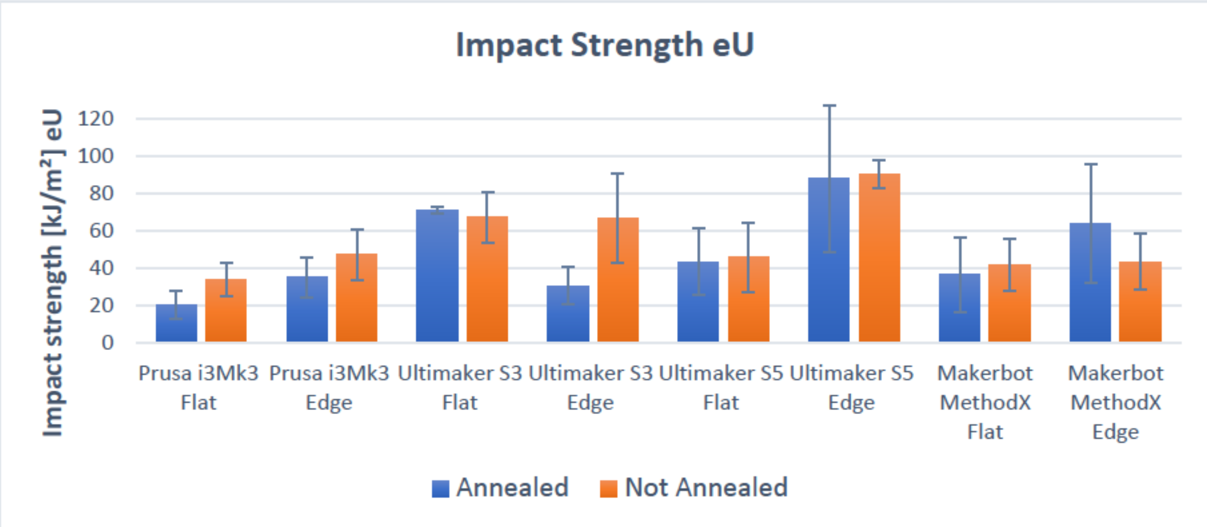

Figure 26: Impact strength eU of specimen.

A statement about whether the Ultimaker S3 or the Ultimaker S5 delivers higher values cannot be made due to the standard deviation. However, the characteristic values of the Prusa i3Mk3s and the Makerbot are inferior to those of the Ultimaker machines in at least one characteristic value. In addition, the values of the "edge" samples are on average higher than those of the "flat" samples.

The behavior of the test specimens in this test is also in line with the expected differences in printer designs. The influence of annealing is lower for "flat" samples, since in this orientation the area of the sample lying on the printing bed is larger. Furthermore, in this orientation the top layer of the specimen is closer to the bed. These two points ensure that there is more surface area to bring energy from the printing bed into the component. These conditions already promote the formation of crystals in the test specimen during printing. Since the specimens printed as "edge" are higher and the distance from the heated printing bed in the Prusa, Ultimaker S3 and Ultimaker S5 is greater, a smaller proportion of the structure is crystallized. This effect is not visible on the Ultimaker S5 due to the high standard deviation.

The even heat in Makerbot MethodX, however, should show a different pattern. It is to be expected that the results of both orientations in treated and untreated state will not differ. Again, a strong deviation in the annealed sample denies a clear result and an unambiguous statement.

4.5 Flexural Strength according to DIN EN ISO 75-2

The last mechanical property to be investigated remains the flexural stiffness. The values for the bending strength are visualized in Figure 27.

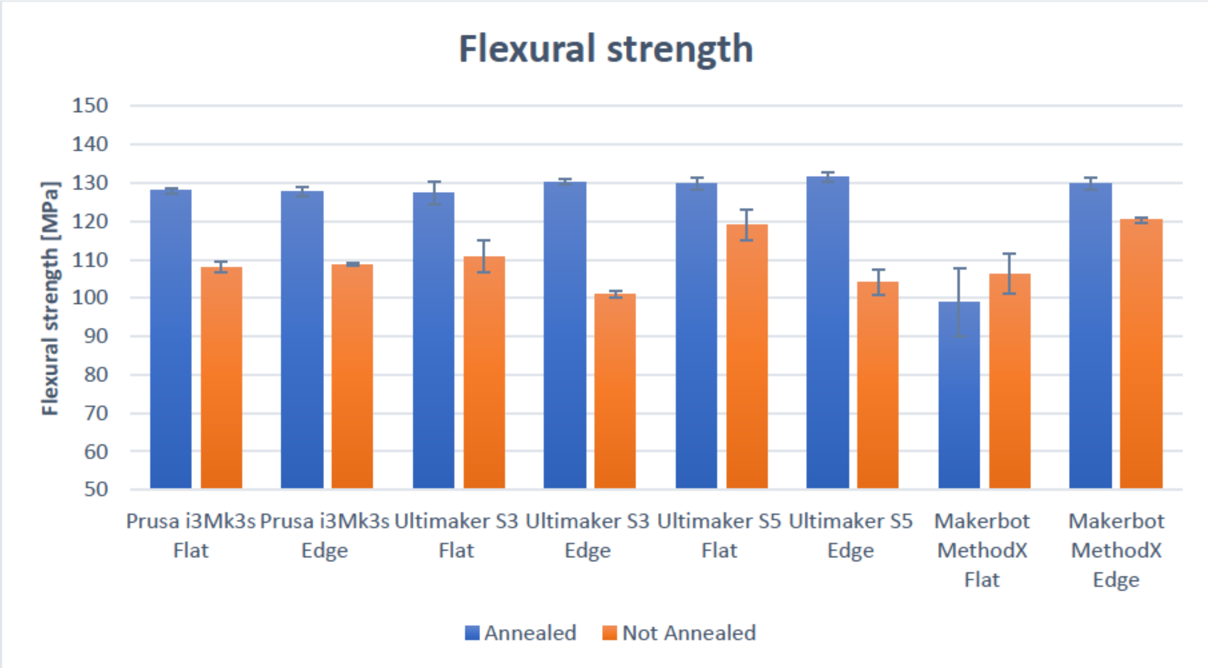

Figure 27: Flexural strength of specimen.

For the Prusa i3Mk3s there is no difference between the two print orientations. For the Ultimaker printers, both show a higher flexural strength in the "flat" orientation for unannealed specimen. The Makerbot shows a similar result to the Ultimaker S5. Except for the samples that were printed as "flat". Here, even higher values are shown for the specimens that were not post-treated. This result is difficult to interpret because of the differences to the other results. The values for the tempered samples do not follow the scheme. Here more detailed investigations could be made to check this error. All other printers show the same bending stiffness in both orientations after tempering.

The elongation of the test specimen behaves like the flexural strength. The elongations of all the tested machines at the highest force can be seen in Figure 28.

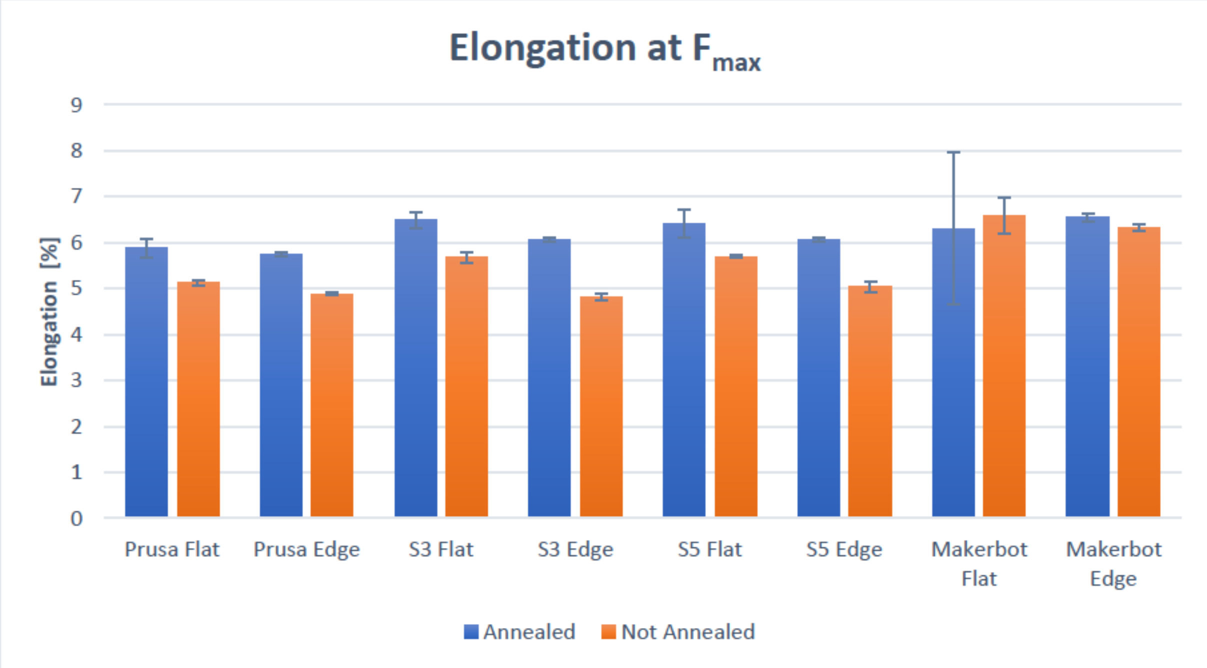

Figure 28: Flexural elongation at F_{max}.

As seen after annealing in the oven, the elongation is increased for all printers except for the samples from the Makerbot. In the Ultimaker S5, differences between the tempered and untreated samples are also smaller.

The results for the elongation support the theory, that the design of the printer has an impact on the properties of a 3D printed part. In the Makerbot with an evenly heated environment, there is no difference between treated and untreated specimens. This again seems to show that the crystalline structures were already formed before the treatment.

For the flexural strength this means that it depends largely on the material of the specimens. After heat treatment the processing quality does not influence the flexural properties anymore. The outer layers contribute a large part to the stability of the component. Possible pores or other defects in the infill or inside the specimen are therefore less important for the flexural strength.

4.6 HDT according to DIN EN ISO 178

In this test the specimens were examined with the HDT Test. The results of the test are shown in Figure 29.

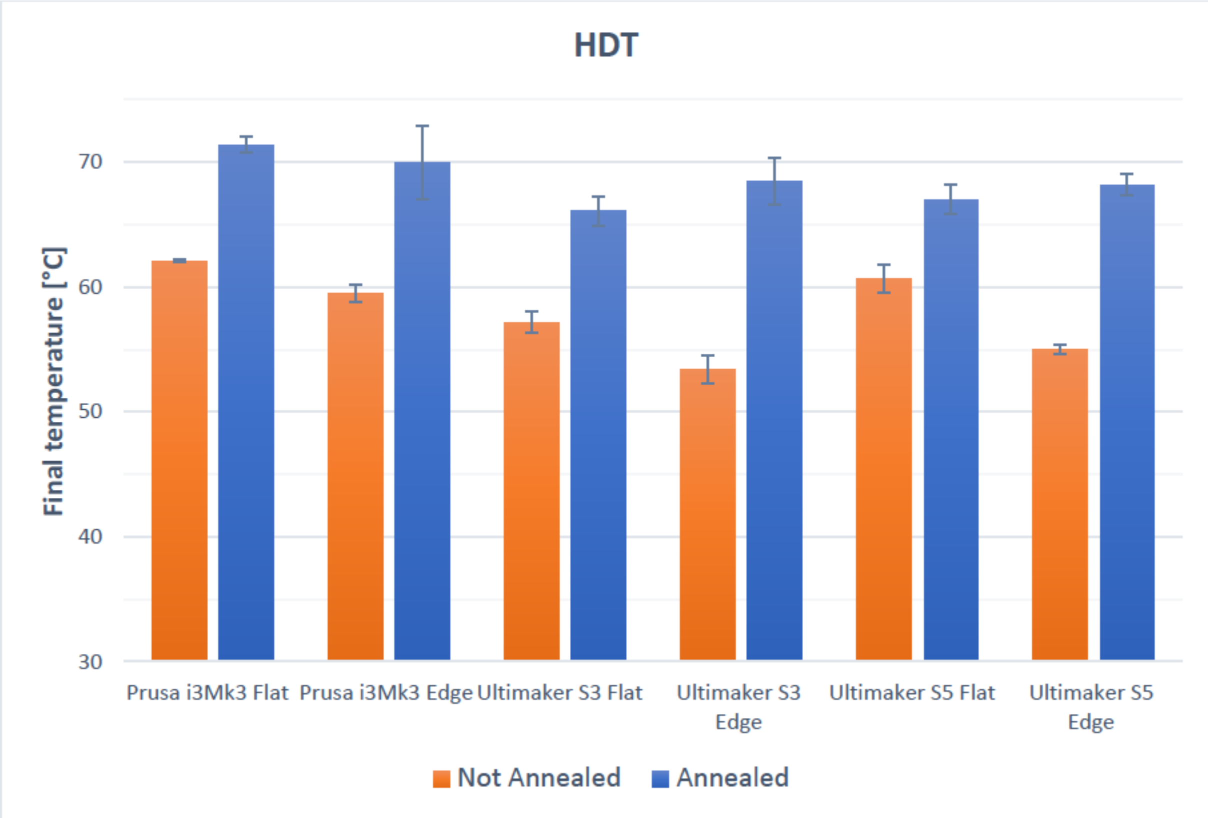

Figure 29: HDT final temperature.

The untreated test specimens directly from the printer vary slightly from one another. These values are between the minimum of 54°C and a maximum of 62°C. However, it can be noted that the "flat" test specimens are slightly superior to those in "edge" orientation. After post-treatment, however, all these differences are balanced out so that they no longer or only slightly differ.

The HDT test cannot be performed with the Makerbot test specimen. These specimens show a strong warping already after printing. Warping in this case means that specimens show a considerable deflection already after they have been detached from the printing platform (Figure 30).

Figure 30: Bend charpy printed on Makerbot MethodX.

The smaller differences in the samples printed as "flat" are again shown by the result, which could already be observed in the impact strength test. Due to this alignment of the test specimens, the amorphous part of the microstructure is lower.

Looking at the values of the HDT test, it becomes clear that the HDT temperature is not a machine characteristic, but rather a material characteristic. Possible errors in the structure of the test specimen, which are very important in mechanical testing, are not visible in the HDT.

4.7 DSC According to DIN EN ISO 11357-1

With the help of DSC analysis, the percentage of crystalline structure can be determined by the amount of heat energy released by the material, or its enthalpy. Therefore, a part of the sample cubes from the pre-test was annealed. These tempered cube samples were then examined together with the untreated cubes. A graph of this DSC analysis can be seen in Figure 31.

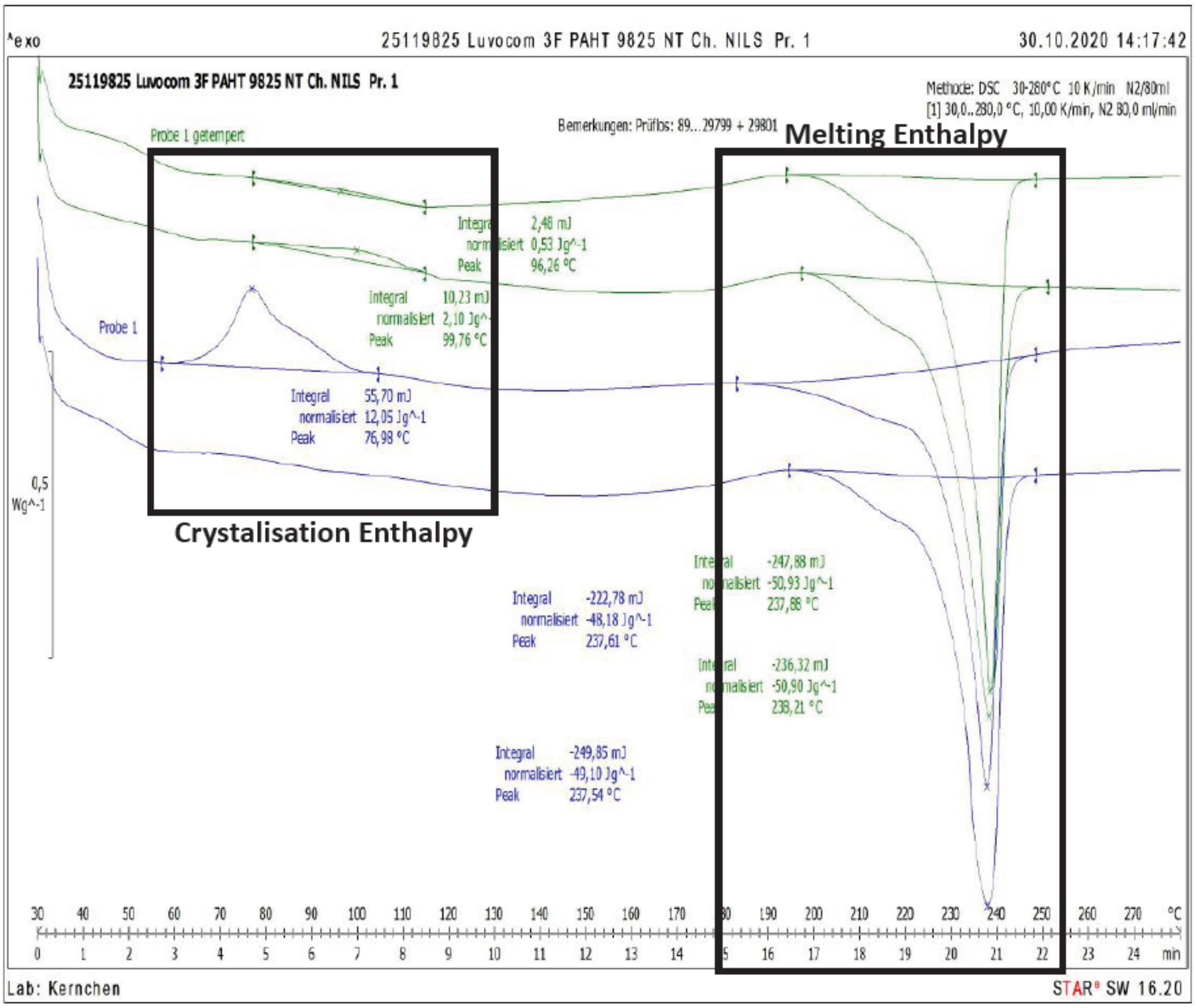

Figure 31: DSC of specimen printed with Prusa i3Mk3s

The enthalpy released over the temperature can be seen here. The green line shows the annealed samples, and the blue line marks the measurement writing of the untreated samples. There is an enthalpy absorption at the same temperature as the glass transition temperature. Here marked as crystallization enthalpy. Another extremum can be seen around the melting point. Here marked with the melting enthalpy.

The crystallization enthalpy occurs in the untreated sample because the material is annealed during the test. This crystallization occurring during the measurement must be corrected later from the result. The melting enthalpy is any enthalpy that is decisive for the percentage of crystalline components in the microstructure.

Comparing the differences between these two extremes with the literature value for a one hundred percent crystalline structure, the crystalline portion of the material can be determined These values are shown in Figure 32 for all tested machines.

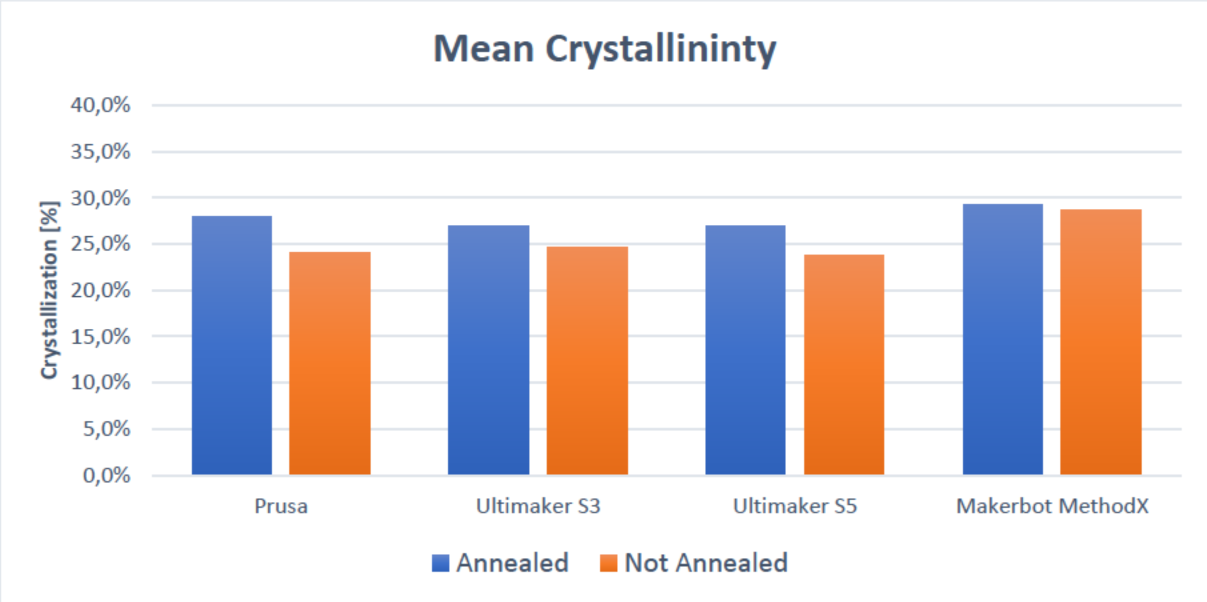

Figure 32: Mean Crystallinity.

To examine the differences in crystal growth more closely, Figure 33 shows the growth of crystals by tempering.

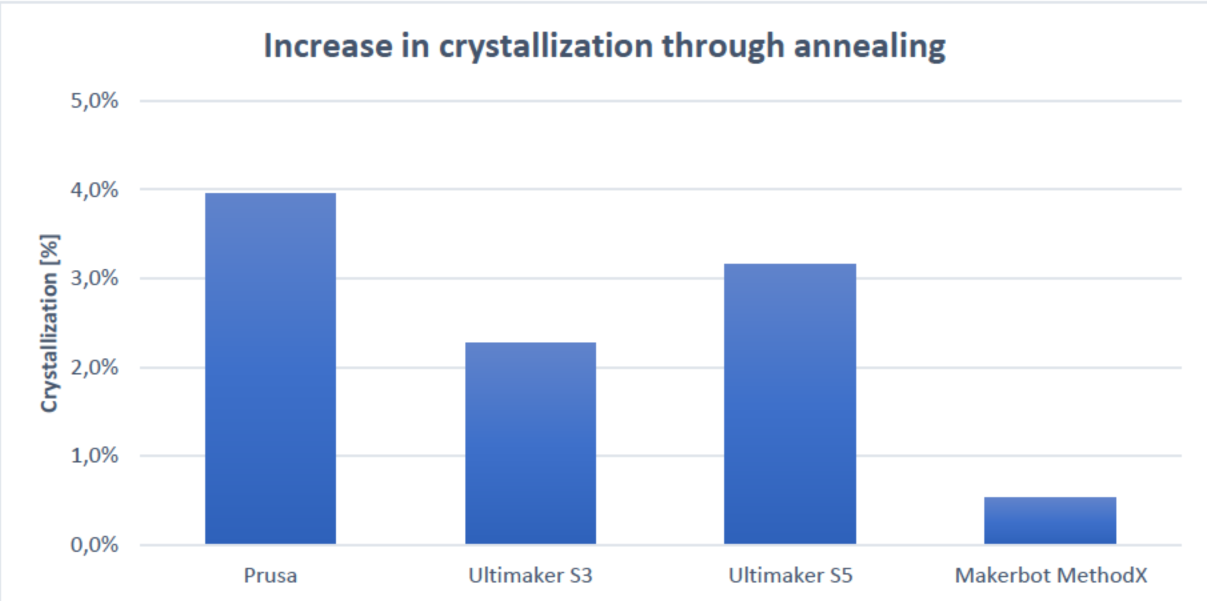

Figure 33: Increase in crystallization through annealing.

The crystal content of 30% is a value that corresponds to a typical value of the crystallinity of a polyamide compound. The growth by subsequent annealing confirms the assumptions already made during the thermal and mechanical tests. The effect of annealing has a greater effect on printers that have good shielding. The Makerbot, which prints in a annealing atmosphere, benefits only marginally from this form of post-treatment.

5 Conclusion

The aim of this thesis was to investigate whether the way an FFF 3D printer is built has an impact on the mechanical and thermal properties of the parts it produces.

The findings summarized in the results section all present a coherent picture. The mechanical properties of a polymer are directly related to the proportion of crystals in its structure. These provide for better mechanical and thermal properties. However, these findings are nothing new. Previous work by Javaid Butt and Raghunath Bhaskar, has already shown that the properties of a semi-crystalline material such as LUVOCOM® PA^{HT} 9825 NT are related to crystal formation [15].

The LUVOCOM® PA^{HT} 9825 NT is a polyamide optimized for 3D printing. Optimized for 3D printing means that the handling of the material has been improved. This is reflected in the optimization of a very slow crystallization process. This slow crystallization is advantageous to avoid stressing the part during printing in an unprotected environment.

Crystallization is therefore often not desired during the processing of polyamides. The results of this study have shown what the formation of these crystals during the printing process means for the mechanical properties of the component. The results of these tests show that the shielding of the part from the environment has a great influence on the properties. It can therefore be said that the crystallinity is proportional to the attempt to conserve the thermal energy. A well-insulated 3D printer has more energy available due to the heat emitted by the printing bed and the HotEnd. It is precisely this energy that can be used during printing to anneal the component. However, it is also apparent that this heat, which is not used during printing, can still be brought into the component subsequently. The same properties can be achieved by subsequent annealing.

The results also indicate that a universal G-code does not promise the same properties. This can be clearly seen with the Prusa printer and the two Ultimaker machines. The Ultimaker S3 and the Ultimaker S5 show very little difference in most tests. The difference between these two machines is primarily evident in the performance before annealing, as the S5 has better shielding. Compared to the Prusa, the two machines show better peak results in almost every mechanical test. The reason for this cannot be formulated with certainty in the context of this study. However, it offers a starting point for further investigations. The Prusa machine was supposed to be capable of the same performance. Rather, it is an indication that each machine requires adapted and customized settings. This also applies to the Makerbot. This printer can produce components with a high degree of crystallinity even during printing. This can be seen not only from the fact that the post-treated components only showed slight differences. The deformation after detachment from the printing bed also shows that the crystals have generated high stresses in the component. The mean values of the tested properties were lower in all tests than with the other machines. This suggests that the sliced G-code was not adapted to the machine and the material used.

In this thesis only the produced properties were investigated from a thermal and mechanical point of view. Other properties such as the effect on the scattering of the results or dimensional accuracy were neglected in the investigations. No statement is made as to the extent to which these other key figures of quality management are influenced by the machines.

Material and machine are in symbiosis in the FFF production. They condition each other to create optimal parts. It is therefore, as happened here, not possible to see a printer as a black box with identical input. At least not if a comparable output is expected.

These results and the associated effort of the manufacturer to create an optimal printing environment are described in the paper with all their advantages and disadvantages. However, what this means for the user has not yet been clearly defined in the results. From the perspective of a production infrastructure, it is extremely important to match the material to the printer being used. This applies if the best possible properties are to be achieved with the material in combination with the respective printer.

It should also be noted that there are significant price differences between the desktop 3D printers tested here. A Prusa i3Mk3s is available for under 1000€, while the Ultimaker S5 and Makerbot MethodX have a price tag of about 5000€. With the Ultimaker S3 somewhere between the machines. In terms of mechanical and thermal properties, as can be seen, this difference is compensated by material handling, adjustments, and post-processing. It is not said that the higher price cannot be justified in other aspects. However, this does not necessarily affect the theoretically achievable properties of the components from the printers.

All in all, the design, and the efforts of the machine manufacturers to better protect the machines from the environment make a difference. However, this difference is not a missed opportunity and can be made up after printing.

6 References

[1] *Terminology for Additive Manufacturing - General Principles - Terminology*.

[2] D. G. Schniederjans, "Adoption of 3D-printing technologies in manufacturing: A survey analysis," *International Journal of Production Economics*, vol. 183, pp. 287–298, 2017, doi: 10.1016/j.ijpe.2016.11.008.

[3] J. Zhang and Y.-G. Jung, Eds., *Additive manufacturing: Materials, processes, quantifications and applications*. Kidlington, Oxford, Cambridge, MA: Butterworth-Heinemann is an imprint of Elsevier, 2018.

[4] L. J. Kumar, P. M. Pandey, and D. I. Wimpenny, Eds., *3D Printing and Additive Manufacturing Technologies*. Singapore: Springer Singapore, 2019.

[5] L. Jyothish Kumar, P. M. Pandey, and D. I. Wimpenny, Eds., *3D printing and additive manufacturing technologies*. Singapore: Springer Nature, 2019.

[6] S. Brischetto, P. Maggiore, and C. G. Ferro, Eds., *Additive manufacturing technologies and applications*. Basel, Beijing, Wuhan, Barcelona, Belgrade: MDPI, 2017.

[7] E. Celik, *Additive Manufacturing: Science and Technology,* 1st ed. Boston: Walter de Gruyter, 2020.

[8] D. M. Devine, Ed., *Polymer-Based Additive Manufacturing: Biomedical Applications,* 1st ed. Cham: Springer, 2019.

[9] L. E. Murr, *Handbook of Materials Structures, Properties, Processing and Performance*. Cham: Springer, 2019.

[10] C. Hopmann and R. Dahlmann, Eds., *Advances in Polymer Processing 2020: Proceedings of the International Symposium on Plastics Technology,* 1st ed. Berlin, Heidelberg: Springer Berlin Heidelberg; Imprint: Springer Vieweg, 2020.

[11] M. Samykano, S. K. Selvamani, K. Kadirgama, W. K. Ngui, G. Kanagaraj, and K. Sudhakar, *Mechanical property of FDM printed ABS: influence of printing parameters*.

[12] T. Wohlers, R. I. Campbell, O. Diegel, R. Huff, and J. Kowen, *Wohlers report 2020: 3D printing and additive manufacturing state of the industry*. Fort Collins, Colo.: Wohlers Associates, 2020.

[13] J. Zhang, X. Feng, H. Patil, R. V. Tiwari, and M. A. Repka, "Coupling 3D printing with hot-melt extrusion to produce controlled-release tablets," *International journal of pharmaceutics*, vol. 519, 1-2, pp. 186–197, 2017, doi: 10.1016/j.ijpharm.2016.12.049.

[14] B. M. Schmitt, C. F. Zirbes, C. Bonin, D. Lohmann, D. C. Lencina, and A. d. C. S. Netto, "A Comparative Study of Cartesian and Delta 3D Printers on Producing PLA Parts," *Mat. Res.*, vol. 20, suppl 2, pp. 883–886, 2017, doi: 10.1590/1980-5373-mr-2016-1039.

[15] Javaid Butt and Raghunath Bhaskar, "Investigating the Effects of Annealing on the Mechanical Properties of FFF-Printed Thermoplastics," *Journal of Manufacturing and Materials Processing*, vol. 4, 38, p 38, 2020, doi: 10.3390/jmmp4020038.

[16] Prusa Research, *Original Prusa i3 MK3S Bausatz.* [Online]. Available: https://shop.prusa3d.com/de/3d-drucker/180-original-prusa-i3-mk3s-bausatz.html (accessed: Nov. 15 2020).

[17] igo3D, *Ultimaker S3 3D-Drucker.* [Online]. Available: https://www.igo3d.com/ultimaker-s3-3d-drucker (accessed: Nov. 15 2020).

[18] igo3D, *Ultimaker S5 Pro Bundle.* [Online]. Available: https://www.igo3d.com/ultimaker-s5-pro-bundle (accessed: Nov. 15 2020).

[19] MakerBot, *MakerBot Method - Professional 3D Printer - Rapid Prototyping 3D Printing.* [Online]. Available: https://www.makerbot.com/de/3d-printers/method/ (accessed: Nov. 15 2020).

[20] A. Fradet *et al.,* “Nomenclature and terminology for dendrimers with regular dendrons and for hyperbranched polymers (IUPAC Recommendations 2017),” *Pure and Applied Chemistry*, vol. 91, no. 3, pp. 523–561, 2019, doi: 10.1515/pac-2016-1217.

[21] O. Horn, “Kunststoff-handbuch. Band VI: Polyamide. Aufbau, Verarbeitung, Eigenschaften und Anwendung. Herausgeg. vonR. Vieweg undA. Müller. Carl Hanser-Verlag, München 1966. 1. Aufl., XVI, 698 S., 477 Abb., 111 Tab., Ln. DM 140.–Bei Vorbest. DM 126,– bei Subskr. d. Gesamtwerks DM 112,–,” *Angew. Chem.*, vol. 79, no. 22, p. 1027, 1967, doi: 10.1002/ange.196707922128.

[22] G. Abts, *Kunststoff-Wissen für Einsteiger,* 2nd ed. München: Hanser, 2014. [Online]. Available: http://www.hanser-elibrary.com/action/showBook?doi= 10.3139/9783446439290

[23] U. Bruder, *Kunststofftechnik leicht gemacht*. München: Hanser, 2016. [Online]. Available: http://www.hanser-fachbuch.de/9783446449572

[24] U. Bruder, *User's guide to plastic,* 2nd ed., 2019.

[25] L. G. Blok, M. L. Longana, H. Yu, and B.K.S. Woods, “An investigation into 3D printing of fibre reinforced thermoplastic composites,” *Additive Manufacturing*, vol. 22, pp. 176–186, 2018, doi: 10.1016/j.addma.2018.04.039.

[26] R. M. Dunn, K. R. Hart, and E. D. Wetzel, *Improving fracture strength of fused filament fabrication parts via thermal annealing in a printed support shell*.

[27] T. Tabi, I. E. Sajo, F. Szabo, A. S. Luyt, and J. G. Kovacs, “Crystalline structure of annealed polylactic acid and its relation to processing,” *Express Polym. Lett.*, vol. 4, no. 10, pp. 659–668, 2010, doi: 10.3144/expresspolymlett.2010.80.

7 Appendix

Technical Datasheet of LUVOCOM® PA^{HT} 9825 NT

LUVOCOM® 3F PAHT 9825 NT

LUVOCOM® 3F
Additive manufacturing solutions

High-temperature polyamide
unreinforced, natural color

Physical properties		Test method	Specimen	Units	Typical value
Specific gravity		ISO 1183-3		g/cm³	1,20
Water absorption	23°C / 24h	ISO 62	MPTS ISO 3167 A	%	<0,3
Melt flow rates (MFR)	250°C / 2,16kg	ISO 1133	pellet	g/10 min	3,6
Melt volume rate (MVR)	250°C / 2,16kg	ISO 1133	pellet	cm³/10 min	3,47
Linear mould shrinkage		DIN 16742	MPTS ISO 3167 A	%	0,3-0,5
Mechanical properties at 23°C / 50% rh					
Tensile strength	dry, @50 mm/min	ISO 527	MPTS ISO 3167 A	MPa	85
Elongation at maximum force	dry, @50 mm/min	ISO 527	MPTS ISO 3167 A	%	3,6
Modulus of elasticity	dry, @1 mm/min	ISO 527	MPTS ISO 3167 A	GPa	3,4
Charpy impact strength	dry	ISO 179 1eU	80x10x4mm	kJ/m²	NB
Thermal properties					
Heat distortion temperature	HDT A	ISO 75	molded sample	°C	90
Continuous service temperature	20.000 h	IEC 60216	MPTS ISO 3167 A	°C	120
Service temperature	during lifetime max. 200h		MPTS ISO 3167 A	°C	160
Coefficient of thermal expansion		ISO 11359	10x8x4 mm	10^{-4}/K	0,5
Thermal conductivity in plane	hot disk	ISO 22007	‖ 60x60x3 mm	W/mK	0,3
Electrical properties					
Insulation resistance strip electrode	R25	DIN IEC 60167	MPTS ISO 3167 A	Ω	$>10^{12}$
Surface resistance	ROB	DIN IEC 60093	Ronde 60x4mm	Ω	$>10^{12}$

Main features

Low influence from moisture and temperature on dimensional stability and electrical properties, compared with PA66

LEHVOSS Group

2020091917272

LUVOCOM® 3F PAHT 9825 NT

LUVOCOM® 3F
Additive manufacturing solutions

High-temperature polyamide unreinforced, natural color

Recommended processing parameters

General		
3D Printing parameters may vary from machine to machine. The following settings may be used as an indication: nozzle temperature: 265 - 290 °C / nozzle material: abrasion resistant / print bed temperature: > 50 °C / layer thickness: > 0,2mm / printing speed 40 - 60 mm/s. The processing notes provided merely represent a recommendation for general use. Due to the large variety of machines, geometries and volumes of parts, etc., it may be necessary to employ different settings according to the specific application. Please contact us for further information.		
Predrying		
It is advisable to predry the granulate with a suitable dryer immediately before processing. The granulate may absorb moisture from the environment.		
Dryer type	Temperature °C	Drying time in h
Dehumidifying dryer	130	6 - 8
Vacuum Dryer	120	4 - 6
Processing		
Zone 1	°C	260 - 300
Zone 2	°C	260 - 300
Zone 3	°C	260 - 300
Nozzle	°C	250 - 290
Melt temperature	°C	280
In general LUVOCOM® 3F can be processed on conventional extrusion machines while observing the usual technical guidelines. Any added fibrous materials or fillers may have an abrasive effect. In this case the cylinder, screw and die should be protected against wear as is usual in the processing of reinforced thermoplastic materials. Lengthy dwell times for the melts in the cylinder should be avoided. Lower the temperatures during interruptions!		
Delivery form & storage		
Unless indicated otherwise, the material is delivered as 3mm long pellets in sealed bags on pallets. Preferably storage should be effected in dry and normally temperatured rooms.		
Additional information		
Filaments produced from this material may be wound into standard size spools.		

09825 01 06 18

Europe and Head Office
Lehmann&Voss&Co. KG
Alsterufer 19
20354 Hamburg
Germany
Tel +49 40 44 197-0
Email: luvocom@lehvoss.de

North America
LEHVOSS North America, LLC
185 South Broad Street
Pawcatuck, CT 06379
USA
Tel +1-855-681-3226
Email: info@lehvoss.us

Asia
LEHVOSS (Shanghai) Chemical Trading Co., Ltd.
Unit 4805, 8 Xingyi Road
Changning District, Shanghai 200336
China
Tel +86 21 62785181
Email: info@lehvoss.cn

LEHVOSS Group

2020091917272

Tensile Test according to DIN EN ISO 527

Lehmann&Voss&Co. LUV

15.10.20

Prüfprotokoll

Prüflosnummer : 890000029655
Material : LUVOCOM® 3F PAHT® 9825 NT à 20 kg
Materialnummer : 25119825-00
Prozessauftrag : 890000029655
Charge : NILS
Prüfer : MsS
Prüfnorm : DIN EN ISO 527
Bemerkung : Job 14.10.20 1x25 W R972
Geschwindigkeit Zugmodul : 1 mm/min
Prüfgeschwindigkeit : 50 mm/min

Prüfergebnisse:

Nr	Zugfestigkeit MPa	Dehnung bei Fmax %	Zugmodul E_t GPa	Bruchspannung MPa	Bruchdehnung %	h mm	b mm
max	1000,00	10,00	10,00				
min	1,00	0,10	0,00				
1	64,57	2,08	3,36	64,44	2,08	3,949	9,894
2	65,92	2,12	3,38	65,91	2,13		
3	66,31	2,13	3,40	66,31	2,13		
4	74,97	2,51	3,33	74,97	2,51		
5	59,88	1,87	3,40	59,88	1,87		

Seriengrafik:

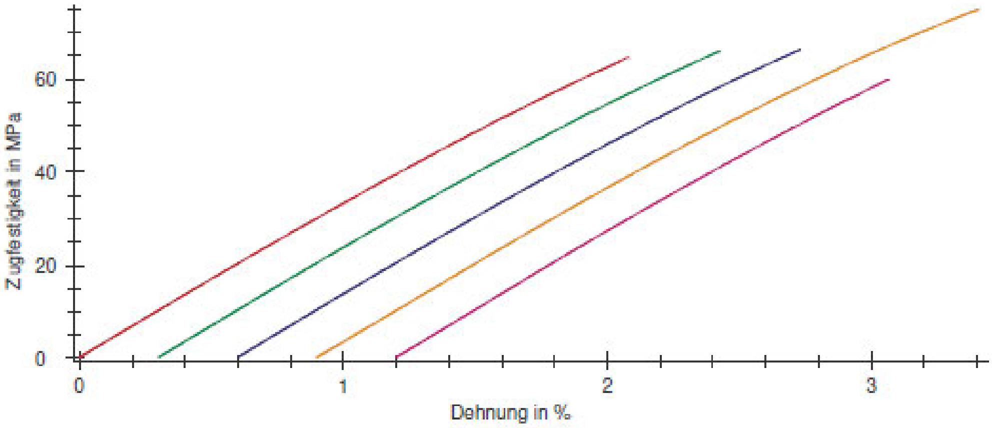

Statistik:

Serie n = 5	Zugfestigkeit MPa	Dehnung bei Fmax %	Zugmodul E_t GPa	Bruchspannung MPa	Bruchdehnung %
x̄	66,33	2,14	3,37	66,30	2,14
s	5,47	0,23	0,03	5,48	0,23
ν [%]	8,24	10,84	0,82	8,26	10,81

Lehmann&Voss&Co.

16.10.20

Prüfprotokoll

Prüflosnummer	:	890000029656
Material	:	LUVOCOM® 3F PAHT® 9825 NT à 20 kg
Materialnummer	:	25119825-00
Prozessauftrag	:	890000029656
Charge	:	NILS
Prüfer	:	MsS
Prüfnorm	:	DIN EN ISO 527
Bemerkung	:	Job 14.10.20 1x25 W R972
Geschwindigkeit Zugmodul	:	1 mm/min
Prüfgeschwindigkeit	:	50 mm/min

Prüfergebnisse:

Nr	Zugfestigkeit MPa	Dehnung bei Fmax %	Zugmodul E_t GPa	Bruchspannung MPa	Bruchdehnung %	h mm	b mm
max	1000,00	10,00	10,00				
min	1,00	0,10	0,00				
1	66,46	2,44	3,11	65,18	2,44	3,925	10,07
2	70,10	2,70	3,07	70,10	2,70		
3	70,35	2,70	3,09	70,35	2,70		
4	69,52	2,62	3,09	67,81	2,63		
5	69,96	2,65	3,10	67,36	2,66		

Seriengrafik:

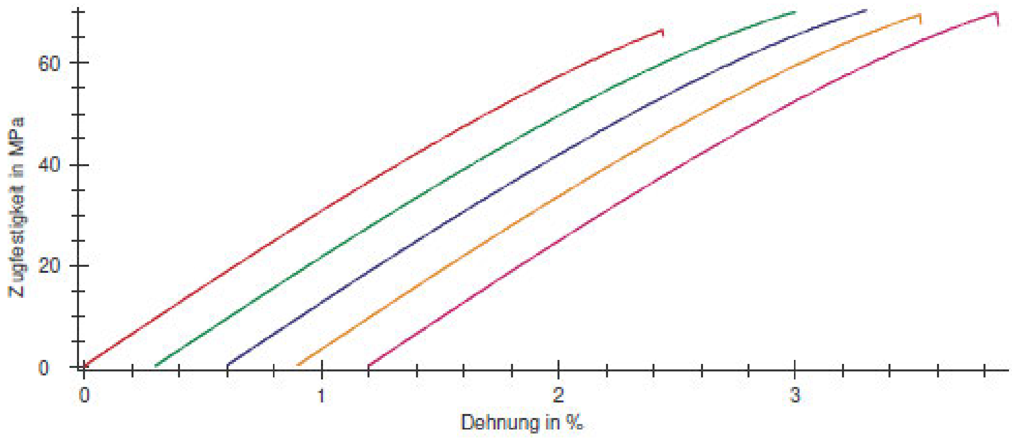

Statistik:

Serie n = 5	Zugfestigkeit MPa	Dehnung bei Fmax %	Zugmodul E_t GPa	Bruchspannung MPa	Bruchdehnung %
x	69,28	2,62	3,09	68,16	2,63
s	1,60	0,11	0,01	2,13	0,11
ν [%]	2,31	4,12	0,45	3,13	4,04

Lehmann&Voss&Co.

15.10.20

Prüfprotokoll

Prüflosnummer	:	890000029657
Material	:	LUVOCOM® 3F PAHT® 9825 NT à 20 kg
Materialnummer	:	25119825-00
Prozessauftrag	:	890000029657
Charge	:	NILS
Prüfer	:	MsS
Prüfnorm	:	DIN EN ISO 527
Bemerkung	:	Job 14.10.20 1x25 W R972
Geschwindigkeit Zugmodul	:	1 mm/min
Prüfgeschwindigkeit	:	50 mm/min

Prüfergebnisse:

Nr	Zugfestigkeit MPa	Dehnung bei Fmax %	Zugmodul E_t GPa	Bruchspannung MPa	Bruchdehnung %	h mm	b mm
max	1000,00	10,00	10,00				
min	1,00	0,10	0,00				
1	62,93	1,97	3,47	60,19	1,97	3,935	10,07
2	65,98	2,16	3,37	64,83	2,17		
3	65,93	2,18	3,30	65,93	2,18		
4	70,91	2,26	3,51	68,45	2,27		
5	49,82	1,53	3,40	48,99	1,53		

Seriengrafik:

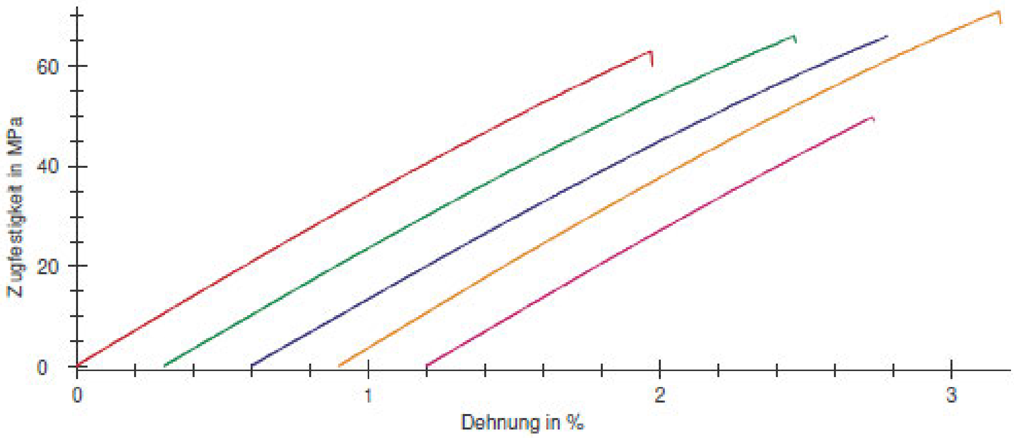

Statistik:

Serie n = 5	Zugfestigkeit MPa	Dehnung bei Fmax %	Zugmodul E_t GPa	Bruchspannung MPa	Bruchdehnung %
$\bar{x}$	63,11	2,02	3,41	61,68	2,02
s	7,96	0,29	0,08	7,70	0,29
ν [%]	12,62	14,60	2,45	12,48	14,56

Lehmann&Voss&Co. 16.10.20

Prüfprotokoll

Prüflosnummer	:	890000029658
Material	:	LUVOCOM® 3F PAHT® 9825 NT à 20 kg
Materialnummer	:	25119825-00
Prozessauftrag	:	890000029658
Charge	:	NILS
Prüfer	:	MsS
Prüfnorm	:	DIN EN ISO 527
Bemerkung	:	Job 14.10.20 1x25 W R972
Geschwindigkeit Zugmodul	:	1 mm/min
Prüfgeschwindigkeit	:	50 mm/min

Prüfergebnisse:

Nr	Zugfestigkeit MPa	Dehnung bei Fmax %	Zugmodul E_t GPa	Bruchspannung MPa	Bruchdehnung %	h mm	b mm
max	1000,00	10,00	10,00				
min	1,00	0,10	0,00				
1	50,76	1,80	2,98	50,39	1,81	3,915	10,21
2	69,40	3,17	2,94	53,68	5,28		
3	68,95	3,18	2,94	55,97	5,15		
4	69,48	3,14	2,97	62,49	4,14		
5	71,16	3,11	3,00	53,14	3,46		

Seriengrafik:

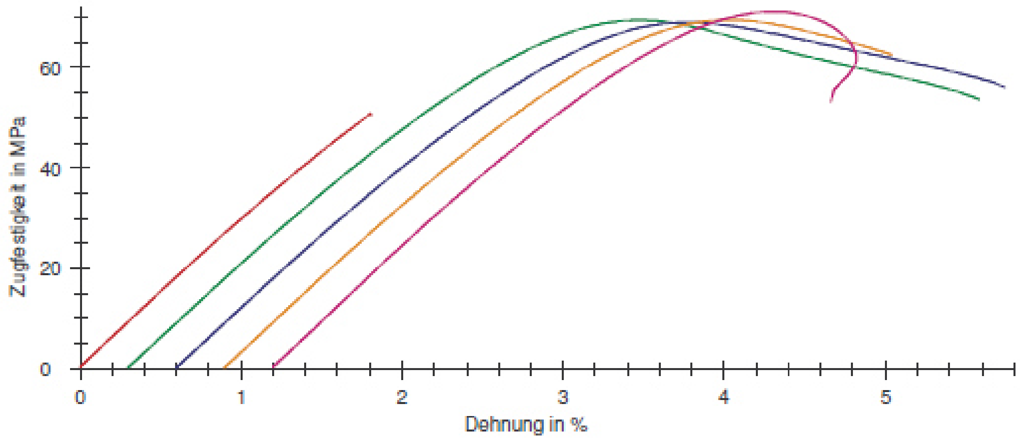

Statistik:

Serie n = 5	Zugfestigkeit MPa	Dehnung bei Fmax %	Zugmodul E_t GPa	Bruchspannung MPa	Bruchdehnung %
x	65,95	2,88	2,96	55,13	3,97
s	8,53	0,60	0,03	4,57	1,42
ν [%]	12,94	20,91	0,88	8,28	35,79

Lehmann&Voss&Co.

02.11.20

Prüfprotokoll

Prüflosnummer	:	890000029873
Material	:	LUVOCOM® 3F PAHT® 9825 NT à 20 kg
Materialnummer	:	25119825-00
Prozessauftrag	:	890000029873
Charge	:	NILS
Prüfer	:	gw
Prüfnorm	:	DIN EN ISO 527
Bemerkung	:	
Geschwindigkeit Zugmodul	:	1 mm/min
Prüfgeschwindigkeit	:	50 mm/min

Prüfergebnisse:

Nr	Zugfestigkeit MPa	Dehnung bei Fmax %	Zugmodul E_t GPa	Bruchspannung MPa	Bruchdehnung %	h mm	b mm
max	1000,00	10,00	10,00				
min	1,00	0,10	0,00				
1	79,62	2,97	3,35	77,45	2,97	3,652	9,985
2	85,58	3,30	3,43	85,58	3,30		
3	70,56	2,44	3,38	70,56	2,44		
4	82,84	3,09	3,39	80,34	3,10		
5	76,85	2,81	3,31	74,87	2,81		

Seriengrafik:

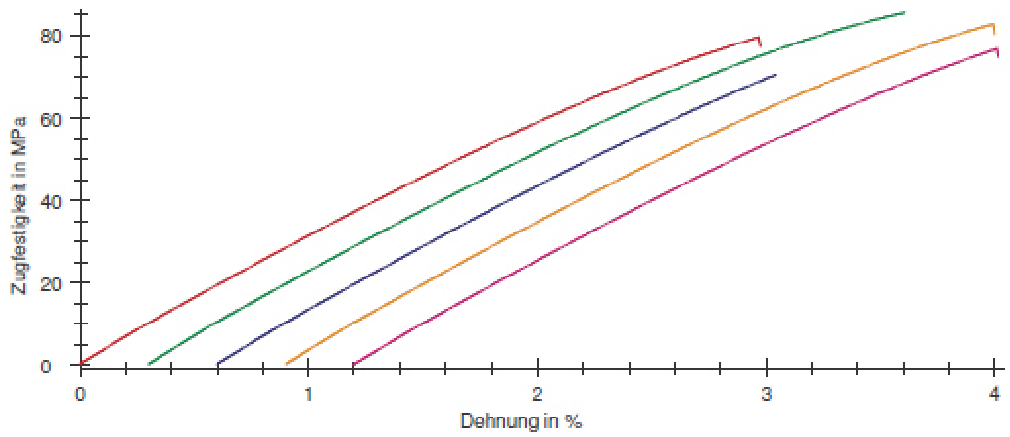

Statistik:

Serie n = 5	Zugfestigkeit MPa	Dehnung bei Fmax %	Zugmodul E_t GPa	Bruchspannung MPa	Bruchdehnung %
$\bar{x}$	79,09	2,92	3,37	77,76	2,93
s	5,79	0,32	0,05	5,66	0,32
ν [%]	7,32	11,08	1,37	7,27	11,09

Lehmann&Voss&Co.

02.11.20

Prüfprotokoll

Prüflosnummer	:	890000029874
Material	:	LUVOCOM® 3F PAHT® 9825 NT à 20 kg
Materialnummer	:	25119825-00
Prozessauftrag	:	890000029874
Charge	:	NILS
Prüfer	:	gw
Prüfnorm	:	DIN EN ISO 527
Bemerkung	:	
Geschwindigkeit Zugmodul	:	1 mm/min
Prüfgeschwindigkeit	:	50 mm/min

Prüfergebnisse:

Nr	Zugfestigkeit MPa	Dehnung bei Fmax %	Zugmodul E_t GPa	Bruchspannung MPa	Bruchdehnung %	h mm	b mm
max	1000,00	10,00	10,00				
min	1,00	0,10	0,00				
1	73,68	2,99	3,11	72,29	2,99	3,886	9,871
2	82,97	3,84	3,23	77,20	4,45		
3	78,93	3,85	3,12	73,41	4,36		
4	71,28	2,77	3,16	71,28	2,77		
5	78,51	3,44	3,16	75,21	3,44		

Seriengrafik:

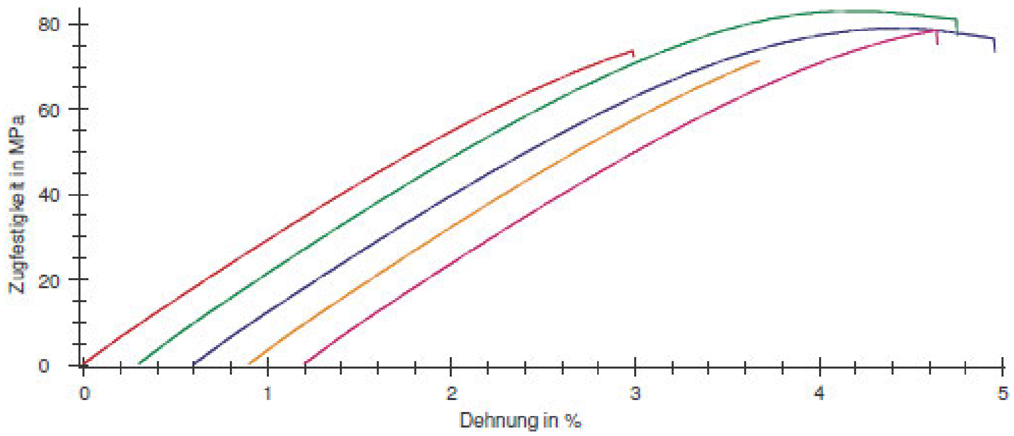

Statistik:

Serie n = 5	Zugfestigkeit MPa	Dehnung bei Fmax %	Zugmodul E_t GPa	Bruchspannung MPa	Bruchdehnung %
$\bar{x}$	77,08	3,38	3,16	73,88	3,60
s	4,62	0,49	0,05	2,36	0,77
ν [%]	6,00	14,52	1,56	3,20	21,39

Lehmann&Voss&Co.

15.10.20

Prüfprotokoll

Prüflosnummer	:	890000029667
Material	:	LUVOCOM® 3F PAHT® 9825 NT à 20 kg
Materialnummer	:	25119825-00
Prozessauftrag	:	890000029667
Charge	:	NILS
Prüfer	:	MsS
Prüfnorm	:	DIN EN ISO 527
Bemerkung	:	Job 14.10.20 1x25 W R972
Geschwindigkeit Zugmodul	:	1 mm/min
Prüfgeschwindigkeit	:	50 mm/min

Prüfergebnisse:

Nr	Zugfestigkeit MPa	Dehnung bei Fmax %	Zugmodul E_t GPa	Bruchspannung MPa	Bruchdehnung %	h mm	b mm
max	1000,00	10,00	10,00				
min	1,00	0,10	0,00				
1	62,00	2,02	3,27	62,00	2,02	3,992	10,08
2	55,38	1,78	3,26	53,44	1,79		
υ 3	~~40,32~~	~~1,24~~	~~3,28~~	~~38,73~~	~~1,25~~		
4	59,32	1,93	3,26	59,32	1,93		
5	63,28	2,03	3,39	61,53	2,03		

Seriengrafik:

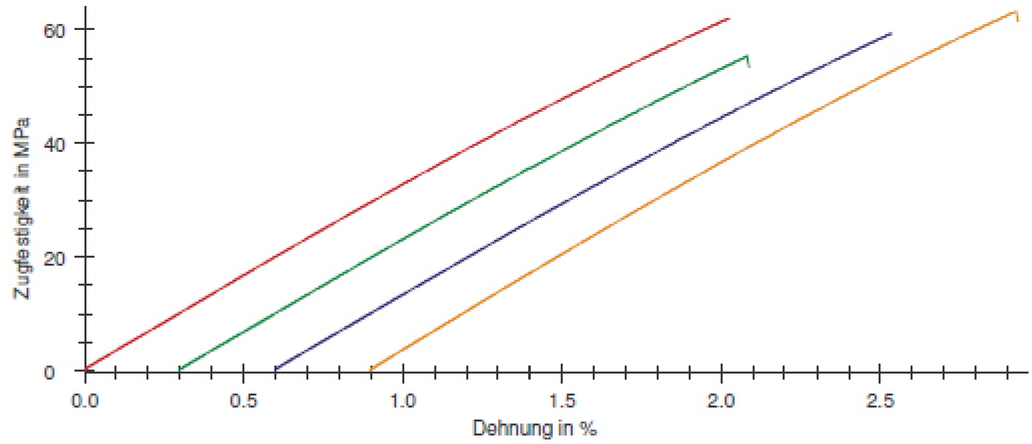

Statistik:

Serie n = 4	Zugfestigkeit MPa	Dehnung bei Fmax %	Zugmodul E_t GPa	Bruchspannung MPa	Bruchdehnung %
$\bar{x}$	59,99	1,94	3,30	59,07	1,94
s	3,49	0,12	0,06	3,93	0,11
ν [%]	5,82	5,93	1,96	6,65	5,88

Lehmann&Voss&Co. LUV

16.10.20

Prüfprotokoll

Prüflosnummer	:	890000029668
Material	:	LUVOCOM® 3F PAHT® 9825 NT à 20 kg
Materialnummer	:	25119825-00
Prozessauftrag	:	890000029668
Charge	:	NILS
Prüfer	:	MsS
Prüfnorm	:	DIN EN ISO 527
Bemerkung	:	Job 14.10.20 1x25 W R972
Geschwindigkeit Zugmodul	:	1 mm/min
Prüfgeschwindigkeit	:	50 mm/min

Prüfergebnisse:

Nr	Zugfestigkeit MPa	Dehnung bei Fmax %	Zugmodul E_t GPa	Bruchspannung MPa	Bruchdehnung %	h mm	b mm
max	1000,00	10,00	10,00				
min	1,00	0,10	0,00				
1	65,96	2,48	3,02	65,96	2,48	3,96	10,28
2	59,62	2,16	3,02	59,62	2,16		
3	74,02	3,37	3,03	44,32	10,07		
4	63,72	2,37	3,03	63,72	2,37		
5	43,11	1,47	3,04	43,11	1,47		

Seriengrafik:

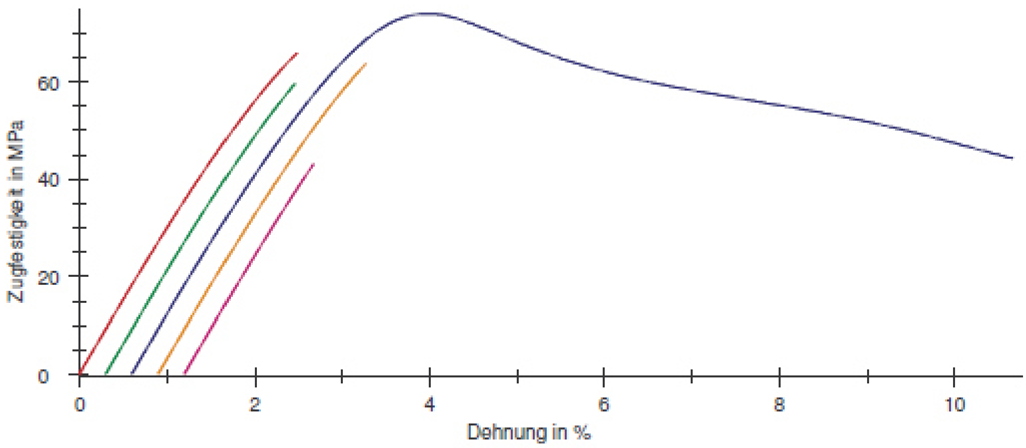

Statistik:

Serie n = 5	Zugfestigkeit MPa	Dehnung bei Fmax %	Zugmodul E_t GPa	Bruchspannung MPa	Bruchdehnung %
$\bar{x}$	61,29	2,37	3,03	55,35	3,71
s	11,43	0,68	0,01	10,86	3,58
ν [%]	18,66	28,84	0,28	19,63	96,40

Lehmann&Voss&Co.

15.10.20

Prüfprotokoll

Prüflosnummer	:	890000029695
Material	:	LUVOCOM® 3F PAHT® 9825 NT à 20 kg
Materialnummer	:	25119825-00
Prozessauftrag	:	890000029695
Charge	:	NILS
Prüfer	:	MsS
Prüfnorm	:	DIN EN ISO 527
Bemerkung	:	Job 14.10.20 1x25 W R972
Geschwindigkeit Zugmodul	:	1 mm/min
Prüfgeschwindigkeit	:	50 mm/min

Prüfergebnisse:

Nr	Zugfestigkeit MPa	Dehnung bei Fmax %	Zugmodul E_t GPa	Bruchspannung MPa	Bruchdehnung %	h mm	b mm
max	1000,00	10,00	10,00				
min	1,00	0,10	0,00				
1	72,55	2,37	3,49	72,55	2,38	4,134	10,1
2	89,32	3,85	3,32	65,19	13,83		
3	75,27	2,50	3,44	71,75	2,50		
4	88,60	3,44	3,41	84,24	3,44		
5	89,31	3,75	3,60	85,54	3,96		

Seriengrafik:

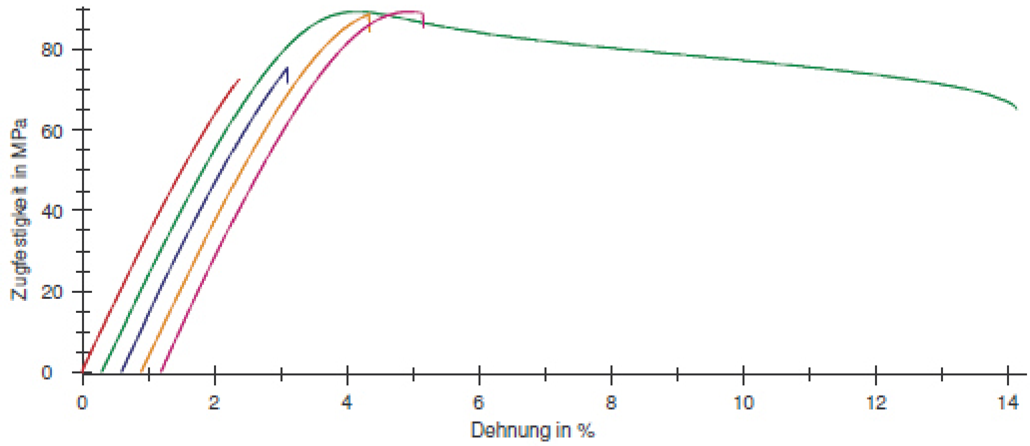

Statistik:

Serie n = 5	Zugfestigkeit MPa	Dehnung bei Fmax %	Zugmodul E_t GPa	Bruchspannung MPa	Bruchdehnung %
$\bar{x}$	83,01	3,18	3,45	75,85	5,22
s	8,37	0,70	0,10	8,74	4,86
ν [%]	10,08	21,99	2,99	11,52	93,01

Lehmann&Voss&Co. LUV

16.10.20

Prüfprotokoll

Prüflosnummer	:	890000029696
Material	:	LUVOCOM® 3F PAHT® 9825 NT à 20 kg
Materialnummer	:	25119825-00
Prozessauftrag	:	890000029696
Charge	:	NILS
Prüfer	:	MsS
Prüfnorm	:	DIN EN ISO 527
Bemerkung	:	Job 14.10.20 1x25 W R972
Geschwindigkeit Zugmodul	:	1 mm/min
Prüfgeschwindigkeit	:	50 mm/min

Prüfergebnisse:

Nr	Zugfestigkeit MPa	Dehnung bei Fmax %	Zugmodul E_t GPa	Bruchspannung MPa	Bruchdehnung %	h mm	b mm
max	1000,00	10,00	10,00				
min	1,00	0,10	0,00				
1	82,45	3,50	3,35	54,95	7,60	4,057	10,07
2	80,63	3,41	3,29	79,67	3,69		
3	82,73	3,45	3,37	48,39	4,40		
4	81,58	3,44	3,34	76,51	3,93		
5	82,00	3,51	3,34	49,00	12,45		

Seriengrafik:

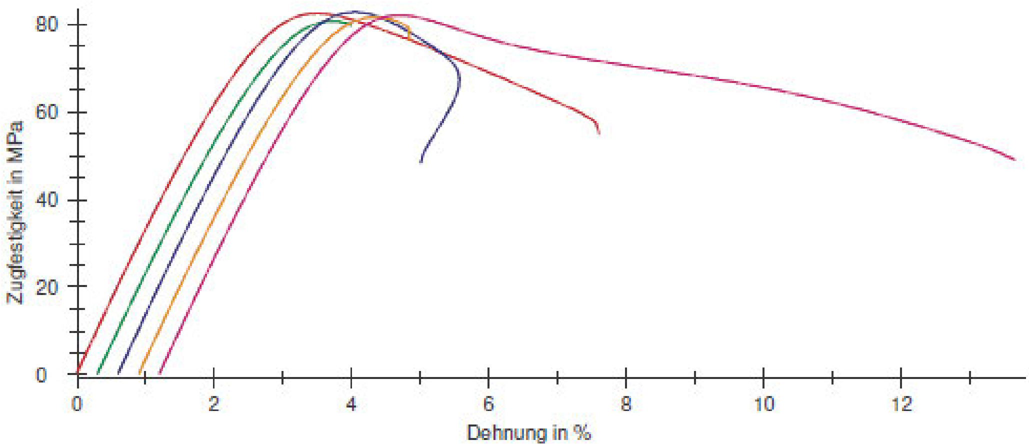

Statistik:

Serie n = 5	Zugfestigkeit MPa	Dehnung bei Fmax %	Zugmodul E_t GPa	Bruchspannung MPa	Bruchdehnung %
$\bar{x}$	81,88	3,46	3,34	61,70	6,42
s	0,82	0,04	0,03	15,22	3,72
ν [%]	1,00	1,25	0,91	24,66	58,04

Lehmann&Voss&Co. — 15.10.20

Prüfprotokoll

Prüflosnummer	:	890000029697
Material	:	LUVOCOM® 3F PAHT® 9825 NT à 20 kg
Materialnummer	:	25119825-00
Prozessauftrag	:	890000029697
Charge	:	NILS
Prüfer	:	MsS
Prüfnorm	:	DIN EN ISO 527
Bemerkung	:	Job 14.10.20 1x25 W R972
Geschwindigkeit Zugmodul	:	1 mm/min
Prüfgeschwindigkeit	:	50 mm/min

Prüfergebnisse:

Nr	Zugfestigkeit MPa	Dehnung bei Fmax %	Zugmodul E_t GPa	Bruchspannung MPa	Bruchdehnung %	h mm	b mm
max	1000,00	10,00	10,00				
min	1,00	0,10	0,00				
1	70,08	2,34	3,34	66,76	2,35	4,126	10,07
2	63,63	2,02	3,38	63,27	2,03		
3	80,43	2,82	3,34	80,43	2,82		
4	59,11	1,88	3,36	56,23	1,88		
5	54,71	1,71	3,38	54,68	1,71		

Seriengrafik:

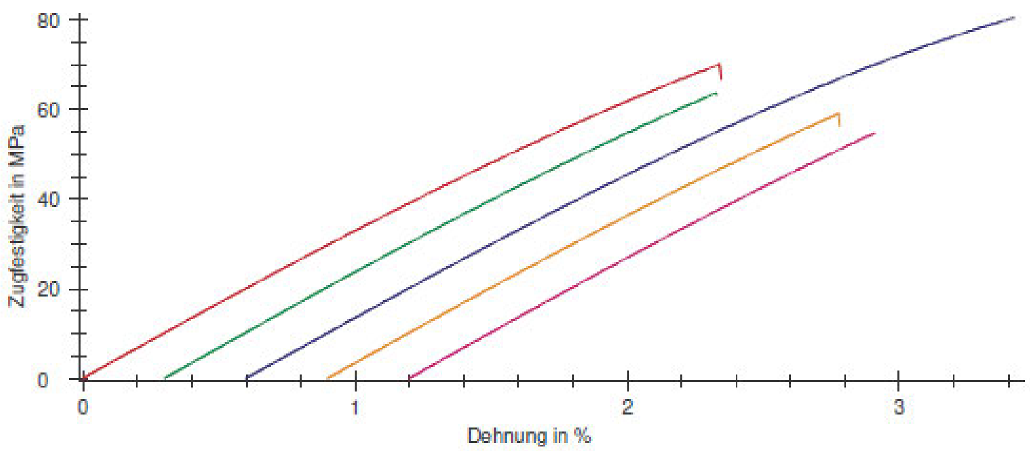

Statistik:

Serie n = 5	Zugfestigkeit MPa	Dehnung bei Fmax %	Zugmodul E_t GPa	Bruchspannung MPa	Bruchdehnung %
$\bar{x}$	65,59	2,15	3,36	64,28	2,16
s	10,06	0,44	0,02	10,31	0,44
ν [%]	15,33	20,44	0,58	16,03	20,33

Lehmann&Voss&Co.

16.10.20

Prüfprotokoll

Prüflosnummer	:	890000029698
Material	:	LUVOCOM® 3F PAHT® 9825 NT à 20 kg
Materialnummer	:	25119825-00
Prozessauftrag	:	890000029698
Charge	:	NILS
Prüfer	:	MsS
Prüfnorm	:	DIN EN ISO 527
Bemerkung	:	Job 14.10.20 1x25 W R972
Geschwindigkeit Zugmodul	:	1 mm/min
Prüfgeschwindigkeit	:	50 mm/min

Prüfergebnisse:

Nr	Zugfestigkeit MPa	Dehnung bei Fmax %	Zugmodul E_t GPa	Bruchspannung MPa	Bruchdehnung %	h mm	b mm
max	1000,00	10,00	10,00				
min	1,00	0,10	0,00				
1	76,33	3,35	3,09	45,77	6,70	4,076	10,09
2	74,01	2,86	3,11	71,80	2,87		
3	76,71	3,18	3,09	76,71	3,18		
4	59,68	2,08	3,11	57,03	2,09		
5	76,96	3,41	3,11	46,09	7,89		

Seriengrafik:

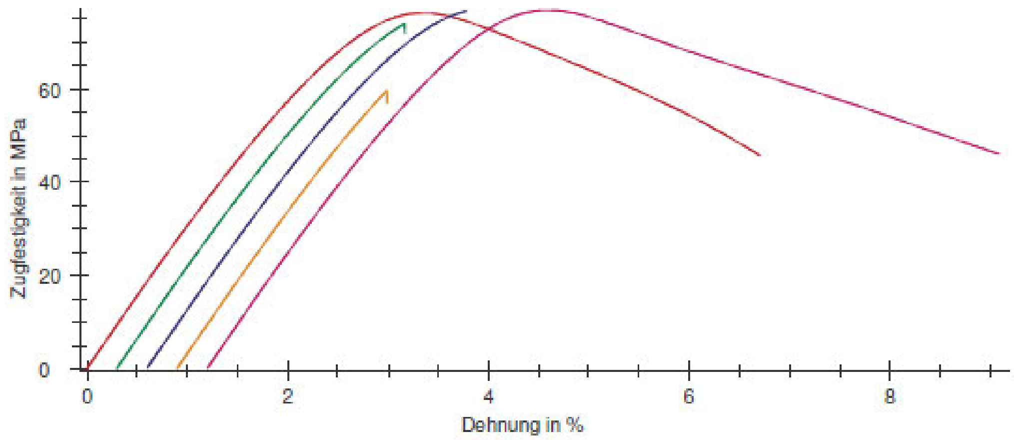

Statistik:

Serie n = 5	Zugfestigkeit MPa	Dehnung bei Fmax %	Zugmodul E_t GPa	Bruchspannung MPa	Bruchdehnung %
$\bar{x}$	72,74	2,98	3,10	59,48	4,55
s	7,39	0,54	0,01	14,34	2,58
ν [%]	10,16	18,21	0,42	24,10	56,68

Lehmann&Voss&Co.

29.10.20

Prüfprotokoll

Prüflosnummer	:	890000029703
Material	:	LUVOCOM® 3F PAHT® 9825 NT à 20 kg
Materialnummer	:	25119825-00
Prozessauftrag	:	890000029703
Charge	:	NILS
Prüfer	:	gw
Prüfnorm	:	DIN EN ISO 527
Bemerkung	:	
Geschwindigkeit Zugmodul	:	1 mm/min
Prüfgeschwindigkeit	:	50 mm/min

Prüfergebnisse:

Nr	Zugfestigkeit MPa	Dehnung bei Fmax %	Zugmodul E_t GPa	Bruchspannung MPa	Bruchdehnung %	h mm	b mm
max	1000,00	10,00	10,00				
min	1,00	0,10	0,00				
1	56,71	1,89	3,22	56,71	1,89	4,272	10,34
2	62,49	2,11	3,28	61,63	2,11		
3	64,19	2,19	3,18	64,19	2,19		
4	63,72	2,16	3,27	63,58	2,17		
5	47,22	1,51	3,24	47,22	1,51		

Seriengrafik:

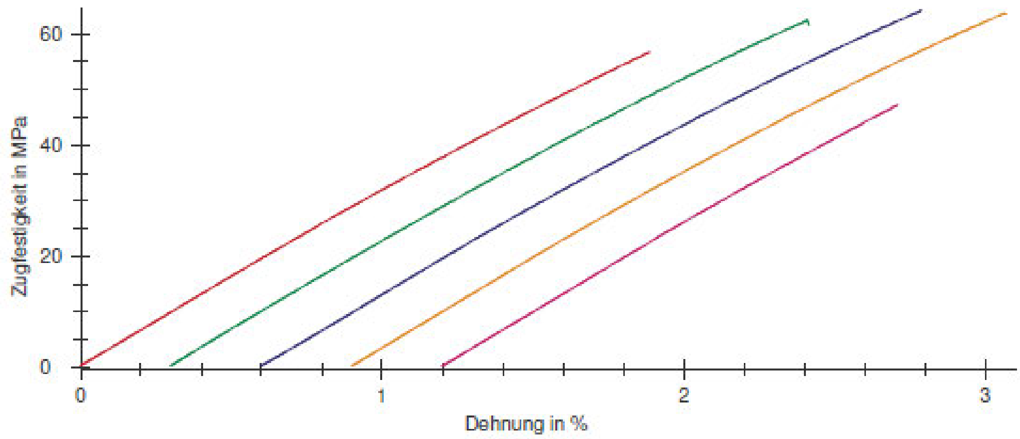

Statistik:

Serie n = 5	Zugfestigkeit MPa	Dehnung bei Fmax %	Zugmodul E_t GPa	Bruchspannung MPa	Bruchdehnung %
$\bar{x}$	58,86	1,97	3,24	58,67	1,97
s	7,16	0,28	0,04	7,04	0,29
ν [%]	12,17	14,44	1,18	12,00	14,50

Lehmann&Voss&Co.

29.10.20

Prüfprotokoll

Prüflosnummer	:	890000029704
Material	:	LUVOCOM® 3F PAHT® 9825 NT à 20 kg
Materialnummer	:	25119825-00
Prozessauftrag	:	890000029704
Charge	:	NILS
Prüfer	:	gw
Prüfnorm	:	DIN EN ISO 527
Bemerkung	:	
Geschwindigkeit Zugmodul	:	1 mm/min
Prüfgeschwindigkeit	:	50 mm/min

Prüfergebnisse:

Nr	Zugfestigkeit MPa	Dehnung bei Fmax %	Zugmodul E_t GPa	Bruchspannung MPa	Bruchdehnung %	h mm	b mm
max	1000,00	10,00	10,00				
min	1,00	0,10	0,00				
1	64,21	2,25	3,27	64,21	2,25	4,336	10,14
2	66,26	2,33	3,13	64,41	2,34		
3	56,75	1,80	3,37	54,20	1,80		
4	56,23	1,92	3,13	56,23	1,92		
5	63,16	2,18	3,05	61,68	2,19		

Seriengrafik:

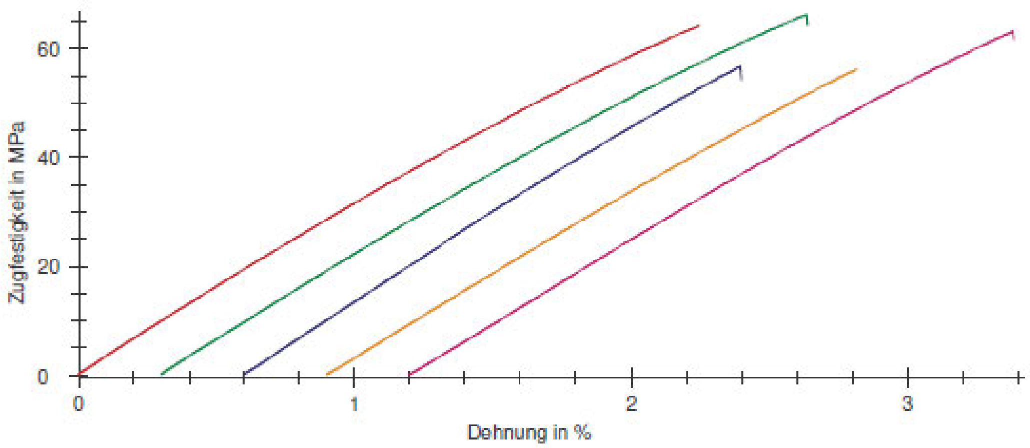

Statistik:

Serie n = 5	Zugfestigkeit MPa	Dehnung bei Fmax %	Zugmodul E_t GPa	Bruchspannung MPa	Bruchdehnung %
$\bar{x}$	61,32	2,10	3,19	60,15	2,10
s	4,55	0,23	0,13	4,68	0,23
ν [%]	7,43	10,90	4,07	7,79	10,91

Impact Strength according to DIN EN ISO 179 1 eU/eA

Lehmann&Voss&Co. LUV

19.10.2020

Prüfprotokoll Schlagzähigkeit

Prüflosnummer	:	890000029659
Material	:	LUVOCOM® 3F PAHT® 9825 NT à 20 kg
Materialnummer	:	25119825-00
Prozessauftrag	:	890000029659
Charge	:	NILS
Prüfer	:	-
Prüfnorm	:	DIN EN ISO 179 1eA

Ergebnisse:

Nr	b_N mm	b mm	h mm	Schlagzähigkeit (ak) kJ/m²	Schlagarbeit [W] J	Versagensart
max				1000,00		
min				1,00		
1	7,992	9,992	4,146	4,01	0,166	s
2				2,22	0,092	s

Seriengrafik:

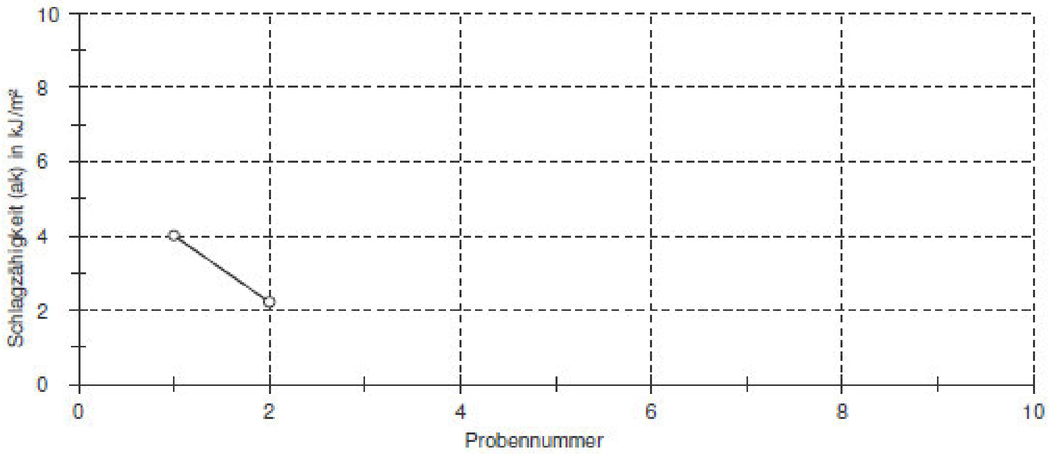

Statistik:

Serie n = 2	Schlagzähigkeit (ak) kJ/m²	Schlagarbeit [W] J
$\bar{x}$	3,12	0,129
s	1,27	0,053
ν [%]	40,69	40,69

25119825-00 PA 890000029659 Ch NILS 1eA.zs2

19.10.2020

Lehmann&Voss&Co.

Prüfprotokoll Schlagzähigkeit

Prüflosnummer	:	890000029659
Material	:	LUVOCOM® 3F PAHT® 9825 NT à 20 kg
Materialnummer	:	25119825-00
Prozessauftrag	:	890000029659
Charge	:	NILS
Prüfer	:	-
Prüfnorm	:	DIN EN ISO 179 1eU
Bemerkung	:	

Ergebnisse:

Nr	b mm	h mm	Schlagzähigkeit (ak) kJ/m²	Schlagarbeit [W] J	Versagensart
max			1000,00		
min			1,00		
1	9,992	4,146	12,57	0,521	s
2			26,94	1,116	s
3			20,59	0,853	s

Seriengrafik:

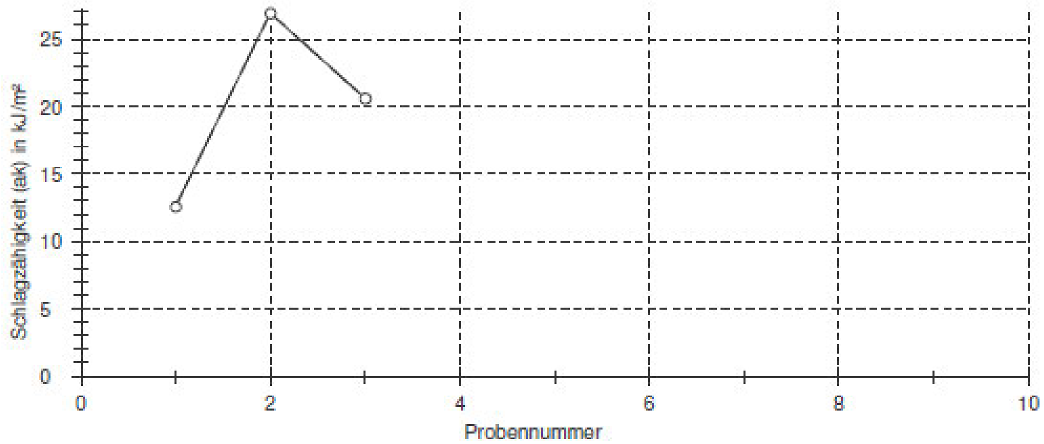

Statistik:

Serie n = 3	Schlagzähigkeit (ak) kJ/m²	Schlagarbeit [W] J
$\bar{x}$	20,03	0,830
s	7,20	0,298
ν [%]	35,93	35,93

25119825-00 PA 890000029659 Ch NILS 1eU.zs2

Lehmann&Voss&Co.

19.10.2020

Prüfprotokoll Schlagzähigkeit

Prüflosnummer	:	890000029660
Material	:	LUVOCOM® 3F PAHT® 9825 NT à 20 kg
Materialnummer	:	25119825-00
Prozessauftrag	:	890000029660
Charge	:	NILS
Prüfer	:	-
Prüfnorm	:	DIN EN ISO 179 1eA

Ergebnisse:

Nr	b_N mm	b mm	h mm	Schlagzähigkeit (ak) kJ/m²	Schlagarbeit [W] J	Versagensart
max				1000,00		
min				1,00		
1	7,866	9,866	4,195	1,96	0,081	s
2				3,89	0,161	s

Seriengrafik:

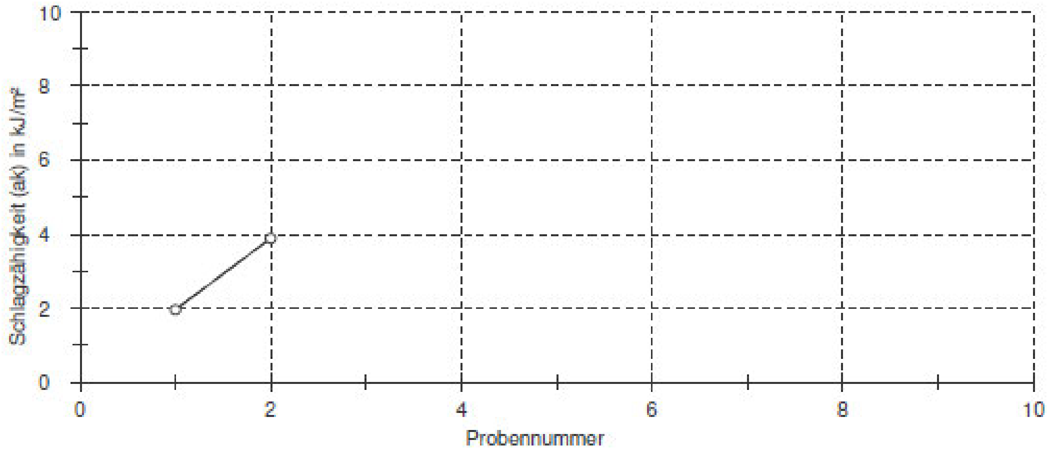

Statistik:

Serie n = 2	Schlagzähigkeit (ak) kJ/m²	Schlagarbeit [W] J
$\bar{x}$	2,92	0,121
s	1,37	0,057
ν [%]	46,73	46,73

25119825-00 PA 890000029660 Ch NILS 1eA.zs2

Lehmann&Voss&Co. LUV

19.10.2020

Prüfprotokoll
Schlagzähigkeit

Prüflosnummer	:	890000029660
Material	:	LUVOCOM® 3F PAHT® 9825 NT à 20 kg
Materialnummer	:	25119825-00
Prozessauftrag	:	890000029660
Charge	:	NILS
Prüfer	:	-
Prüfnorm	:	DIN EN ISO 179 1eU
Bemerkung	:	

Ergebnisse:

Nr	b mm	h mm	Schlagzähigkeit (ak) kJ/m²	Schlagarbeit [W] J	Versagensart
max			1000,00		
min			1,00		
1	9,866	4,195	32,90	1,362	s
2			24,72	1,023	s
3			43,23	1,789	t

Seriengrafik:

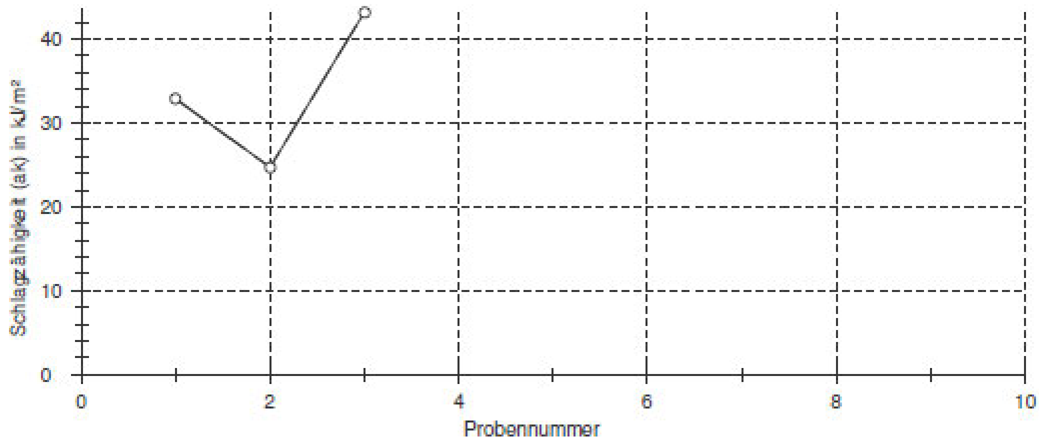

Statistik:

Serie n = 3	Schlagzähigkeit (ak) kJ/m²	Schlagarbeit [W] J
x	33,61	1,391
s	9,27	0,384
ν [%]	27,59	27,59

25119825-00 PA 890000029660 Ch NILS 1eU.zs2

Lehmann&Voss&Co.

20.10.2020

Prüfprotokoll
Schlagzähigkeit

Prüflosnummer	:	890000029661
Material	:	LUVOCOM® 3F PAHT® 9825 NT à 20 kg
Materialnummer	:	25119825-00
Prozessauftrag	:	890000029661
Charge	:	NILS
Prüfer	:	-
Prüfnorm	:	DIN EN ISO 179 1eA

Ergebnisse:

Nr	b_N mm	b mm	h mm	Schlagzähigkeit (ak) kJ/m²	Schlagarbeit [W] J	Versagensart
max				1000,00		
min				1,00		
1	8,246	10,25	3,931	2,06	0,083	s
2				1,58	0,064	s

Seriengrafik:

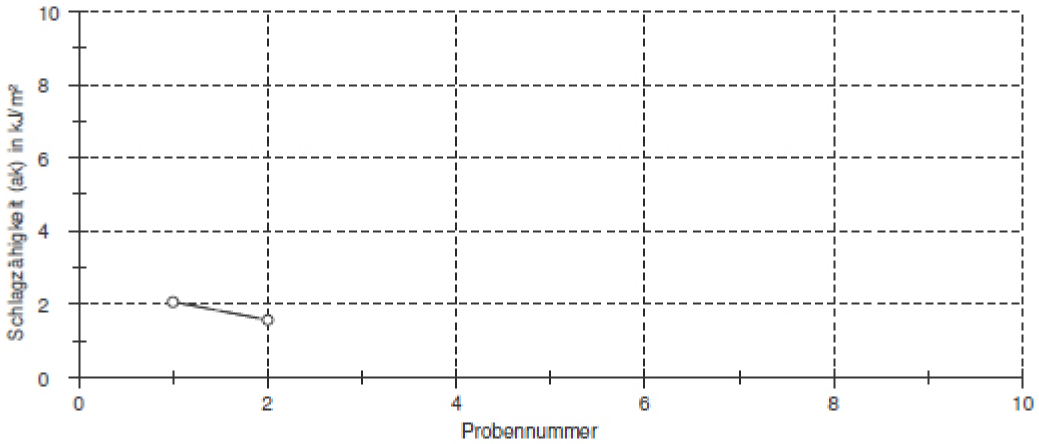

Statistik:

Serie n = 2	Schlagzähigkeit (ak) kJ/m²	Schlagarbeit [W] J
x̄	1,82	0,073
s	0,34	0,014
ν [%]	18,89	18,89

25119825-00 PA 890000029661 Ch NILS 1eA.zs2

Lehmann&Voss&Co.

20.10.2020

Prüfprotokoll
Schlagzähigkeit

Prüflosnummer	:	890000029661
Material	:	LUVOCOM® 3F PAHT® 9825 NT à 20 kg
Materialnummer	:	25119825-00
Prozessauftrag	:	890000029661
Charge	:	NILS
Prüfer	:	-
Prüfnorm	:	DIN EN ISO 179 1eU

Ergebnisse:

Nr	b mm	h mm	Schlagzähigkeit (ak) kJ/m²	Schlagarbeit [W] J	Versagensart
max			1000,00		
min			1,00		
1	10,25	3,931	41,80	1,683	s
2			40,31	1,623	t
3			22,55	0,908	t

Seriengrafik:

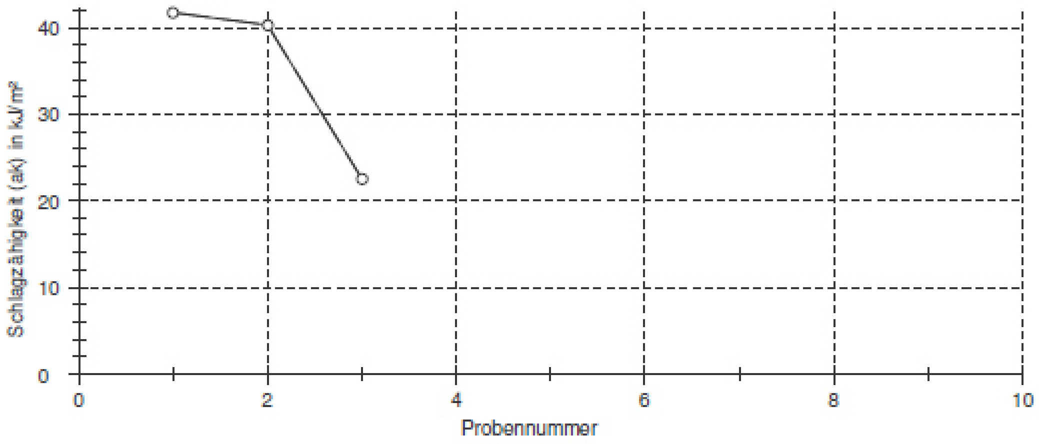

Statistik:

Serie n = 3	Schlagzähigkeit (ak) kJ/m²	Schlagarbeit [W] J
$\bar{x}$	34,88	1,405
s	10,71	0,431
ν [%]	30,70	30,70

25119825-00 PA 890000029661 Ch NILS 1eU.zs2

19.10.2020

Lehmann&Voss&Co.

Prüfprotokoll
Schlagzähigkeit

Prüflosnummer	:	890000029662
Material	:	LUVOCOM® 3F PAHT® 9825 NT à 20 kg
Materialnummer	:	25119825-00
Prozessauftrag	:	890000029662
Charge	:	NILS
Prüfer	:	-
Prüfnorm	:	DIN EN ISO 179 1eA

Ergebnisse:

Nr	b_N mm	b mm	h mm	Schlagzähigkeit (ak) kJ/m²	Schlagarbeit [W] J	Versagensart
max				1000,00		
min				1,00		
1	8,181	10,18	3,91	3,79	0,151	s
2				1,94	0,077	s

Seriengrafik:

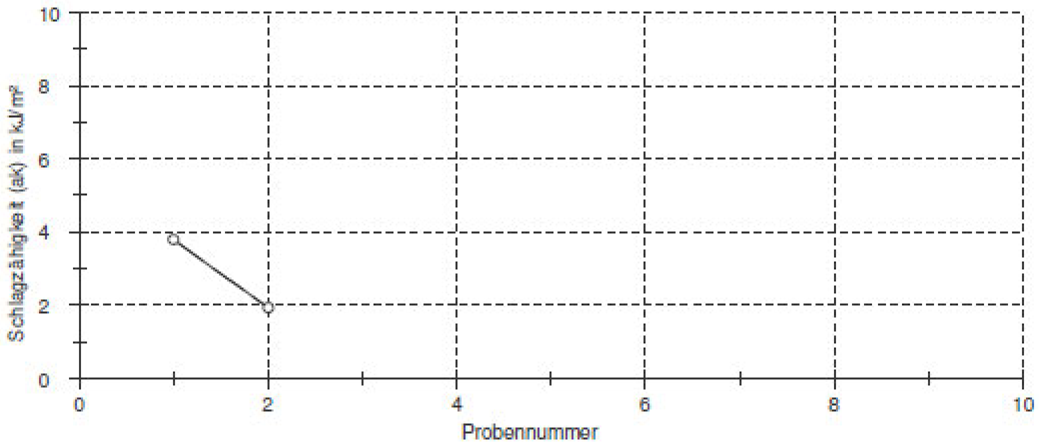

Statistik:

Serie n = 2	Schlagzähigkeit (ak) kJ/m²	Schlagarbeit [W] J
$\bar{x}$	2,87	0,114
s	1,31	0,052
ν [%]	45,62	45,62

25119825-00 PA 890000029662 Ch NILS 1eA.zs2

Lehmann&Voss&Co.

19.10.2020

Prüfprotokoll
Schlagzähigkeit

Prüflosnummer	:	890000029662
Material	:	LUVOCOM® 3F PAHT® 9825 NT à 20 kg
Materialnummer	:	25119825-00
Prozessauftrag	:	890000029662
Charge	:	NILS
Prüfer	:	-
Prüfnorm	:	DIN EN ISO 179 1eU
Bemerkung	:	

Ergebnisse:

Nr	b mm	h mm	Schlagzähigkeit (ak) kJ/m²	Schlagarbeit [W] J	Versagensart
max			1000,00		
min			1,00		
1	10,18	3,91	34,15	1,359	t
2			45,59	1,815	t
3			60,86	2,423	t

Seriengrafik:

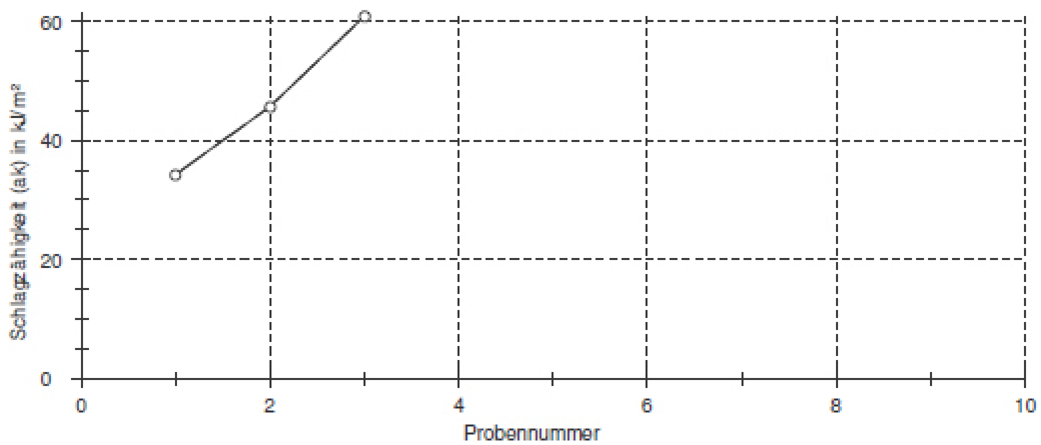

Statistik:

Serie n = 3	Schlagzähigkeit (ak) kJ/m²	Schlagarbeit [W] J
$\bar{x}$	46,87	1,866
s	13,40	0,533
ν [%]	28,60	28,60

25119825-00 PA 890000029662 Ch NILS 1eU.zs2

Lehmann&Voss&Co.

20.10.2020

Prüfprotokoll
Schlagzähigkeit

Prüflosnummer	:	890000029669
Material	:	LUVOCOM® 3F PAHT® 9825 NT à 20 kg
Materialnummer	:	25119825-00
Prozessauftrag	:	890000029669
Charge	:	NILS
Prüfer	:	-
Prüfnorm	:	DIN EN ISO 179 1eA

Ergebnisse:

Nr	b_N mm	b mm	h mm	Schlagzähigkeit (ak) kJ/m²	Schlagarbeit [W] J	Versagensart
max				1000,00		
min				1,00		
1	7,962	9,962	3,769	4,10	0,154	s
2				3,88	0,146	s

Seriengrafik:

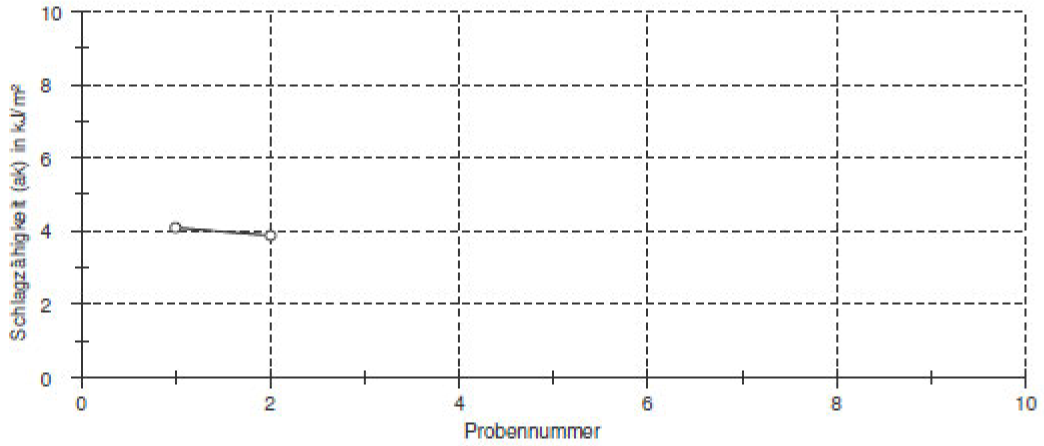

Statistik:

Serie n = 2	Schlagzähigkeit (ak) kJ/m²	Schlagarbeit [W] J
$\bar{x}$	3,99	0,150
s	0,16	0,006
ν [%]	3,94	3,94

25119825-00 PA 890000029669 Ch NILS 1eA.zs2

Lehmann&Voss&Co.

20.10.2020

Prüfprotokoll
Schlagzähigkeit

Prüflosnummer	:	890000029669
Material	:	LUVOCOM® 3F PAHT® 9825 NT à 20 kg
Materialnummer	:	25119825-00
Prozessauftrag	:	890000029669
Charge	:	NILS
Prüfer	:	-
Prüfnorm	:	DIN EN ISO 179 1eU
Bemerkung	:	

Ergebnisse:

Nr	b mm	h mm	Schlagzähigkeit (ak) kJ/m²	Schlagarbeit [W] J	Versagensart
max			1000,00		
min			1,00		
1	9,962	3,769	69,09	2,594	s
2			71,96	2,702	t
3			72,37	2,717	s

Seriengrafik:

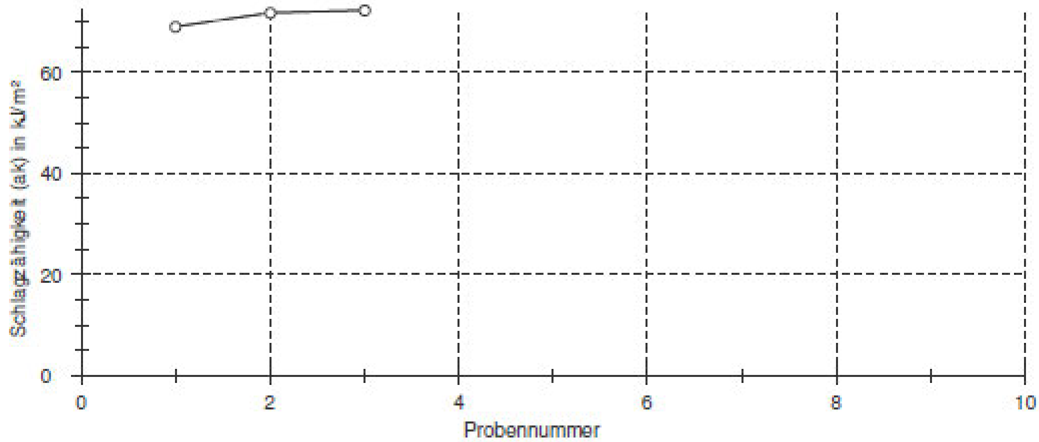

Statistik:

Serie n = 3	Schlagzähigkeit (ak) kJ/m²	Schlagarbeit [W] J
$\bar{x}$	71,14	2,671
s	1,79	0,067
ν [%]	2,51	2,51

25119825-00 PA 890000029669 Ch NILS 1eU.zs2

Lehmann&Voss&Co.

19.10.2020

Prüfprotokoll
Schlagzähigkeit

Prüflosnummer : 890000029670
Material : LUVOCOM® 3F PAHT® 9825 NT à 20 kg
Materialnummer : 25119825-00
Prozessauftrag : 890000029670
Charge : NILS
Prüfer : -
Prüfnorm : DIN EN ISO 179 1eA

Ergebnisse:

Nr	b_N mm	b mm	h mm	Schlagzähigkeit (ak) kJ/m²	Schlagarbeit [W] J	Versagensart
max				1000,00		
min				1,00		
1	8	10	3,96	43,59	1,726	s
2				46,04	1,823	t

Seriengrafik:

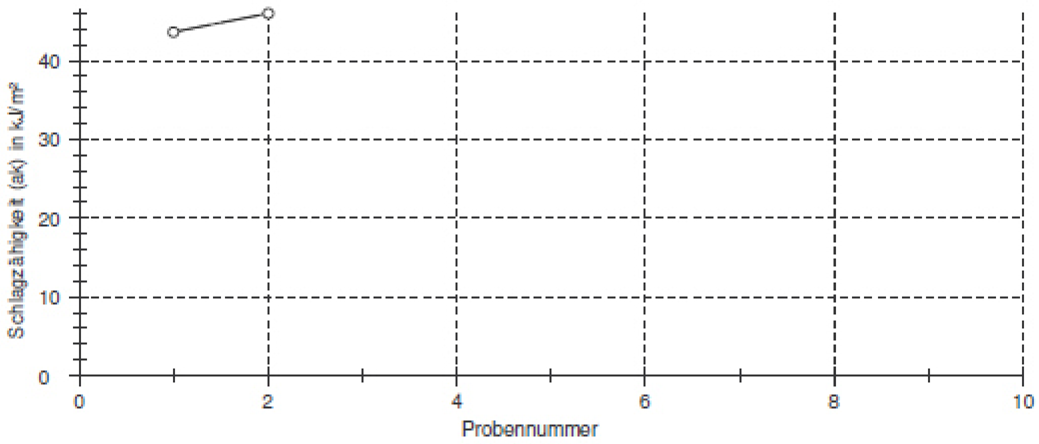

Statistik:

Serie n = 2	Schlagzähigkeit (ak) kJ/m²	Schlagarbeit [W] J
$\bar{x}$	44,82	1,775
s	1,73	0,069
v [%]	3,86	3,86

25119825-00 PA 890000029670 Ch NILS 1eA.zs2

Lehmann&Voss&Co.

19.10.2020

Prüfprotokoll
Schlagzähigkeit

Prüflosnummer	:	890000029670
Material	:	LUVOCOM® 3F PAHT® 9825 NT à 20 kg
Materialnummer	:	25119825-00
Prozessauftrag	:	890000029670
Charge	:	NILS
Prüfer	:	-
Prüfnorm	:	DIN EN ISO 179 1eU
Bemerkung	:	

Ergebnisse:

Nr	b mm	h mm	Schlagzähigkeit (ak) kJ/m²	Schlagarbeit [W] J	Versagensart
max			1000,00		
min			1,00		
1	10	3,96	51,44	2,037	t
2			74,95	2,968	b
3			74,53	2,951	t

Seriengrafik:

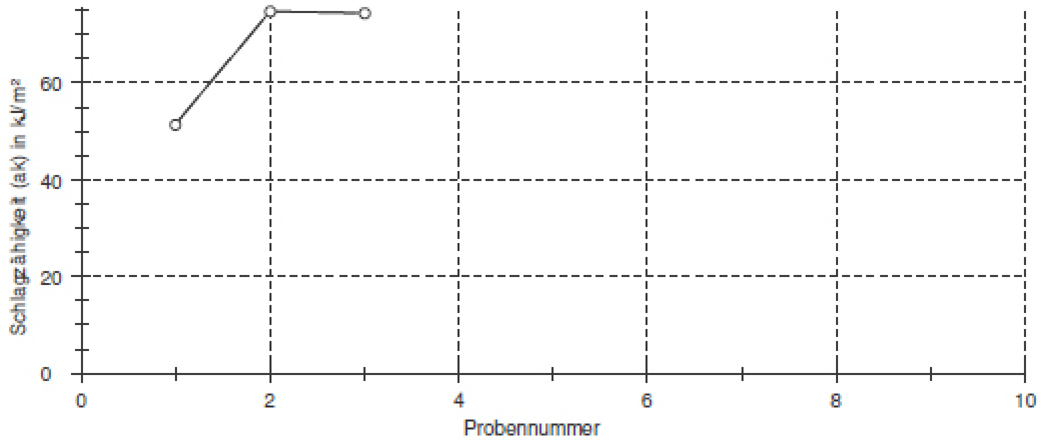

Statistik:

Serie n = 3	Schlagzähigkeit (ak) kJ/m²	Schlagarbeit [W] J
$\bar{x}$	66,97	2,652
s	13,45	0,533
ν [%]	20,09	20,09

25119825-00 PA 890000029670 Ch NILS 1eU.zs2

Lehmann&Voss&Co. LUV

20.10.2020

Prüfprotokoll
Schlagzähigkeit

Prüflosnummer	:	890000029671
Material	:	LUVOCOM® 3F PAHT® 9825 NT à 20 kg
Materialnummer	:	25119825-00
Prozessauftrag	:	890000029671
Charge	:	NILS
Prüfer	:	-
Prüfnorm	:	DIN EN ISO 179 1eA

Ergebnisse:

Nr	b_N mm	b mm	h mm	Schlagzähigkeit (ak) kJ/m²	Schlagarbeit [W] J	Versagensart
max				1000,00		
min				1,00		
1	7,885	9,885	4,039	2,52	0,101	s
2				3,55	0,142	s

Seriengrafik:

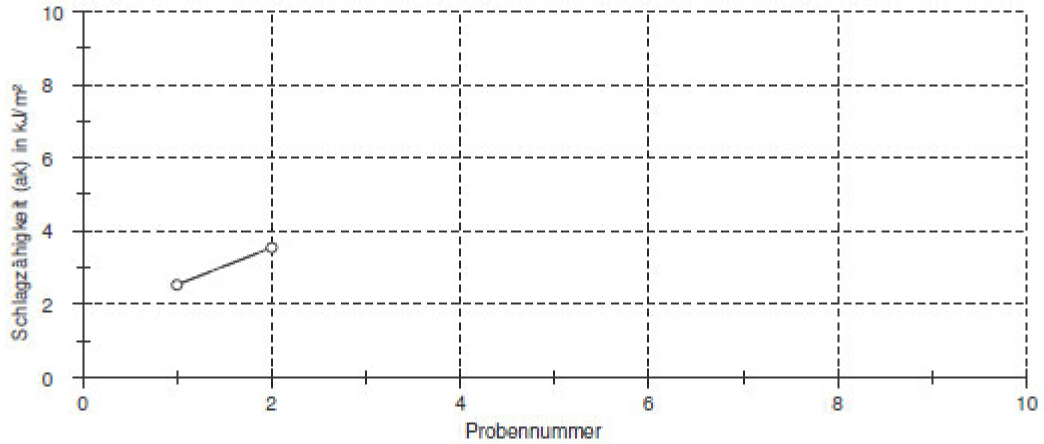

Statistik:

Serie n = 2	Schlagzähigkeit (ak) kJ/m²	Schlagarbeit [W] J
$\bar{x}$	3,04	0,121
s	0,73	0,029
v [%]	23,95	23,95

25119825-00 PA 890000029671 Ch NILS 1eA.zs2

Lehmann&Voss&Co.

20.10.2020

Prüfprotokoll
Schlagzähigkeit

Prüflosnummer	:	890000029671
Material	:	LUVOCOM® 3F PAHT® 9825 NT à 20 kg
Materialnummer	:	25119825-00
Prozessauftrag	:	890000029671
Charge	:	NILS
Prüfer	:	-
Prüfnorm	:	DIN EN ISO 179 1eU
Bemerkung	:	

Ergebnisse:

Nr	b mm	h mm	Schlagzähigkeit (ak) kJ/m²	Schlagarbeit [W] J	Versagensart
max			1000,00		
min			1,00		
1	9,885	4,039	24,52	0,979	s
2			24,65	0,984	s
3			41,99	1,676	t

Seriengrafik:

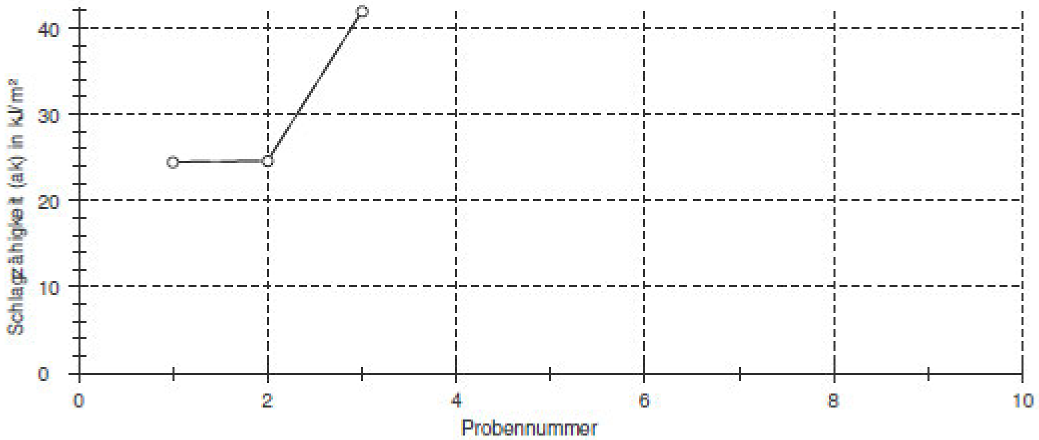

Statistik:

Serie n = 3	Schlagzähigkeit (ak) kJ/m²	Schlagarbeit [W] J
$\bar{x}$	30,38	1,213
s	10,05	0,401
ν [%]	33,07	33,07

25119825-00 PA 890000029671 Ch NILS 1eU.zs2

Lehmann&Voss&Co.

19.10.2020

Prüfprotokoll
Schlagzähigkeit

Prüflosnummer	:	890000029672
Material	:	LUVOCOM® 3F PAHT® 9825 NT à 20 kg
Materialnummer	:	25119825-00
Prozessauftrag	:	890000029672
Charge	:	NILS
Prüfer	:	-
Prüfnorm	:	DIN EN ISO 179 1eA

Ergebnisse:

Nr	b_N mm	b mm	h mm	Schlagzähigkeit (ak) kJ/m²	Schlagarbeit [W] J	Versagensart
max				1000,00		
min				1,00		
1	7,958	9,958	4,083	3,64	0,148	s
2				3,77	0,153	s

Seriengrafik:

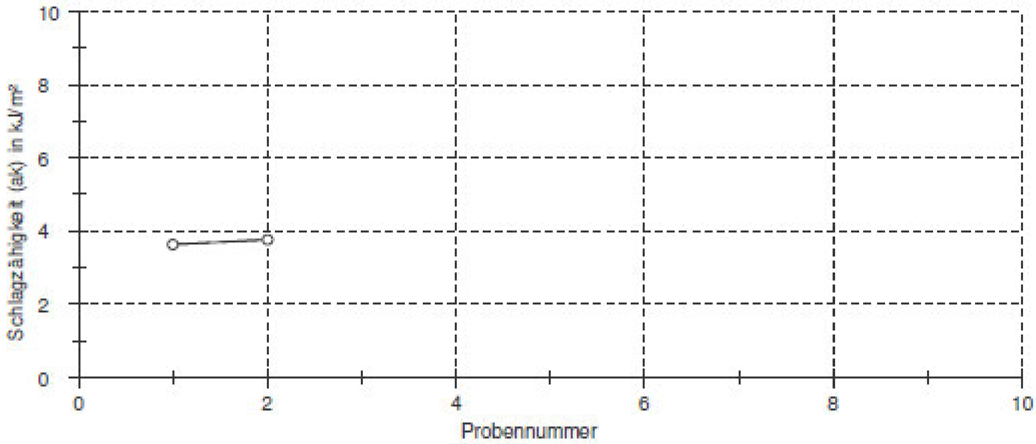

Statistik:

Serie n = 2	Schlagzähigkeit (ak) kJ/m²	Schlagarbeit [W] J
$\bar{x}$	3,70	0,151
s	0,09	0,004
ν [%]	2,50	2,50

25119825-00 PA 890000029672 Ch NILS 1eA.zs2

Lehmann&Voss&Co.

19.10.2020

Prüfprotokoll
Schlagzähigkeit

Prüflosnummer	:	890000029672
Material	:	LUVOCOM® 3F PAHT® 9825 NT à 20 kg
Materialnummer	:	25119825-00
Prozessauftrag	:	890000029672
Charge	:	NILS
Prüfer	:	-
Prüfnorm	:	DIN EN ISO 179 1eU
Bemerkung	:	

Ergebnisse:

Nr	b mm	h mm	Schlagzähigkeit (ak) kJ/m²	Schlagarbeit [W] J	Versagensart
max			1000,00		
min			1,00		
1	9,958	4,083	40,12	1,631	s
2			73,42	2,985	b
3			86,56	3,520	t

Seriengrafik:

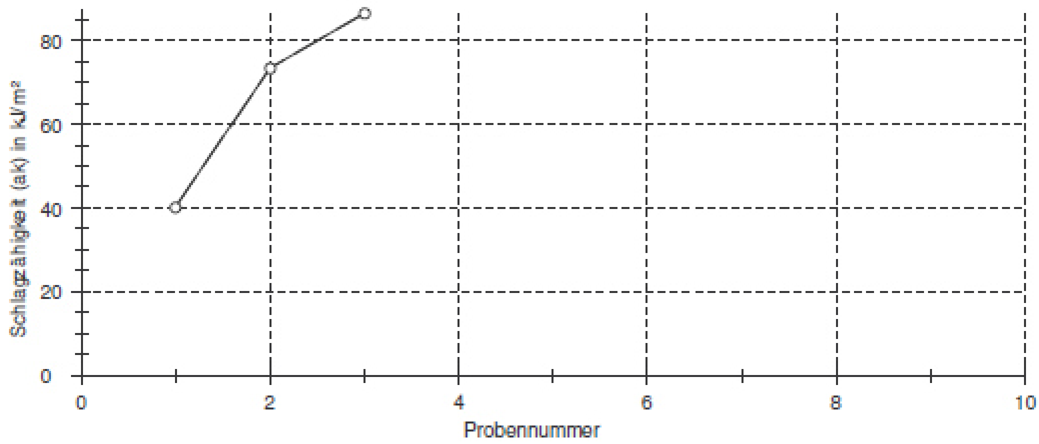

Statistik:

Serie n = 3	Schlagzähigkeit (ak) kJ/m²	Schlagarbeit [W] J
$\bar{x}$	66,70	2,712
s	23,94	0,973
ν [%]	35,89	35,89

25119825-00 PA 890000029672 Ch NILS 1eU.zs2

19.10.2020

Lehmann&Voss&Co.

Prüfprotokoll
Schlagzähigkeit

Prüflosnummer	:	890000029699
Material	:	LUVOCOM® 3F PAHT® 9825 NT à 20 kg
Materialnummer	:	25119825-00
Prozessauftrag	:	890000029699
Charge	:	NILS
Prüfer	:	-
Prüfnorm	:	DIN EN ISO 179 1eA

Ergebnisse:

Nr	b_N mm	b mm	h mm	Schlagzähigkeit (ak) kJ/m²	Schlagarbeit [W] J	Versagensart
max				1000,00		
min				1,00		
1	8,084	10,08	4,15	4,38	0,183	s
2				4,03	0,169	s

Seriengrafik:

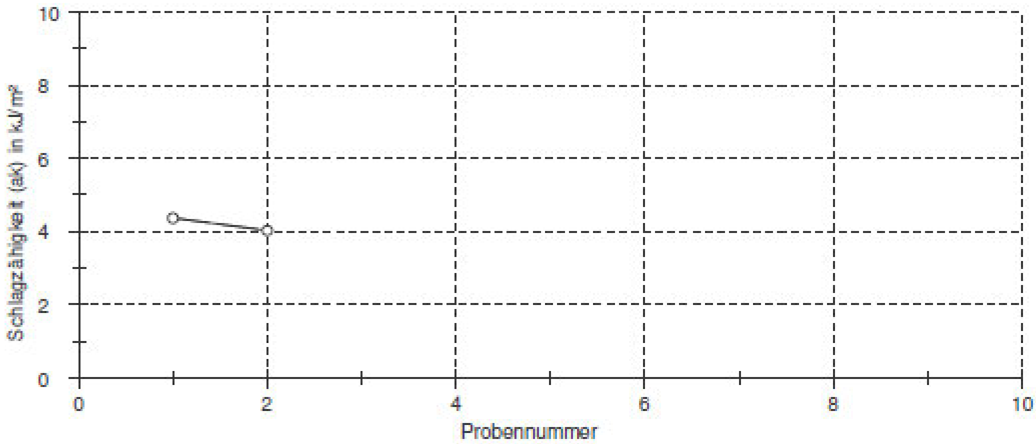

Statistik:

Serie n = 2	Schlagzähigkeit (ak) kJ/m²	Schlagarbeit [W] J
x̄	4,20	0,176
s	0,25	0,010
ν [%]	5,89	5,89

25119825-00 PA 890000029699 Ch NILS 1eA.zs2

Lehmann&Voss&Co.

19.10.2020

Prüfprotokoll
Schlagzähigkeit

Prüflosnummer : 890000029699
Material : LUVOCOM® 3F PAHT® 9825 NT à 20 kg
Materialnummer : 25119825-00
Prozessauftrag : 890000029699
Charge : NILS
Prüfer : -
Prüfnorm : DIN EN ISO 179 1eU
Bemerkung :

Ergebnisse:

Nr	b mm	h mm	Schlagzähigkeit (ak) kJ/m²	Schlagarbeit [W] J	Versagensart
max			1000,00		
min			1,00		
1	10,08	4,15	63,47	2,656	t
2			35,30	1,477	s
3			30,60	1,281	s

Seriengrafik:

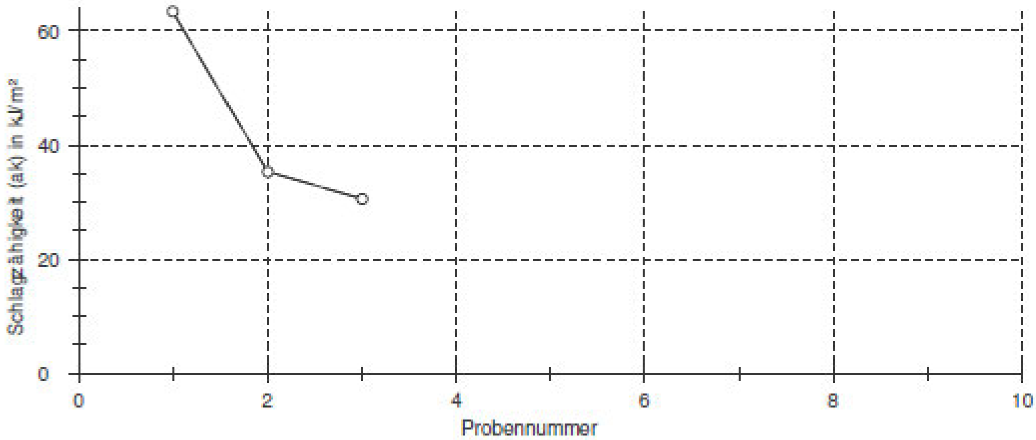

Statistik:

Serie n = 3	Schlagzähigkeit (ak) kJ/m²	Schlagarbeit [W] J
$\bar{x}$	43,12	1,804
s	17,77	0,744
ν [%]	41,22	41,22

25119825-00 PA 890000029699 Ch NILS 1eU.zs2

Lehmann&Voss&Co.

19.10.2020

Prüfprotokoll
Schlagzähigkeit

Prüflosnummer	:	890000029700
Material	:	LUVOCOM® 3F PAHT® 9825 NT à 20 kg
Materialnummer	:	25119825-00
Prozessauftrag	:	890000029700
Charge	:	NILS
Prüfer	:	-
Prüfnorm	:	DIN EN ISO 179 1eA

Ergebnisse:

Nr	b_N mm	b mm	h mm	Schlagzähigkeit (ak) kJ/m²	Schlagarbeit [W] J	Versagensart
max				1000,00		
min				1,00		
1	7,995	9,995	4,07	6,72	0,273	s
2				3,92	0,159	s

Seriengrafik:

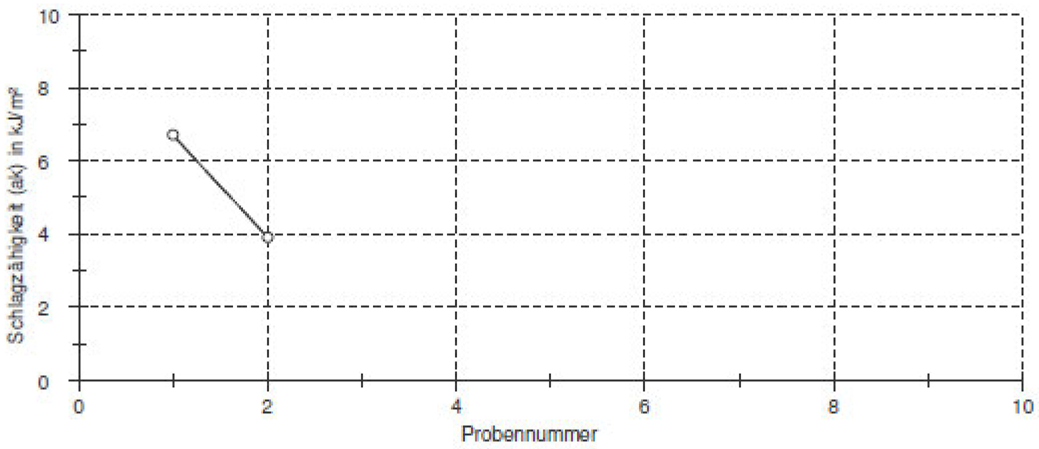

Statistik:

Serie n = 2	Schlagzähigkeit (ak) kJ/m²	Schlagarbeit [W] J
$\bar{x}$	5,32	0,216
s	1,98	0,081
ν [%]	37,27	37,27

25119825-00 PA 890000029700 Ch NILS 1eA.zs2

19.10.2020

Lehmann&Voss&Co.

Prüfprotokoll
Schlagzähigkeit

Prüflosnummer : 890000029700
Material : LUVOCOM® 3F PAHT® 9825 NT à 20 kg
Materialnummer : 25119825-00
Prozessauftrag : 890000029700
Charge : NILS
Prüfer : -
Prüfnorm : DIN EN ISO 179 1eU
Bemerkung :

Ergebnisse:

Nr	b mm	h mm	Schlagzähigkeit (ak) kJ/m²	Schlagarbeit [W] J	Versagensart
max			1000,00		
min			1,00		
1	9,995	4,07	37,31	1,518	t
2			66,98	2,725	s
3			32,66	1,329	s

Seriengrafik:

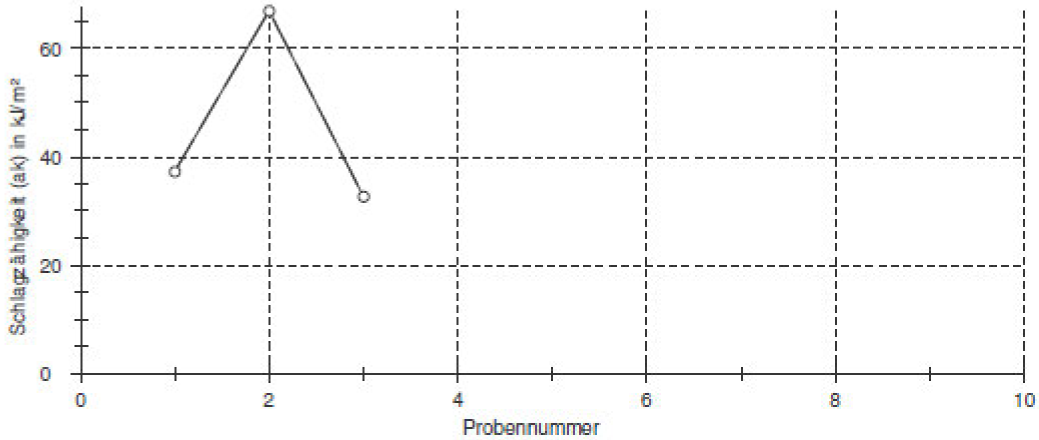

Statistik:

Serie n = 3	Schlagzähigkeit (ak) kJ/m²	Schlagarbeit [W] J
$\bar{x}$	45,65	1,857
s	18,62	0,757
ν [%]	40,79	40,79

25119825-00 PA 890000029700 Ch NILS 1eU.zs2

Lehmann&Voss&Co.

20.10.2020

Prüfprotokoll
Schlagzähigkeit

Prüflosnummer : 890000029701
Material : LUVOCOM® 3F PAHT® 9825 NT à 20 kg
Materialnummer : 25119825-00
Prozessauftrag : 890000029701
Charge : NILS
Prüfer : -
Prüfnorm : DIN EN ISO 179 1eA

Ergebnisse:

Nr	b_N mm	b mm	h mm	Schlagzähigkeit (ak) kJ/m²	Schlagarbeit [W] J	Versagensart
max				1000,00		
min				1,00		
1	7,952	9,952	4,048	3,79	0,152	s
2				3,75	0,151	s

Seriengrafik:

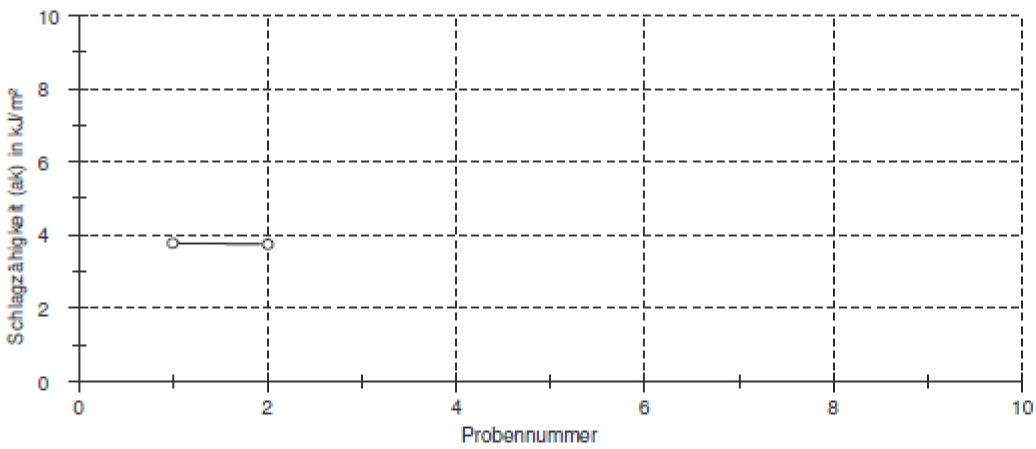

Statistik:

Serie n = 2	Schlagzähigkeit (ak) kJ/m²	Schlagarbeit [W] J
$\bar{x}$	3,77	0,152
s	0,03	0,001
ν [%]	0,71	0,71

25119825-00 PA 890000029701 Ch NILS 1eA.zs2

Lehmann&Voss&Co.

20.10.2020

Prüfprotokoll
Schlagzähigkeit

Prüflosnummer	:	890000029701
Material	:	LUVOCOM® 3F PAHT® 9825 NT à 20 kg
Materialnummer	:	25119825-00
Prozessauftrag	:	890000029701
Charge	:	NILS
Prüfer	:	-
Prüfnorm	:	DIN EN ISO 179 1eU
Bemerkung	:	

Ergebnisse:

Nr	b mm	h mm	Schlagzähigkeit (ak) kJ/m²	Schlagarbeit [W] J	Versagensart
max			1000,00		
min			1,00		
1	9,952	4,048	131,49	5,297	t
2			76,29	3,073	t
3			55,20	2,223	t

Seriengrafik:

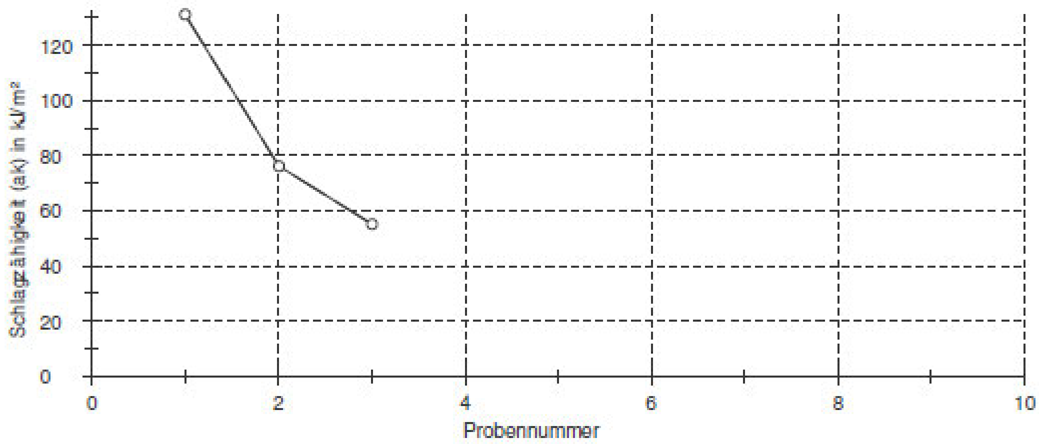

Statistik:

Serie n = 3	Schlagzähigkeit (ak) kJ/m²	Schlagarbeit [W] J
$\bar{x}$	87,66	3,531
s	39,40	1,587
ν [%]	44,94	44,94

25119825-00 PA 890000029701 Ch NILS 1eU.zs2

Lehmann&Voss&Co.

19.10.2020

Prüfprotokoll
Schlagzähigkeit

Prüflosnummer : 890000029702
Material : LUVOCOM® 3F PAHT® 9825 NT à 20 kg
Materialnummer : 25119825-00
Prozessauftrag : 890000029702
Charge : NILS
Prüfer : -
Prüfnorm : DIN EN ISO 179 1eA

Ergebnisse:

Nr	b_N mm	b mm	h mm	Schlagzähigkeit (ak) kJ/m²	Schlagarbeit [W] J	Versagensart
max				1000,00		
min				1,00		
1	8,004	10	4,011	3,67	0,147	s
2				3,72	0,149	s

Seriengrafik:

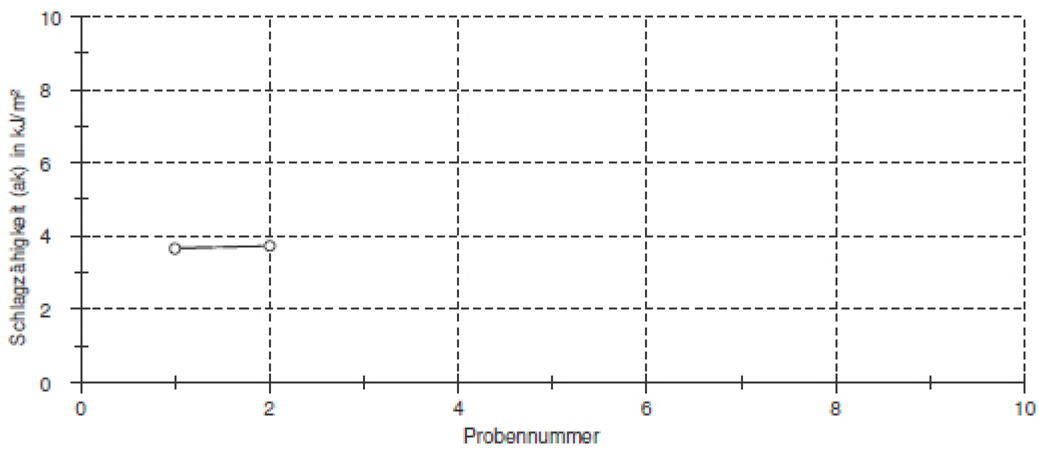

Statistik:

Serie n = 2	Schlagzähigkeit (ak) kJ/m²	Schlagarbeit [W] J
x̄	3,70	0,148
s	0,04	0,002
ν [%]	1,09	1,09

25119825-00 PA 890000029702 Ch NILS 1eA.zs2

Lehmann&Voss&Co.

19.10.2020

Prüfprotokoll
Schlagzähigkeit

Prüflosnummer	:	890000029702
Material	:	LUVOCOM® 3F PAHT® 9825 NT à 20 kg
Materialnummer	:	25119825-00
Prozessauftrag	:	890000029702
Charge	:	NILS
Prüfer	:	-
Prüfnorm	:	DIN EN ISO 179 1eU
Bemerkung	:	

Ergebnisse:

Nr	b mm	h mm	Schlagzähigkeit (ak) kJ/m²	Schlagarbeit [W] J	Versagensart
max			1000,00		
min			1,00		
1	10	4,011	82,52	3,312	t
2			90,48	3,631	t
3			97,86	3,927	t

Seriengrafik:

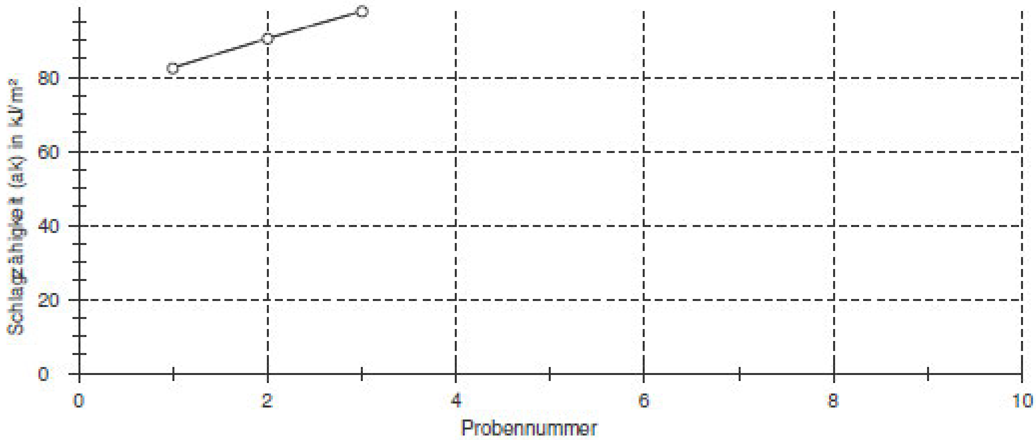

Statistik:

Serie n = 3	Schlagzähigkeit (ak) kJ/m²	Schlagarbeit [W] J
$\bar{x}$	90,29	3,623
s	7,67	0,308
ν [%]	8,50	8,50

25119825-00 PA 890000029702 Ch NILS 1eU.zs2

Lehmann&Voss&Co.

02.11.2020

Prüfprotokoll
Schlagzähigkeit

Prüflosnummer	:	890000029705
Material	:	LUVOCOM® 3F PAHT® 9825 NT à 20 kg
Materialnummer	:	25119825-00
Prozessauftrag	:	890000029705
Charge	:	NILS
Prüfer	:	-
Prüfnorm	:	DIN EN ISO 179 1eA

Ergebnisse:

Nr	b_N mm	b mm	h mm	Schlagzähigkeit (ak) kJ/m²	Schlagarbeit [W] J	Versagensart
max				1000,00		
min				1,00		
1	7,951	9,951	4,139	4,62	0,190	s
2				5,20	0,214	s
3				5,24	0,216	s
4				5,24	0,216	s

Seriengrafik:

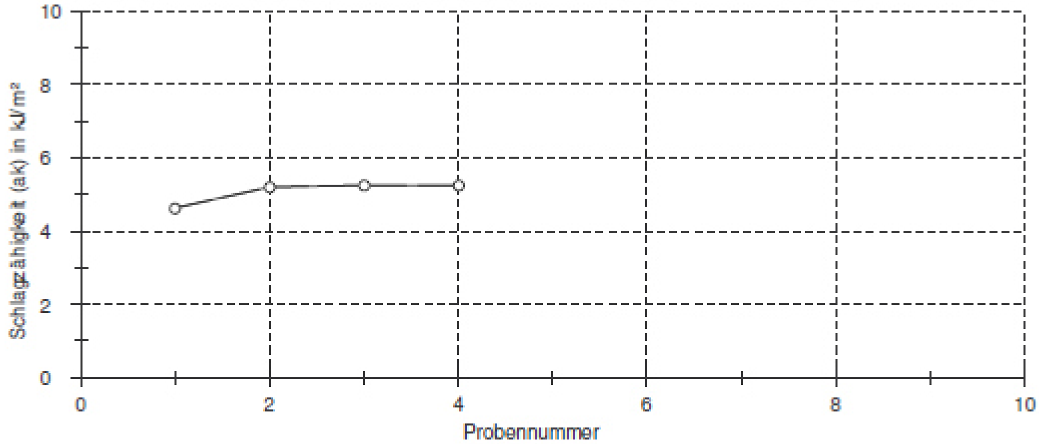

Statistik:

Serie n = 4	Schlagzähigkeit (ak) kJ/m²	Schlagarbeit [W] J
$\bar{x}$	5,08	0,209
s	0,31	0,013
ν [%]	6,05	6,05

25119825-00 PA 890000029705 Ch NILS 1eA 1.zs2

Lehmann&Voss&Co.

02.11.2020

Prüfprotokoll
Schlagzähigkeit

Prüflosnummer : 890000029705
Material : LUVOCOM® 3F PAHT® 9825 NT à 20 kg
Materialnummer : 25119825-00
Prozessauftrag : 890000029705
Charge : NILS
Prüfer : -
Prüfnorm : DIN EN ISO 179 1eU
Bemerkung :

Ergebnisse:

Nr	b mm	h mm	Schlagzähigkeit (ak) kJ/m²	Schlagarbeit [W] J	Versagensart
max			1000,00		
min			1,00		
1	9,951	4,139	66,66	2,746	t
2			42,44	1,748	t
3			11,99	0,494	s
4			29,25	1,205	t
5			31,12	1,282	t

Seriengrafik:

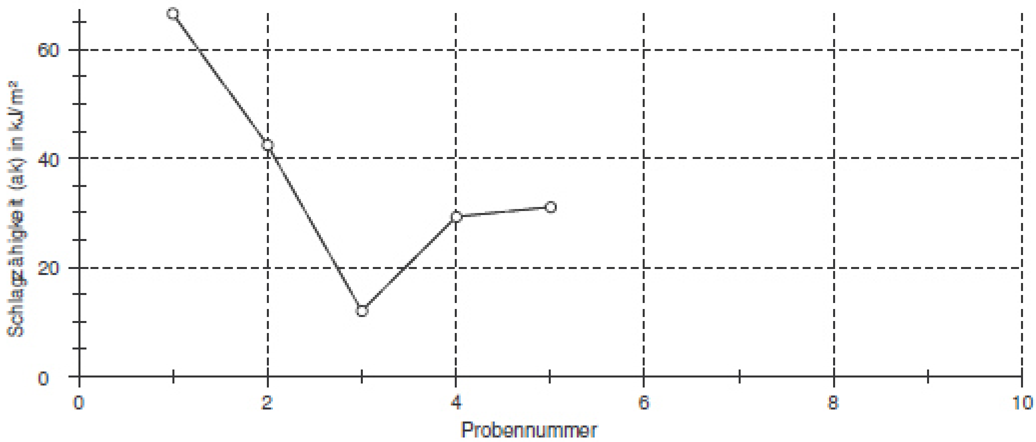

Statistik:

Serie n = 5	Schlagzähigkeit (ak) kJ/m²	Schlagarbeit [W] J
$\bar{x}$	36,29	1,495
s	20,17	0,831
ν [%]	55,57	55,57

25119825-00 PA 890000029705 Ch NILS 1eU.zs2

Lehmann&Voss&Co.

02.11.2020

Prüfprotokoll
Schlagzähigkeit

Prüflosnummer : 890000029706
Material : LUVOCOM® 3F PAHT® 9825 NT à 20 kg
Materialnummer : 25119825-00
Prozessauftrag : 890000029706
Charge : NILS
Prüfer : -
Prüfnorm : DIN EN ISO 179 1eA

Ergebnisse:

Nr	b_N mm	b mm	h mm	Schlagzähigkeit (ak) kJ/m²	Schlagarbeit [W] J	Versagensart
max				1000,00		
min				1,00		
1	8,049	10,05	4,152	5,97	0,249	t
2				3,85	0,161	s
3				3,76	0,157	s
4				3,58	0,149	s
5				4,63	0,193	s

Seriengrafik:

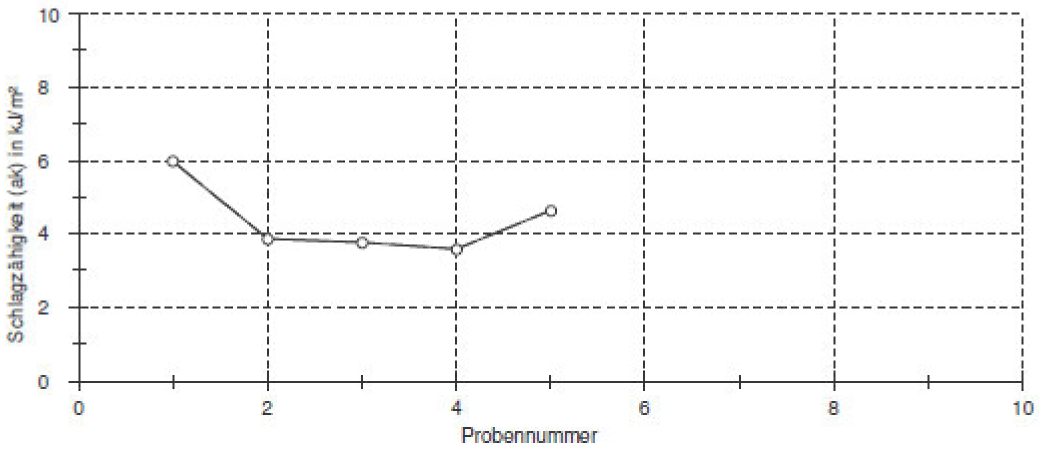

Statistik:

Serie n = 5	Schlagzähigkeit (ak) kJ/m²	Schlagarbeit [W] J
$\bar{x}$	4,36	0,182
s	0,99	0,041
ν [%]	22,65	22,65

25119825-00 PA 890000029706 Ch NILS 1eA.zs2

Lehmann&Voss&Co.

02.11.2020

Prüfprotokoll
Schlagzähigkeit

Prüflosnummer	:	890000029706
Material	:	LUVOCOM® 3F PAHT® 9825 NT à 20 kg
Materialnummer	:	25119825-00
Prozessauftrag	:	890000029706
Charge	:	NILS
Prüfer	:	-
Prüfnorm	:	DIN EN ISO 179 1eU
Bemerkung	:	

Ergebnisse:

Nr	b mm	h mm	Schlagzähigkeit (ak) kJ/m²	Schlagarbeit [W] J	Versagensart
max			1000,00		
min			1,00		
1	10,05	4,152	35,00	1,460	s
2			27,07	1,130	t
3			33,90	1,415	s
4			59,98	2,503	t
5			51,48	2,148	s

Seriengrafik:

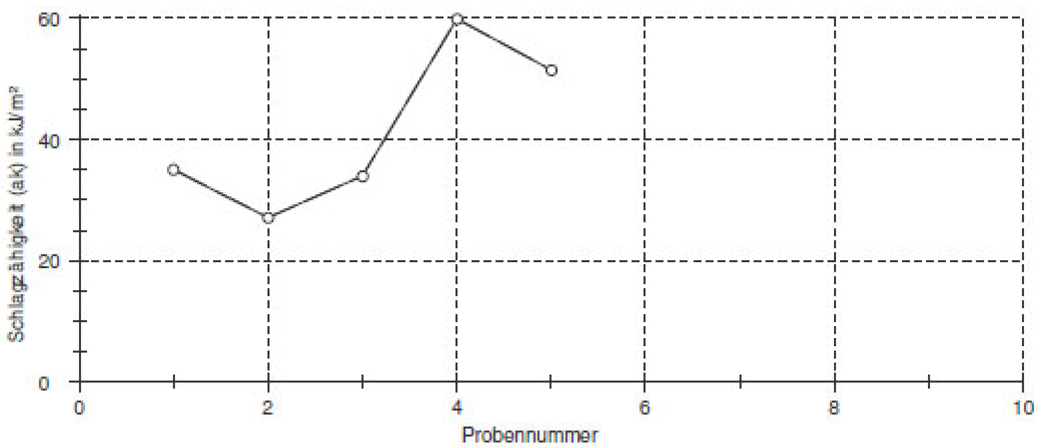

Statistik:

Serie n = 5	Schlagzähigkeit (ak) kJ/m²	Schlagarbeit [W] J
$\bar{x}$	41,49	1,731
s	13,69	0,571
ν [%]	32,99	32,99

25119825-00 PA 890000029706 Ch NILS 1eU.zs2

Lehmann&Voss&Co.

02.11.2020

Prüfprotokoll
Schlagzähigkeit

Prüflosnummer	:	890000029707
Material	:	LUVOCOM® 3F PAHT® 9825 NT à 20 kg
Materialnummer	:	25119825-00
Prozessauftrag	:	890000029707
Charge	:	NILS
Prüfer	:	-
Prüfnorm	:	DIN EN ISO 179 1eA

Ergebnisse:

Nr	b_N mm	b mm	h mm	Schlagzähigkeit (ak) kJ/m²	Schlagarbeit [W] J	Versagensart
max				1000,00		
min				1,00		
1	7,901	9,901	4,009	3,56	0,141	s
2				2,50	0,099	s
3				3,67	0,146	s
4				1,91	0,076	s

Seriengrafik:

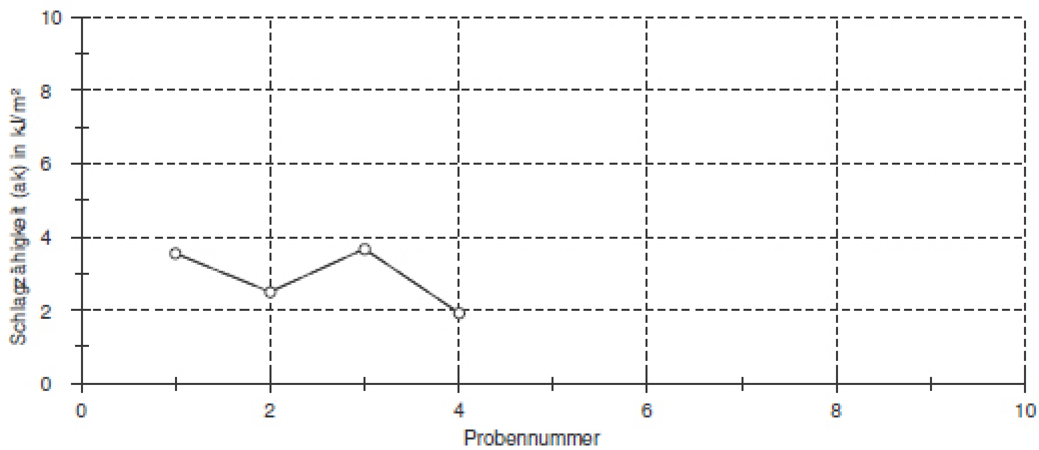

Statistik:

Serie n = 4	Schlagzähigkeit (ak) kJ/m²	Schlagarbeit [W] J
$\bar{x}$	2,91	0,115
s	0,85	0,034
ν [%]	29,14	29,14

25119825-00 PA 890000029707 Ch NILS 1eA.zs2

Lehmann&Voss&Co.

02.11.2020

Prüfprotokoll
Schlagzähigkeit

Prüflosnummer : 890000029707
Material : LUVOCOM® 3F PAHT® 9825 NT à 20 kg
Materialnummer : 25119825-00
Prozessauftrag : 890000029707
Charge : NILS
Prüfer : -
Prüfnorm : DIN EN ISO 179 1eU
Bemerkung :

Ergebnisse:

Nr	b mm	h mm	Schlagzähigkeit (ak) kJ/m²	Schlagarbeit [W] J	Versagensart
max			1000,00		
min			1,00		
1	9,901	4,009	109,19	4,334	t
2			74,73	2,966	s
3			25,44	1,010	t
4			45,16	1,793	t
5			63,03	2,502	s

Seriengrafik:

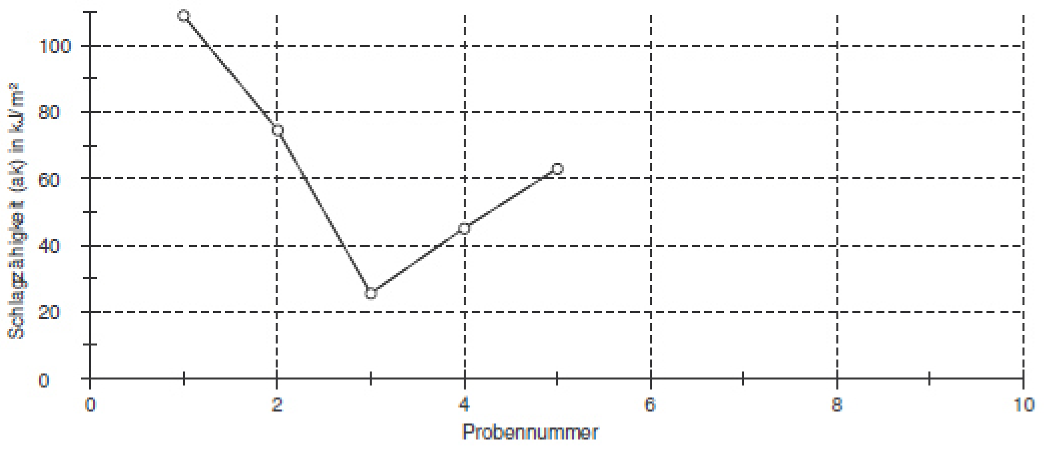

Statistik:

Serie n = 5	Schlagzähigkeit (ak) kJ/m²	Schlagarbeit [W] J
$\bar{x}$	63,51	2,521
s	31,62	1,255
ν [%]	49,79	49,79

25119825-00 PA 890000029707 Ch NILS 1eU.zs2

Lehmann&Voss&Co.

02.11.2020

Prüfprotokoll
Schlagzähigkeit

Prüflosnummer	:	890000029708
Material	:	LUVOCOM® 3F PAHT® 9825 NT à 20 kg
Materialnummer	:	25119825-00
Prozessauftrag	:	890000029708
Charge	:	NILS
Prüfer	:	-
Prüfnorm	:	DIN EN ISO 179 1eA

Ergebnisse:

Nr	b_N mm	b mm	h mm	Schlagzähigkeit (ak) kJ/m²	Schlagarbeit [W] J	Versagensart
max				1000,00		
min				1,00		
1	8,224	10,22	4,19	3,79	0,162	s
2				3,60	0,154	s
3				3,67	0,157	s
4				3,70	0,159	s
5				3,45	0,148	s

Seriengrafik:

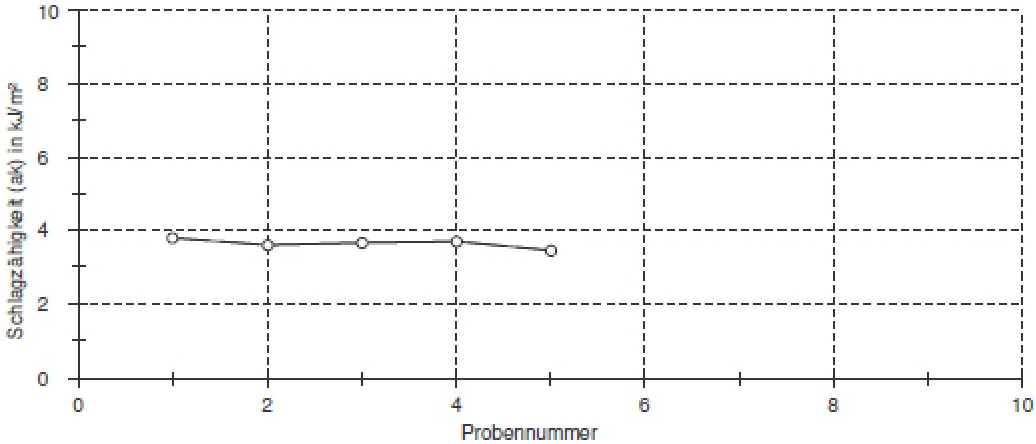

Statistik:

Serie n = 5	Schlagzähigkeit (ak) kJ/m²	Schlagarbeit [W] J
$\bar{x}$	3,64	0,156
s	0,13	0,005
ν [%]	3,47	3,47

25119825-00 PA 890000029708 Ch NILS 1eA.zs2

Lehmann&Voss&Co.

02.11.2020

Prüfprotokoll
Schlagzähigkeit

Prüflosnummer : 890000029708
Material : LUVOCOM® 3F PAHT® 9825 NT à 20 kg
Materialnummer : 25119825-00
Prozessauftrag : 890000029708
Charge : NILS
Prüfer : -
Prüfnorm : DIN EN ISO 179 1eU
Bemerkung :

Ergebnisse:

Nr	b mm	h mm	Schlagzähigkeit (ak) kJ/m²	Schlagarbeit [W] J	Versagensart
max			1000,00		
min			1,00		
1	10,22	4,19	26,22	1,123	s
2			50,74	2,173	t
3			47,66	2,042	s
4			29,29	1,255	t
5			61,97	2,655	s

Seriengrafik:

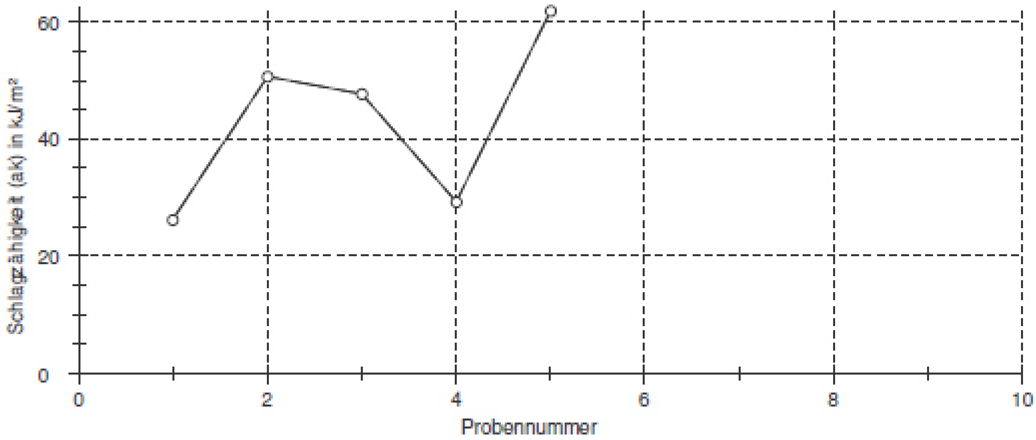

Statistik:

Serie n = 5	Schlagzähigkeit (ak) kJ/m²	Schlagarbeit [W] J
$\bar{x}$	43,17	1,850
s	15,09	0,646
ν [%]	34,95	34,95

25119825-00 PA 890000029708 Ch NILS 1eU.zs2

Flexural Strength according to DIN EN ISO 75-2

Lehmann&Voss&Co.

16.10.20

Prüfprotokoll

Prüflosnummer	:	890000029659
Material	:	LUVOCOM® 3F PAHT® 9825 NT à 20 kg
Materialnummer	:	25119825-00
Prozessauftrag	:	890000029659
Charge	:	NILS
Prüfer	:	MsS
Bemerkung	:	
Prüfnorm	:	DIN EN ISO 178
Geschwindigkeit Biegemodul	:	2 mm/min
Prüfgeschwindigkeit	:	10 mm/min

Prüfergebnisse:

Nr	Biegefestigkeit MPa	Dehnung bei Fmax %	Biegemodul GPa	Biegefestigkeit bei Bruch MPa	Bruchdehnung %	h mm	b mm
max	500,00	3,00	50,00		3,00		
min	1,00	0,10	1,00		0,10		
1	128,75	>5,85	3,11	-	-	4,189	9,935
2	129,30	>6,05	3,13	-	-	4,183	9,929
3	128,77	>5,95	3,21	-	-	4,182	9,947
4	127,56	>5,55	3,09	126	>5,58	4,2	9,974
5	128,56	>5,99	3,11	-	-	4,202	9,911

Seriengrafik:

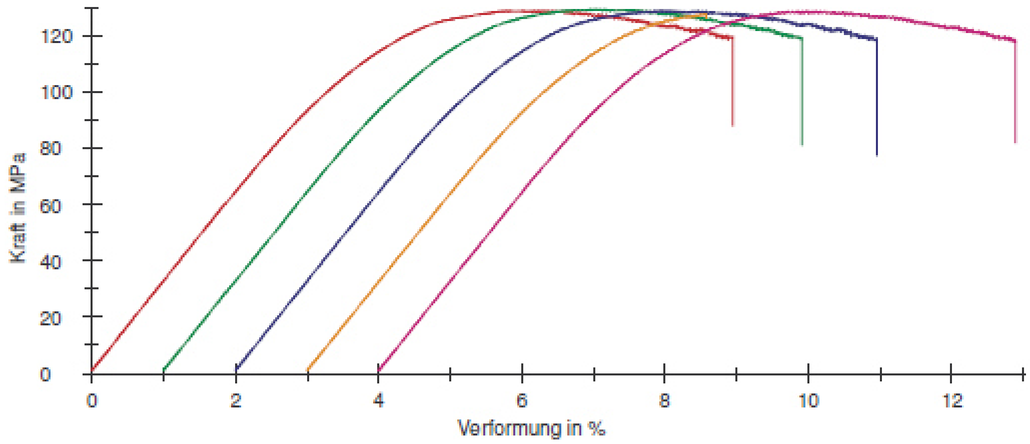

Statistik:

Serie n = 5	Biegefestigkeit MPa	Dehnung bei Fmax %	Biegemodul GPa	Biegefestigkeit bei Bruch MPa	Bruchdehnung %	h mm	b mm
$\bar{x}$	128,59	5,88	3,13	126	5,58	4,191	9,939
s	0,64	0,20	0,05	-	-	0,009406	0,02339
ν [%]	0,50	3,34	1,52	-	-	0,22	0,24

Lehmann&Voss&Co. LUV

16.10.20

Prüfprotokoll

Prüflosnummer	:	890000029660
Material	:	LUVOCOM® 3F PAHT® 9825 NT à 20 kg
Materialnummer	:	25119825-00
Prozessauftrag	:	890000029660
Charge	:	NILS
Prüfer	:	MsS
Bemerkung	:	
Prüfnorm	:	DIN EN ISO 178
Geschwindigkeit Biegemodul	:	2 mm/min
Prüfgeschwindigkeit	:	10 mm/min

Prüfergebnisse:

Nr	Biegefestigkeit MPa	Dehnung bei Fmax %	Biegemodul GPa	Biegefestigkeit bei Bruch MPa	Bruchdehnung %	h mm	b mm
max	500,00	3,00	50,00		3,00		
min	1,00	0,10	1,00		0,10		
1	109,03	>5,14	2,89	92,7	>8,92	4,157	9,919
2	107,51	>5,06	2,88	91,4	>9,03	4,188	9,884
3	109,41	>5,16	2,90	-	-	4,212	9,903
4	108,07	>5,10	2,85	-	-	4,21	9,932
5	105,86	>5,21	2,85	-	-	4,216	9,875

Seriengrafik:

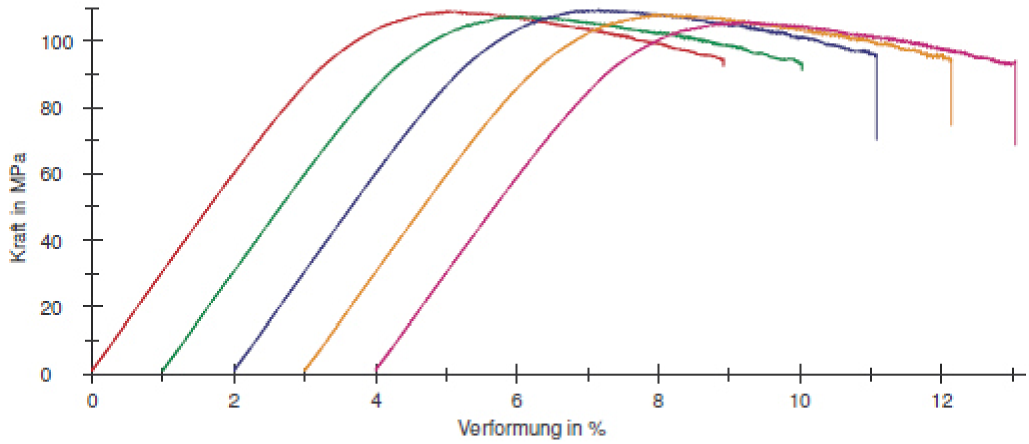

Statistik:

Serie n = 5	Biegefestigkeit MPa	Dehnung bei Fmax %	Biegemodul GPa	Biegefestigkeit bei Bruch MPa	Bruchdehnung %	h mm	b mm
x	107,97	5,13	2,87	92,0	8,98	4,197	9,903
s	1,40	0,06	0,03	0,915	0,08	0,0247	0,02367
ν [%]	1,30	1,10	0,88	0,99	0,86	0,59	0,24

Lehmann&Voss&Co.

16.10.20

Prüfprotokoll

Prüflosnummer	:	890000029661
Material	:	LUVOCOM® 3F PAHT® 9825 NT à 20 kg
Materialnummer	:	25119825-00
Prozessauftrag	:	890000029661
Charge	:	NILS
Prüfer	:	MsS
Bemerkung	:	
Prüfnorm	:	DIN EN ISO 178
Geschwindigkeit Biegemodul	:	2 mm/min
Prüfgeschwindigkeit	:	10 mm/min

Prüfergebnisse:

Nr	Biegefestigkeit MPa	Dehnung bei Fmax %	Biegemodul GPa	Biegefestigkeit bei Bruch MPa	Bruchdehnung %	h mm	b mm
max	500,00	3,00	50,00		3,00		
min	1,00	0,10	1,00		0,10		
1	128,47	>5,76	2,90	-	-	3,949	10,2
2	126,26	>5,66	3,02	-	-	3,928	10,28
3	126,70	>5,77	2,94	-	-	3,929	10,23
4	129,41	>5,71	3,07	-	-	3,95	10,2
5	127,59	>5,80	2,74	-	-	3,94	10,19

Seriengrafik:

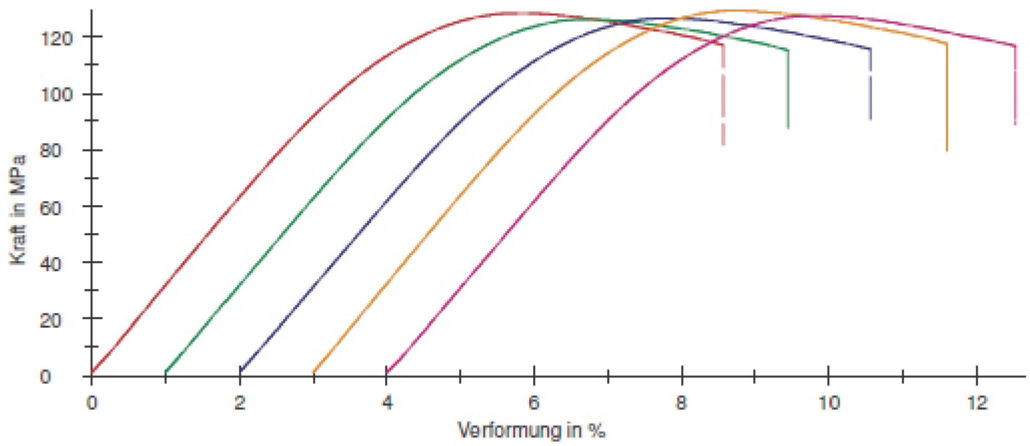

Statistik:

Serie n = 5	Biegefestigkeit MPa	Dehnung bei Fmax %	Biegemodul GPa	Biegefestigkeit bei Bruch MPa	Bruchdehnung %	h mm	b mm
$\bar{x}$	127,69	5,74	2,94	-	-	3,939	10,22
s	1,28	0,05	0,13	-	-	0,01052	0,03896
ν [%]	1,01	0,93	4,33	-	-	0,27	0,38

Lehmann&Voss&Co. LUV

15.10.20

Prüfprotokoll

Prüflosnummer	:	890000029662
Material	:	LUVOCOM® 3F PAHT® 9825 NT à 20 kg
Materialnummer	:	25119825-00
Prozessauftrag	:	890000029662
Charge	:	NILS
Prüfer	:	MsS
Bemerkung	:	
Prüfnorm	:	DIN EN ISO 178
Geschwindigkeit Biegemodul	:	2 mm/min
Prüfgeschwindigkeit	:	10 mm/min

Prüfergebnisse:

Nr	Biegefestigkeit MPa	Dehnung bei Fmax %	Biegemodul GPa	Biegefestigkeit bei Bruch MPa	Bruchdehnung %	h mm	b mm
max	500,00	3,00	50,00		3,00		
min	1,00	0,10	1,00		0,10		
1	108,46	>4,83	2,79	92,2	>8,45	3,927	10,2
2	108,64	>4,88	2,86	92,3	>8,47	3,922	10,2
3	108,38	>4,91	2,75	92,1	>8,46	3,94	10,16
4	108,88	>4,91	2,83	92,5	>8,48	3,942	10,22
5	109,51	>4,89	2,82	93,1	>8,43	3,919	10,18

Seriengrafik:

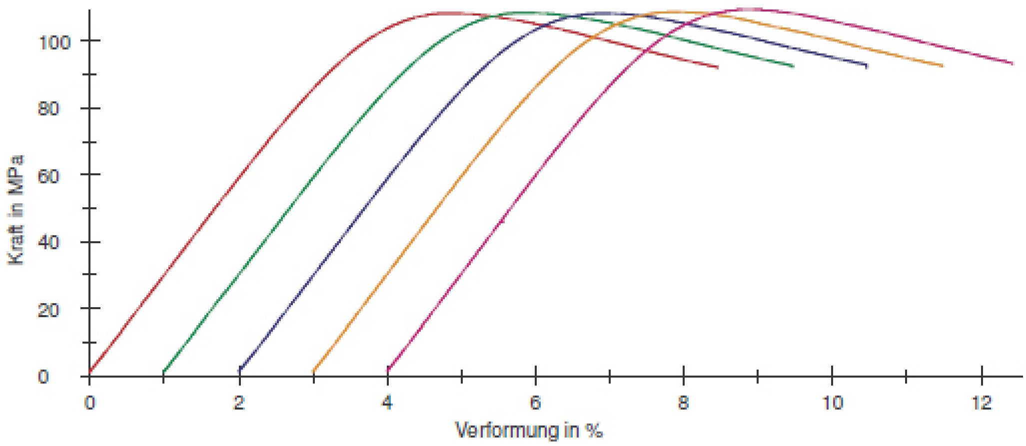

Statistik:

Serie n = 5	Biegefestigkeit MPa	Dehnung bei Fmax %	Biegemodul GPa	Biegefestigkeit bei Bruch MPa	Bruchdehnung %	h mm	b mm
x̄	108,78	4,88	2,81	92,5	8,46	3,93	10,19
s	0,45	0,03	0,04	0,386	0,02	0,01037	0,02134
ν [%]	0,42	0,71	1,41	0,42	0,21	0,26	0,21

Lehmann&Voss&Co.

16.10.20

Prüfprotokoll

Prüflosnummer	:	890000029669
Material	:	LUVOCOM® 3F PAHT® 9825 NT à 20 kg
Materialnummer	:	25119825-00
Prozessauftrag	:	890000029669
Charge	:	NILS
Prüfer	:	MsS
Bemerkung	:	
Prüfnorm	:	DIN EN ISO 178
Geschwindigkeit Biegemodul	:	2 mm/min
Prüfgeschwindigkeit	:	10 mm/min

Prüfergebnisse:

Nr	Biegefestigkeit MPa	Dehnung bei Fmax %	Biegemodul GPa	Biegefestigkeit bei Bruch MPa	Bruchdehnung %	h mm	b mm
max	500,00	3,00	50,00		3,00		
min	1,00	0,10	1,00		0,10		
1	128,29	>6,28	3,19	-	-	3,933	9,924
2	128,86	>6,42	3,21	-	-	3,928	9,872
3	128,55	>6,42	3,18	-	-	3,93	9,966
4	122,27	>6,68	2,98	-	-	3,937	9,975
5	129,54	>6,65	3,19	-	-	3,919	9,909

Seriengrafik:

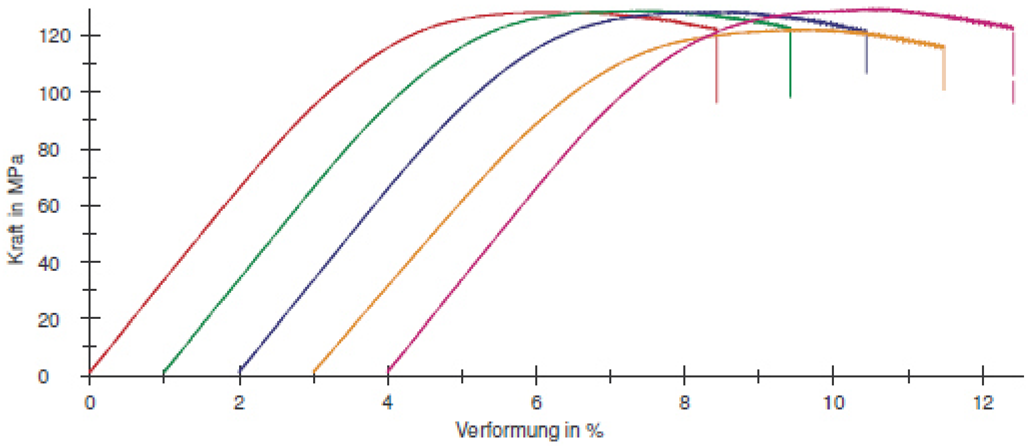

Statistik:

Serie n = 5	Biegefestigkeit MPa	Dehnung bei Fmax %	Biegemodul GPa	Biegefestigkeit bei Bruch MPa	Bruchdehnung %	h mm	b mm
$\bar{x}$	127,50	6,49	3,15	-	-	3,929	9,929
s	2,96	0,17	0,10	-	-	0,006898	0,0423
ν [%]	2,32	2,67	3,02	-	-	0,18	0,43

Lehmann&Voss&Co. 15.10.20

Prüfprotokoll

Prüflosnummer	:	890000029670
Material	:	LUVOCOM® 3F PAHT® 9825 NT à 20 kg
Materialnummer	:	25119825-00
Prozessauftrag	:	890000029670
Charge	:	NILS
Prüfer	:	MsS
Bemerkung	:	
Prüfnorm	:	DIN EN ISO 178
Geschwindigkeit Biegemodul	:	2 mm/min
Prüfgeschwindigkeit	:	10 mm/min

Prüfergebnisse:

Nr	Biegefestigkeit MPa	Dehnung bei Fmax %	Biegemodul GPa	Biegefestigkeit bei Bruch MPa	Bruchdehnung %	h mm	b mm
max	500,00	3,00	50,00		3,00		
min	1,00	0,10	1,00		0,10		
1	106,46	>5,58	2,78	-	-	3,824	10
2	112,17	>5,64	2,92	-	-	3,993	10,07
3	112,01	>5,86	2,82	-	-	3,996	10,05
4	116,78	>5,63	2,98	-	-	3,999	9,96
5	106,85	>5,69	2,69	-	-	4,009	10,06

Seriengrafik:

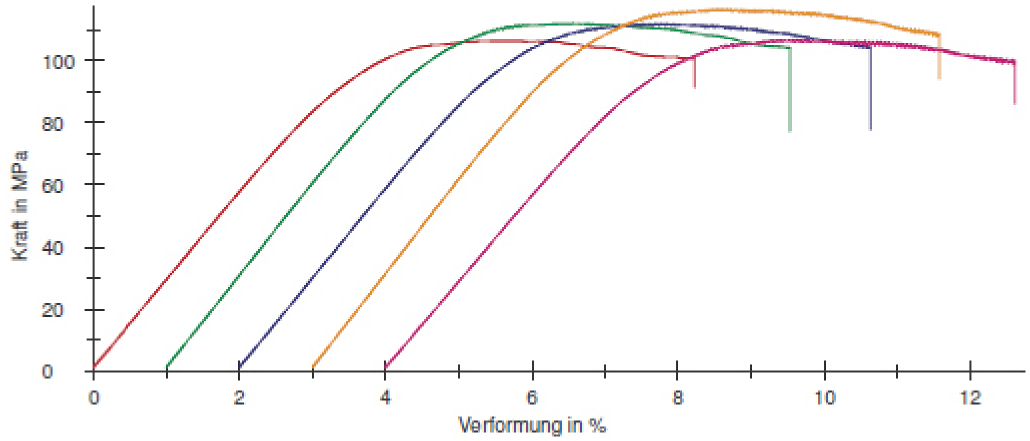

Statistik:

Serie n = 5	Biegefestigkeit MPa	Dehnung bei Fmax %	Biegemodul GPa	Biegefestigkeit bei Bruch MPa	Bruchdehnung %	h mm	b mm
$\bar{x}$	110,85	5,68	2,84	-	-	3,964	10,03
s	4,29	0,11	0,12	-	-	0,07849	0,04779
ν [%]	3,87	1,87	4,07	-	-	1,98	0,48

Lehmann&Voss&Co. 16.10.20

Prüfprotokoll

Prüflosnummer	:	890000029671
Material	:	LUVOCOM® 3F PAHT® 9825 NT à 20 kg
Materialnummer	:	25119825-00
Prozessauftrag	:	890000029671
Charge	:	NILS
Prüfer	:	MsS
Bemerkung	:	
Prüfnorm	:	DIN EN ISO 178
Geschwindigkeit Biegemodul	:	2 mm/min
Prüfgeschwindigkeit	:	10 mm/min

Prüfergebnisse:

Nr	Biegefestigkeit MPa	Dehnung bei Fmax %	Biegemodul GPa	Biegefestigkeit bei Bruch MPa	Bruchdehnung %	h mm	b mm
max	500,00	3,00	50,00		3,00		
min	1,00	0,10	1,00		0,10		
1	129,27	>6,09	2,92	-	-	4,097	9,823
2	130,16	>6,05	2,92	-	-	4,039	9,842
3	129,92	>6,05	2,83	-	-	4,052	9,855
4	130,89	>6,00	2,98	-	-	4,05	9,855
5	131,05	>6,14	2,94	-	-	4,058	9,85

Seriengrafik:

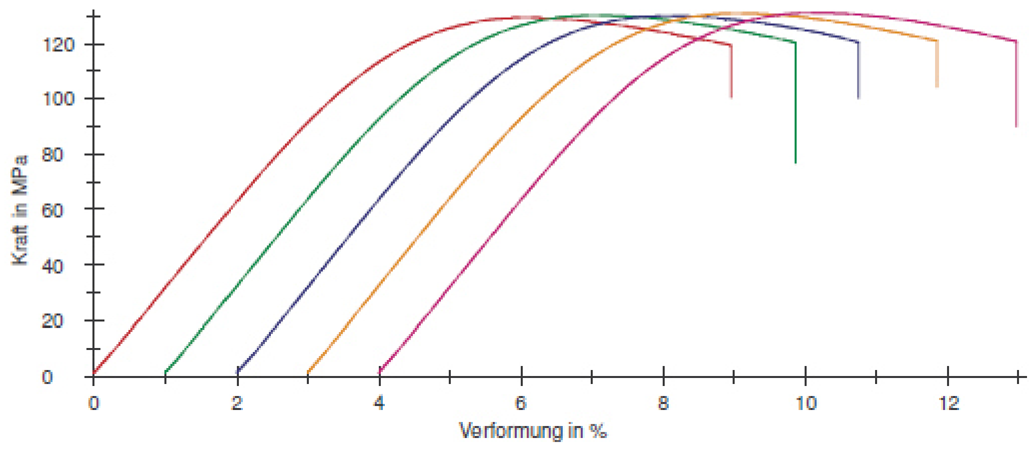

Statistik:

Serie n = 5	Biegefestigkeit MPa	Dehnung bei Fmax %	Biegemodul GPa	Biegefestigkeit bei Bruch MPa	Bruchdehnung %	h mm	b mm
x	130,26	6,07	2,92	-	-	4,059	9,845
s	0,73	0,05	0,05	-	-	0,02225	0,0134
ν [%]	0,56	0,86	1,81	-	-	0,55	0,14

Lehmann&Voss&Co.

16.10.20

Prüfprotokoll

Prüflosnummer	:	890000029672
Material	:	LUVOCOM® 3F PAHT® 9825 NT à 20 kg
Materialnummer	:	25119825-00
Prozessauftrag	:	890000029672
Charge	:	NILS
Prüfer	:	MsS
Bemerkung	:	
Prüfnorm	:	DIN EN ISO 178
Geschwindigkeit Biegemodul	:	2 mm/min
Prüfgeschwindigkeit	:	10 mm/min

Prüfergebnisse:

Nr	Biegefestigkeit MPa	Dehnung bei Fmax %	Biegemodul GPa	Biegefestigkeit bei Bruch MPa	Bruchdehnung %	h mm	b mm
max	500,00	3,00	50,00		3,00		
min	1,00	0,10	1,00		0,10		
1	100,00	>4,78	2,55	85,0	>8,93	4,092	9,973
2	101,40	>4,89	2,70	-	-	4,083	9,969
3	100,45	>4,87	2,74	-	-	4,102	9,947
4	100,39	>4,72	2,77	85,3	>8,94	4,131	9,848
5	102,17	>4,85	2,67	-	-	4,081	9,917

Seriengrafik:

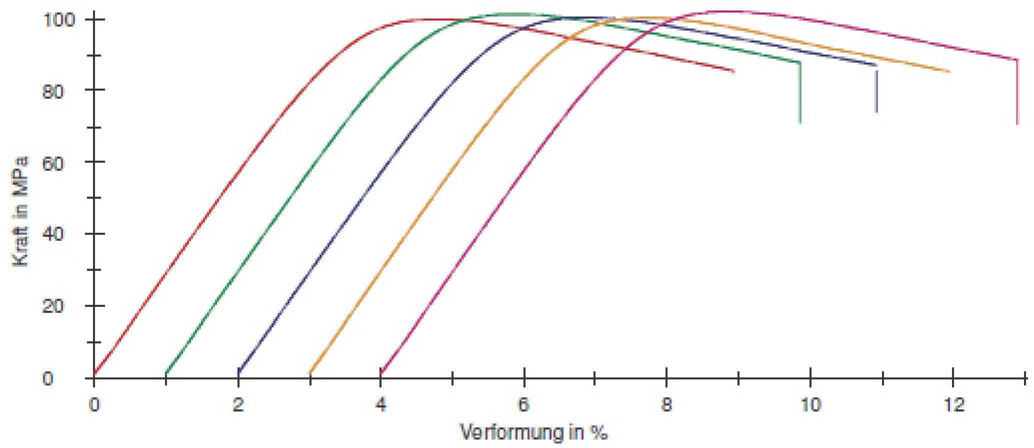

Statistik:

Serie n = 5	Biegefestigkeit MPa	Dehnung bei Fmax %	Biegemodul GPa	Biegefestigkeit bei Bruch MPa	Bruchdehnung %	h mm	b mm
x	100,88	4,82	2,69	85,2	8,93	4,098	9,931
s	0,89	0,07	0,09	0,240	0,01	0,02023	0,05135
ν [%]	0,88	1,46	3,20	0,28	0,10	0,49	0,52

Lehmann&Voss&Co. LUV

16.10.20

Prüfprotokoll

Prüflosnummer	:	890000029699
Material	:	LUVOCOM® 3F PAHT® 9825 NT à 20 kg
Materialnummer	:	25119825-00
Prozessauftrag	:	890000029699
Charge	:	NILS
Prüfer	:	MsS
Bemerkung	:	
Prüfnorm	:	DIN EN ISO 178
Geschwindigkeit Biegemodul	:	2 mm/min
Prüfgeschwindigkeit	:	10 mm/min

Prüfergebnisse:

Nr	Biegefestigkeit MPa	Dehnung bei Fmax %	Biegemodul GPa	Biegefestigkeit bei Bruch MPa	Bruchdehnung %	h mm	b mm
max	500,00	3,00	50,00		3,00		
min	1,00	0,10	1,00		0,10		
1	127,36	>6,14	3,08	-	-	4,183	10,22
2	130,30	>6,20	3,16	-	-	4,173	10,07
3	129,85	>6,26	3,10	-	-	4,171	10,08
4	130,82	>6,75	3,13	-	-	4,16	10,07
5	130,78	>6,76	3,12	-	-	4,124	10,13

Seriengrafik:

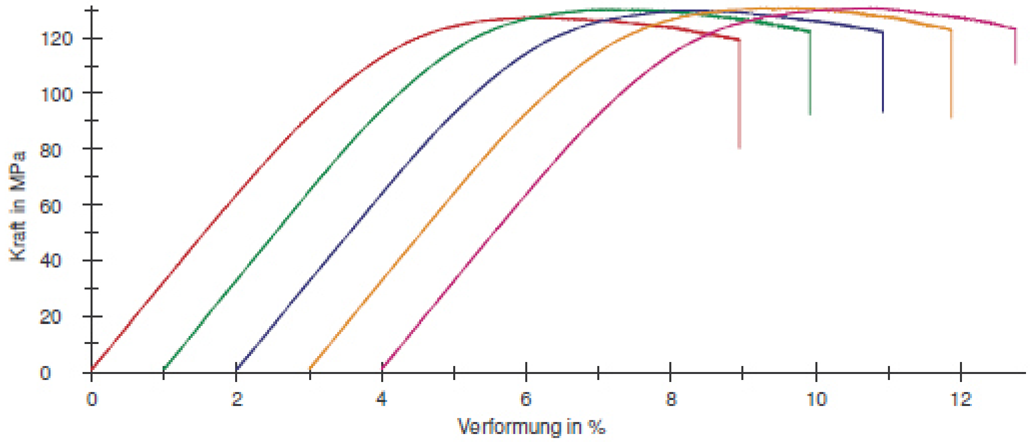

Statistik:

Serie n = 5	Biegefestigkeit MPa	Dehnung bei Fmax %	Biegemodul GPa	Biegefestigkeit bei Bruch MPa	Bruchdehnung %	h mm	b mm
x	129,82	6,42	3,12	-	-	4,162	10,11
s	1,43	0,31	0,03	-	-	0,02279	0,06321
ν [%]	1,10	4,76	0,92	-	-	0,55	0,63

Lehmann&Voss&Co. 15.10.20

Prüfprotokoll

Prüflosnummer	:	890000029700
Material	:	LUVOCOM® 3F PAHT® 9825 NT à 20 kg
Materialnummer	:	25119825-00
Prozessauftrag	:	890000029700
Charge	:	NILS
Prüfer	:	MsS
Bemerkung	:	
Prüfnorm	:	DIN EN ISO 178
Geschwindigkeit Biegemodul	:	2 mm/min
Prüfgeschwindigkeit	:	10 mm/min

Prüfergebnisse:

Nr	Biegefestigkeit MPa	Dehnung bei Fmax %	Biegemodul GPa	Biegefestigkeit bei Bruch MPa	Bruchdehnung %	h mm	b mm
max	500,00	3,00	50,00		3,00		
min	1,00	0,10	1,00		0,10		
1	121,35	>5,67	3,10	-	-	4,062	9,983
2	120,75	>5,70	3,08	-	-	4,077	10,02
3	120,90	>5,74	3,09	-	-	4,057	10,02
4	120,55	>5,69	3,06	-	-	4,031	10,01
5	112,01	>5,67	2,87	-	-	4,081	9,992

Seriengrafik:

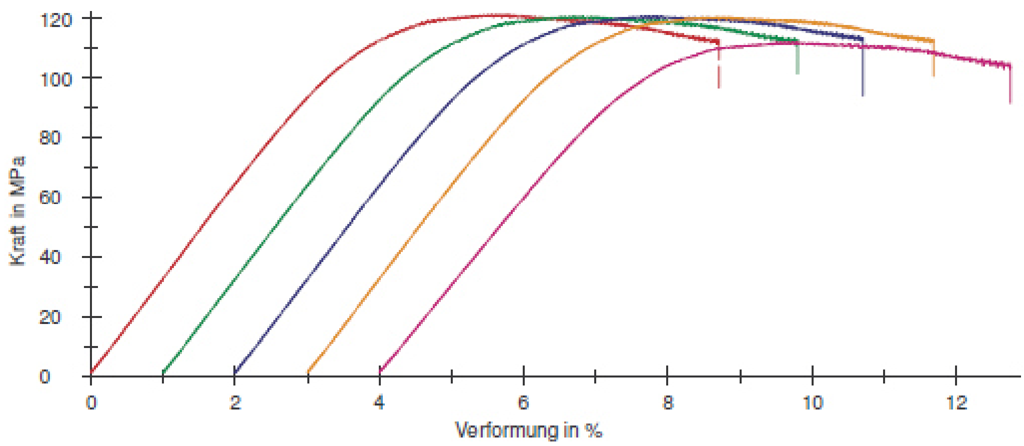

Statistik:

Serie n = 5	Biegefestigkeit MPa	Dehnung bei Fmax %	Biegemodul GPa	Biegefestigkeit bei Bruch MPa	Bruchdehnung %	h mm	b mm
x̄	119,11	5,70	3,04	-	-	4,061	10,01
s	3,98	0,03	0,10	-	-	0,01995	0,01746
ν [%]	3,34	0,47	3,16	-	-	0,49	0,17

Lehmann&Voss&Co.

16.10.20

Prüfprotokoll

Prüflosnummer	:	890000029701
Material	:	LUVOCOM® 3F PAHT® 9825 NT à 20 kg
Materialnummer	:	25119825-00
Prozessauftrag	:	890000029701
Charge	:	NILS
Prüfer	:	MsS
Bemerkung	:	
Prüfnorm	:	DIN EN ISO 178
Geschwindigkeit Biegemodul	:	2 mm/min
Prüfgeschwindigkeit	:	10 mm/min

Prüfergebnisse:

Nr	Biegefestigkeit MPa	Dehnung bei Fmax %	Biegemodul GPa	Biegefestigkeit bei Bruch MPa	Bruchdehnung %	h mm	b mm
max	500,00	3,00	50,00		3,00		
min	1,00	0,10	1,00		0,10		
1	132,11	>6,07	3,09	-	-	4,048	9,911
2	131,43	>6,14	2,85	-	-	3,996	9,883
3	131,86	>6,04	3,11	-	-	4,033	9,939
4	132,69	>6,03	3,06	-	-	4,041	9,913
5	129,41	>6,07	3,06	-	-	4,039	9,921

Seriengrafik:

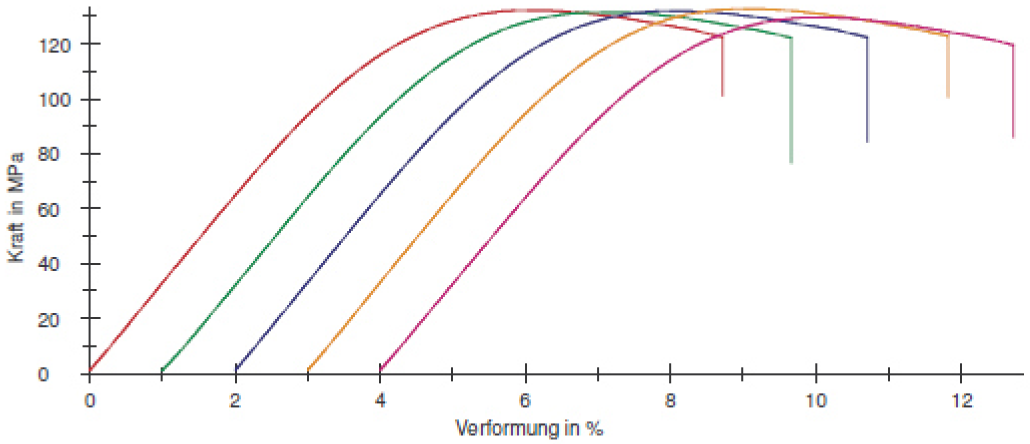

Statistik:

Serie n = 5	Biegefestigkeit MPa	Dehnung bei Fmax %	Biegemodul GPa	Biegefestigkeit bei Bruch MPa	Bruchdehnung %	h mm	b mm
$\bar{x}$	131,50	6,07	3,03	-	-	4,031	9,913
s	1,25	0,04	0,10	-	-	0,0204	0,02027
ν [%]	0,95	0,70	3,38	-	-	0,51	0,20

Lehmann&Voss&Co.

16.10.20

Prüfprotokoll

Prüflosnummer	:	890000029702
Material	:	LUVOCOM® 3F PAHT® 9825 NT à 20 kg
Materialnummer	:	25119825-00
Prozessauftrag	:	890000029702
Charge	:	NILS
Prüfer	:	MsS
Bemerkung	:	
Prüfnorm	:	DIN EN ISO 178
Geschwindigkeit Biegemodul	:	2 mm/min
Prüfgeschwindigkeit	:	10 mm/min

Prüfergebnisse:

Nr	Biegefestigkeit MPa	Dehnung bei Fmax %	Biegemodul GPa	Biegefestigkeit bei Bruch MPa	Bruchdehnung %	h mm	b mm
max	500,00	3,00	50,00		3,00		
min	1,00	0,10	1,00		0,10		
1	107,22	>5,17	2,56	-	-	4,023	10,04
2	106,54	>5,11	2,83	-	-	4,033	10,07
3	99,79	>4,95	2,69	84,8	>8,78	4,048	10,07
4	105,18	>5,10	2,79	-	-	4,017	10,08
5	101,81	>4,88	2,50	-	-	4,007	10,06

Seriengrafik:

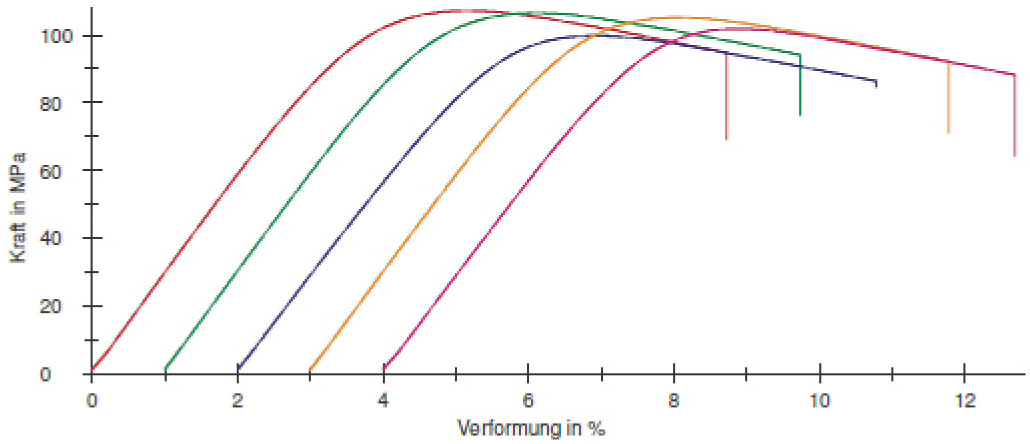

Statistik:

Serie n = 5	Biegefestigkeit MPa	Dehnung bei Fmax %	Biegemodul GPa	Biegefestigkeit bei Bruch MPa	Bruchdehnung %	h mm	b mm
x̄	104,11	5,04	2,67	84,8	8,78	4,026	10,07
s	3,19	0,12	0,14	-	-	0,016	0,01474
ν [%]	3,06	2,39	5,32	-	-	0,40	0,15

Lehmann&Voss&Co. 29.10.20

Prüfprotokoll

Prüflosnummer	:	890000029705
Material	:	LUVOCOM® 3F PAHT® 9825 NT à 20 kg
Materialnummer	:	25119825-00
Prozessauftrag	:	890000029705
Charge	:	NILS
Prüfer	:	gw
Bemerkung	:	
Prüfnorm	:	DIN EN ISO 178
Geschwindigkeit Biegemodul	:	2 mm/min
Prüfgeschwindigkeit	:	10 mm/min

Prüfergebnisse:

Nr	Biegefestigkeit MPa	Dehnung bei Fmax %	Biegemodul GPa	Biegefestigkeit bei Bruch MPa	Bruchdehnung %	h mm	b mm
max	500,00	3,00	50,00		3,00		
min	1,00	0,10	1,00		0,10		
1	107,85	>7,36	2,37	-	-	4,176	10,15
2	104,95	>7,50	1,96	-	-	4,186	10,09
3	102,78	>7,67	1,90	-	-	4,191	10,13
4	90,47	>4,50	2,12	90,5	>4,50	4,19	10,1
5	88,74	>4,51	2,02	88,7	>4,51	4,206	10,14

Seriengrafik:

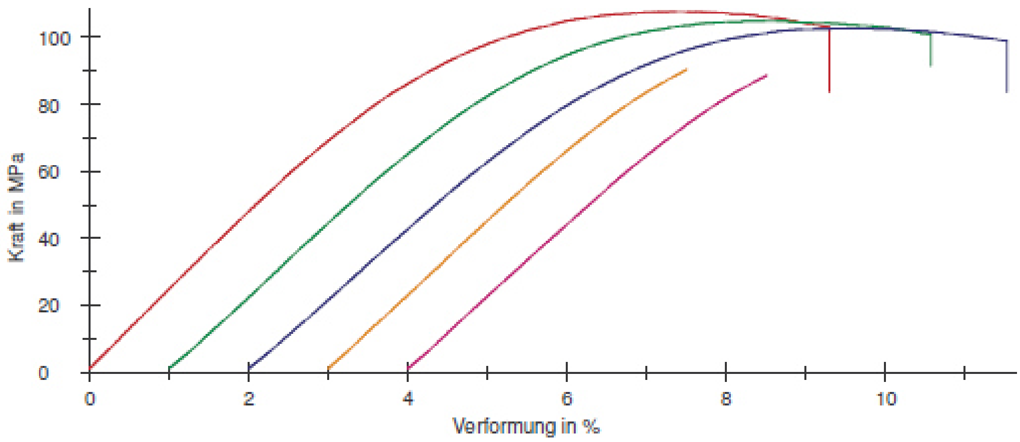

Statistik:

Serie n = 5	Biegefestigkeit MPa	Dehnung bei Fmax %	Biegemodul GPa	Biegefestigkeit bei Bruch MPa	Bruchdehnung %	h mm	b mm
$\bar{x}$	98,96	6,31	2,08	89,6	4,50	4,19	10,12
s	8,75	1,65	0,18	1,22	0,01	0,01087	0,0255
ν [%]	8,84	26,17	8,89	1,36	0,13	0,26	0,25

Lehmann&Voss&Co. 29.10.20

Prüfprotokoll

Prüflosnummer	:	890000029706
Material	:	LUVOCOM® 3F PAHT® 9825 NT à 20 kg
Materialnummer	:	25119825-00
Prozessauftrag	:	890000029706
Charge	:	NILS
Prüfer	:	gw
Bemerkung	:	
Prüfnorm	:	DIN EN ISO 178
Geschwindigkeit Biegemodul	:	2 mm/min
Prüfgeschwindigkeit	:	10 mm/min

Prüfergebnisse:

Nr	Biegefestigkeit MPa	Dehnung bei Fmax %	Biegemodul GPa	Biegefestigkeit bei Bruch MPa	Bruchdehnung %	h mm	b mm
max	500,00	3,00	50,00		3,00		
min	1,00	0,10	1,00		0,10		
1	104,00	>6,52	2,53	-	-	4,103	10,18
2	108,92	>6,23	2,52	-	-	4,077	10,16
3	106,54	>6,89	2,29	-	-	4,167	9,963
4	113,11	>6,18	2,63	-	-	4,066	10,04
5	99,12	>7,07	2,05	-	-	4,16	10,11

Seriengrafik:

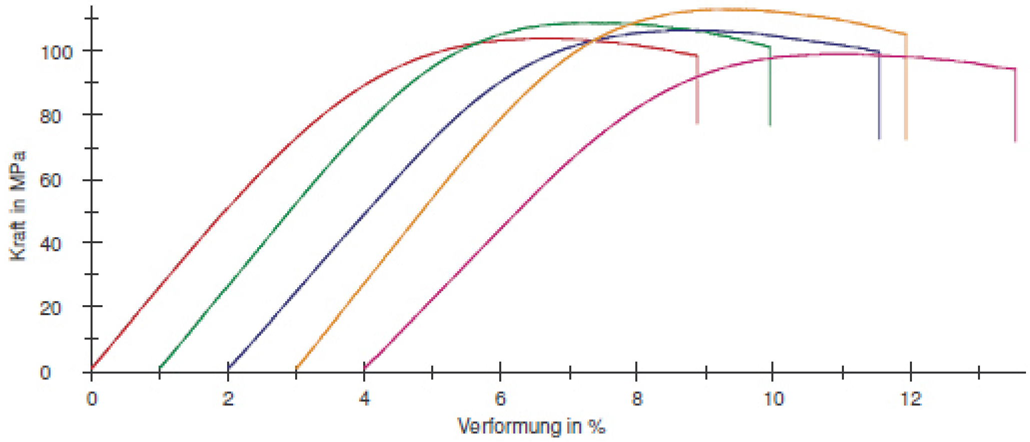

Statistik:

Serie n = 5	Biegefestigkeit MPa	Dehnung bei Fmax %	Biegemodul GPa	Biegefestigkeit bei Bruch MPa	Bruchdehnung %	h mm	b mm
x	106,34	6,58	2,40	-	-	4,115	10,09
s	5,25	0,39	0,23	-	-	0,04686	0,08869
ν [%]	4,93	5,96	9,73	-	-	1,14	0,88

Lehmann&Voss&Co. LUV

29.10.20

Prüfprotokoll

Prüflosnummer	:	890000029707
Material	:	LUVOCOM® 3F PAHT® 9825 NT à 20 kg
Materialnummer	:	25119825-00
Prozessauftrag	:	890000029707
Charge	:	NILS
Prüfer	:	gw
Bemerkung	:	
Prüfnorm	:	DIN EN ISO 178
Geschwindigkeit Biegemodul	:	2 mm/min
Prüfgeschwindigkeit	:	10 mm/min

Prüfergebnisse:

Nr	Biegefestigkeit MPa	Dehnung bei Fmax %	Biegemodul GPa	Biegefestigkeit bei Bruch MPa	Bruchdehnung %	h mm	b mm
max	500,00	3,00	50,00		3,00		
min	1,00	0,10	1,00		0,10		
1	128,68	>6,64	2,79	-	-	4,182	10,32
2	130,90	>6,53	2,73	122	>8,19	4,15	10,32
3	127,92	>6,65	2,67	-	-	4,203	10,35
4	130,24	>6,44	2,77	-	-	4,155	10,36
5	131,21	>6,51	2,73	-	-	4,167	10,27

Seriengrafik:

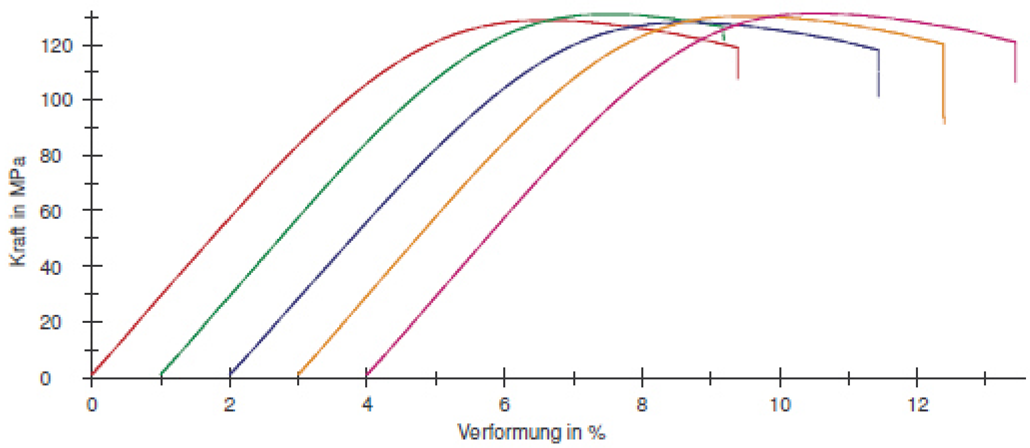

Statistik:

Serie n = 5	Biegefestigkeit MPa	Dehnung bei Fmax %	Biegemodul GPa	Biegefestigkeit bei Bruch MPa	Bruchdehnung %	h mm	b mm
x̄	129,79	6,55	2,74	122	8,19	4,172	10,33
s	1,43	0,09	0,05	-	-	0,02132	0,03753
ν [%]	1,10	1,37	1,72	-	-	0,51	0,36

Lehmann&Voss&Co.

29.10.20

Prüfprotokoll

Prüflosnummer	:	890000029708
Material	:	LUVOCOM® 3F PAHT® 9825 NT à 20 kg
Materialnummer	:	25119825-00
Prozessauftrag	:	890000029708
Charge	:	NILS
Prüfer	:	gw
Bemerkung	:	
Prüfnorm	:	DIN EN ISO 178
Geschwindigkeit Biegemodul	:	2 mm/min
Prüfgeschwindigkeit	:	10 mm/min

Prüfergebnisse:

Nr	Biegefestigkeit MPa	Dehnung bei Fmax %	Biegemodul GPa	Biegefestigkeit bei Bruch MPa	Bruchdehnung %	h mm	b mm
max	500,00	3,00	50,00		3,00		
min	1,00	0,10	1,00		0,10		
1	120,26	>6,25	2,69	-	-	4,251	10,31
2	120,71	>6,36	2,75	-	-	4,208	10,38
3	118,95	>6,29	2,56	-	-	4,215	10,47
4	121,00	>6,35	2,76	-	-	4,232	10,32
5	120,44	>6,39	2,43	-	-	4,246	10,41

Seriengrafik:

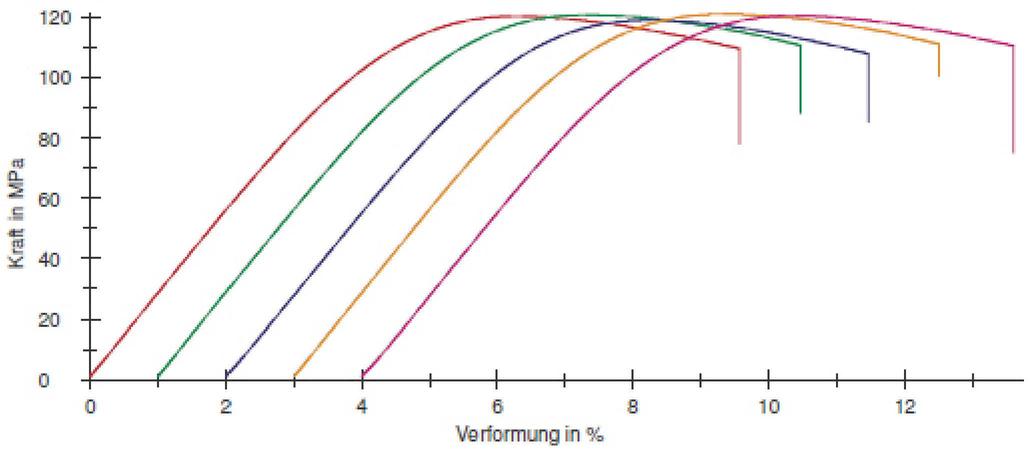

Statistik:

Serie n = 5	Biegefestigkeit MPa	Dehnung bei Fmax %	Biegemodul GPa	Biegefestigkeit bei Bruch MPa	Bruchdehnung %	h mm	b mm
$\bar{x}$	120,27	6,33	2,64	-	-	4,23	10,38
s	0,79	0,06	0,14	-	-	0,01872	0,06461
ν [%]	0,66	0,90	5,27	-	-	0,44	0,62

HDT according to DIN EN ISO 178

Test-Erläuterung

Probe-Namen: 25119825 Ch NILS PL 89-29659

Gruppe	1
Material-Code	
Standardtest	HDT ISO 75-2
Standardtestmethode	A (1,8 MPa - 120 °C/h)
Heizrate	120 °C/h
Biegespannung	1,800 [MPa]
Stützweite	64,00 [mm]
Länge	80,00 [mm]
Breite	10,00 [mm]
Stärke	4,00 [mm]
Testende Durchbiegung	0,34 [mm]

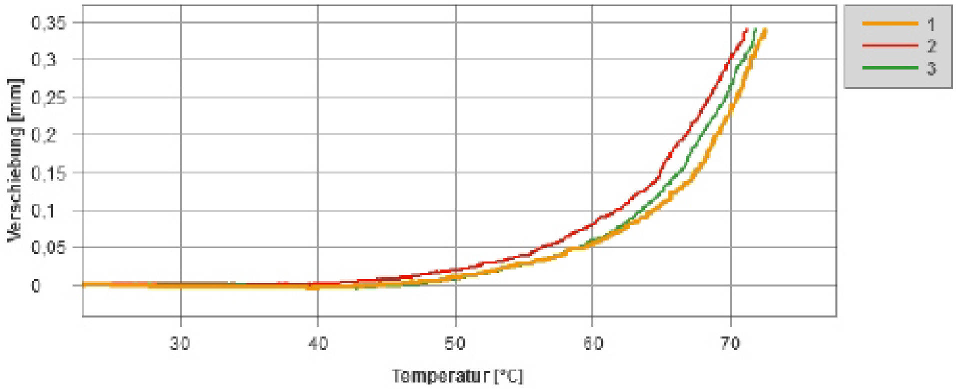

	Endzustand	Endgültige Verschiebung [mm]	Endtemperatur [°C]
1	Getestet	0,340	72,5
2	Getestet	0,340	71,2
3	Getestet	0,340	71,8
Mittelwert		0,340	71,8
Std dev		0,00	0,65
Bereich		0,000	1,3

Test-Erläuterung

Probe-Namen: 25119825 Ch NILS =PL 89-29660

Gruppe	1
Material-Code	
Standardtest	HDT ISO 75-2
Standardtestmethode	A (1.8 MPa - 120 °C/h)
Heizrate	120 °C/h
Biegespannung	1,800 [MPa]
Stützweite	64,00 [mm]
Länge	80,00 [mm]
Breite	10,00 [mm]
Stärke	4,00 [mm]
Testende Durchbiegung	0,34 [mm]

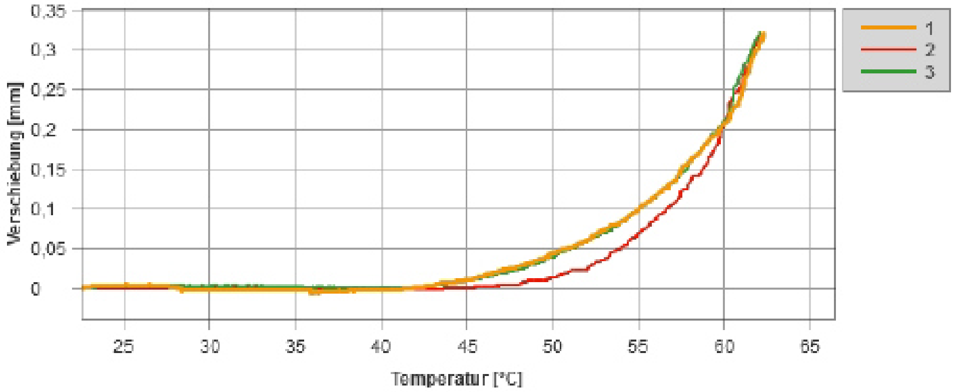

	Endzustand	Endgültige Verschiebung [mm]	Endtemperatur [°C]
1	Getestet	0,320	62,3
2	Getestet	0,320	62,1
3	Getestet	0,320	62,1
Mittelwert		0,320	62,2
Std dev		0,00	0,12
Bereich		0,000	0,2

Test-Erläuterung

Probe-Namen: 25119825 Ch NILS PL 89-29661

Gruppe	1
Material-Code	
Standardtest	HDT ISO 75-2
Standardtestmethode	A (1.8 MPa - 120 °C/h)
Heizrate	120 °C/h
Biegespannung	1,800 [MPa]
Stützweite	64,00 [mm]
Länge	80,00 [mm]
Breite	10,00 [mm]
Stärke	4,00 [mm]
Testende Durchbiegung	0,34 [mm]

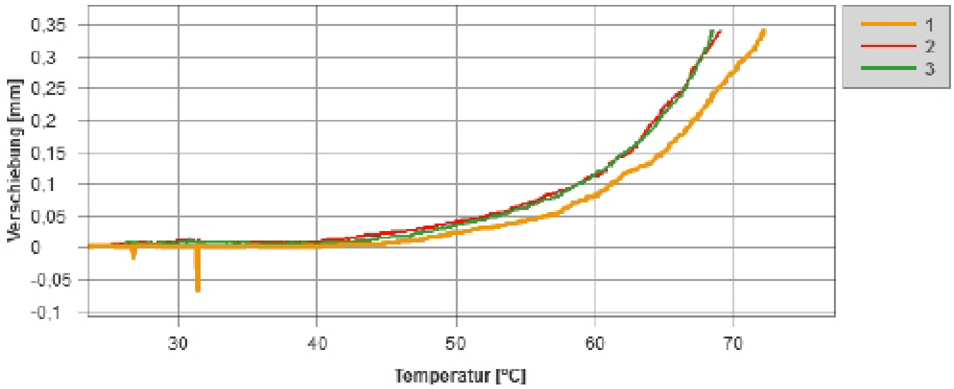

	Endzustand	Endgültige Verschiebung [mm]	Endtemperatur [°C]
1	Getestet	0,340	72,2
2	Getestet	0,340	69,1
3	Getestet	0,340	68,6
Mittelwert		0,340	70,0
Std dev		0,00	1,95
Bereich		0,000	3,6

Test-Erläuterung

Probe-Namen: 25119825 Ch NILS PL 89-29662

Gruppe	1
Material-Code	
Standardtest	HDT ISO 75-2
Standardtestmethode	A (1.8 MPa - 120 °C/h)
Heizrate	120 °C/h
Biegespannung	1,800 [MPa]
Stützweite	64,00 [mm]
Länge	80,00 [mm]
Breite	10,00 [mm]
Stärke	4,00 [mm]
Testende Durchbiegung	0,34 [mm]

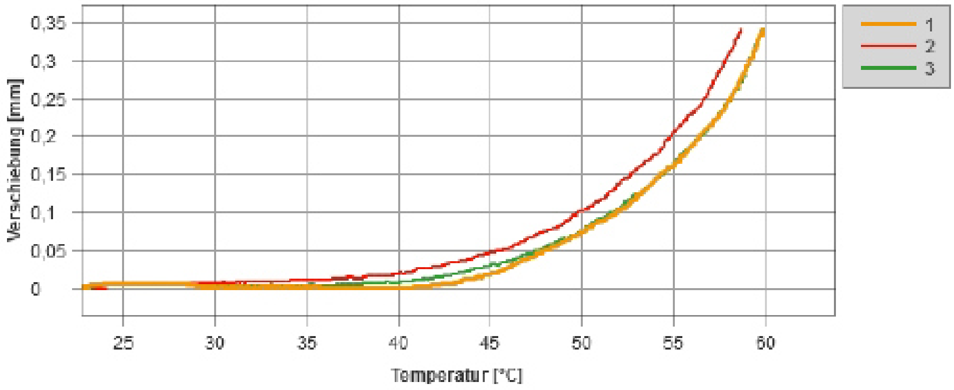

	Endzustand	Endgültige Verschiebung [mm]	Endtemperatur [°C]
1	Getestet	0,340	59,8
2	Getestet	0,340	58,7
3	Getestet	0,340	59,9
Mittelwert		0,340	59,5
Std dev		0,00	0,67
Bereich		0,000	1,2

Test-Erläuterung

Probe-Namen: 25119825 Ch NILS PL 89-29669

Gruppe	1
Material-Code	
Standardtest	HDT ISO 75-2
Standardtestmethode	A (1.8 MPa - 120 °C/h)
Heizrate	120 °C/h
Biegespannung	1,800 [MPa]
Stützweite	64,00 [mm]
Länge	80,00 [mm]
Breite	10,00 [mm]
Stärke	4,00 [mm]
Testende Durchbiegung	0,34 [mm]

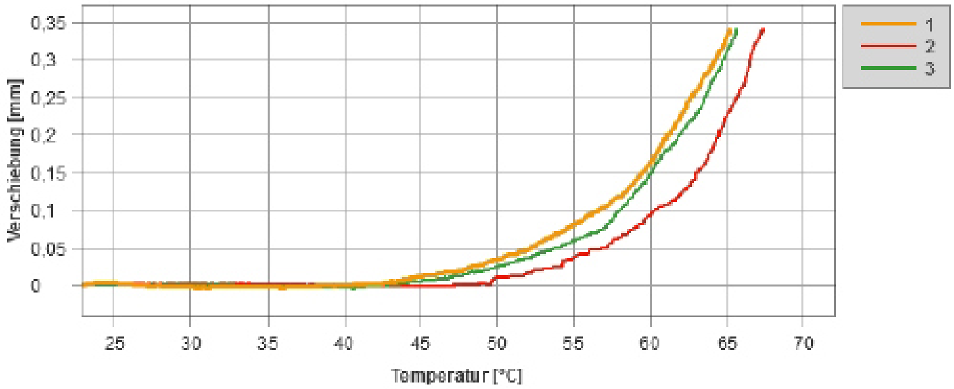

	Endzustand	Endgültige Verschiebung [mm]	Endtemperatur [°C]
1	Getestet	0,340	65,2
2	Getestet	0,340	67,4
3	Getestet	0,340	65,7
Mittelwert		0,340	66,1
Std dev		0,00	1,15
Bereich		0,000	2,2

Test-Erläuterung

Probe-Namen: 25119825 Ch NILS 89-29670

Gruppe	1
Material-Code	
Standardtest	HDT ISO 75-2
Standardtestmethode	A (1.8 MPa - 120 °C/h)
Heizrate	120 °C/h
Biegespannung	1,800 [MPa]
Stützweite	64,00 [mm]
Länge	80,00 [mm]
Breite	10,00 [mm]
Stärke	4,00 [mm]
Testende Durchbiegung	0,34 [mm]

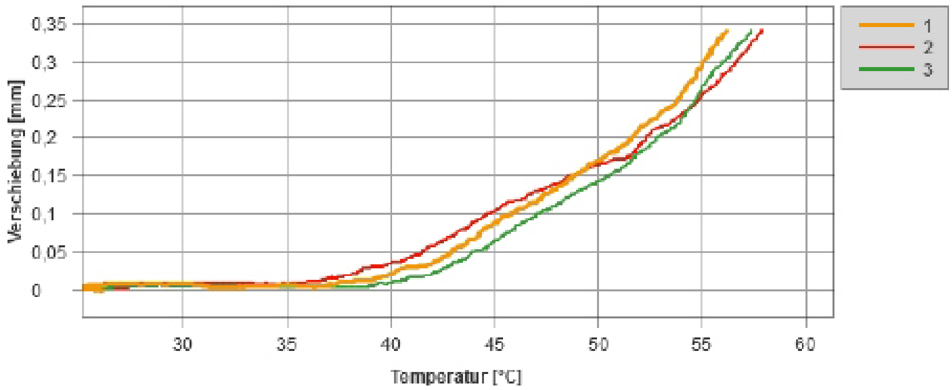

	Endzustand	Endgültige Verschiebung [mm]	Endtemperatur [°C]
1	Getestet	0,340	56,2
2	Getestet	0,340	57,9
3	Getestet	0,340	57,4
Mittelwert		0,340	57,2
Std dev		0,00	0,87
Bereich		0,000	1,7

Test-Erläuterung

Probe-Namen: 25119825 CH NILS Pl 89-29671

Gruppe	1
Material-Code	
Standardtest	HDT ISO 75-2
Standardtestmethode	A (1.8 MPa - 120 °C/h)
Heizrate	120 °C/h
Biegespannung	1,800 [MPa]
Stützweite	64,00 [mm]
Länge	80,00 [mm]
Breite	10,00 [mm]
Stärke	4,00 [mm]
Testende Durchbiegung	0,34 [mm]

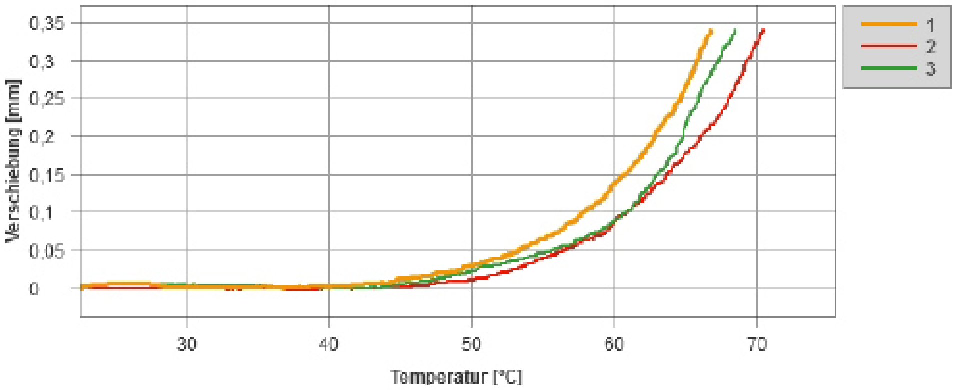

	Endzustand	Endgültige Verschiebung [mm]	Endtemperatur [°C]
1	Getestet	0,340	66,8
2	Getestet	0,340	70,5
3	Getestet	0,340	68,5
Mittelwert		0,340	68,6
Std dev		0,00	1,85
Bereich		0,000	3,7

Test-Erläuterung

Probe-Namen: 25119825 Ch NILS PL 89-29672

Gruppe	1
Material-Code	
Standardtest	HDT ISO 75-2
Standardtestmethode	A (1.8 MPa - 120 °C/h)
Heizrate	120 °C/h
Biegespannung	1,800 [MPa]
Stützweite	64,00 [mm]
Länge	80,00 [mm]
Breite	10,00 [mm]
Stärke	4,00 [mm]
Testende Durchbiegung	0,34 [mm]

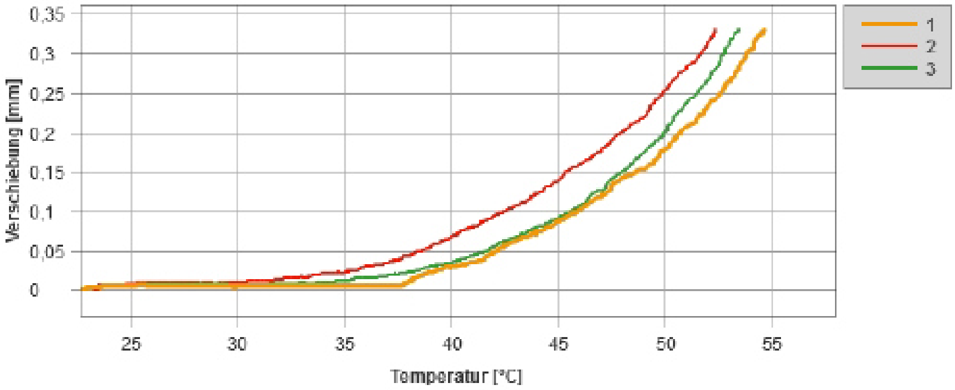

	Endzustand	Endgültige Verschiebung [mm]	Endtemperatur [°C]
1	Getestet	0,330	54,6
2	Getestet	0,330	52,3
3	Getestet	0,330	53,4
Mittelwert		0,330	53,4
Std dev		0,00	1,15
Bereich		0,000	2,3

Test-Erläuterung

Probe-Namen: 25119825 Ch Nils PL 89-29699

Gruppe	1
Material-Code	
Standardtest	HDT ISO 75-2
Standardtestmethode	A (1.8 MPa - 120 °C/h)
Heizrate	120 °C/h
Biegespannung	1,800 [MPa]
Stützweite	64,00 [mm]
Länge	80,00 [mm]
Breite	10,00 [mm]
Stärke	4,00 [mm]
Testende Durchbiegung	0,34 [mm]

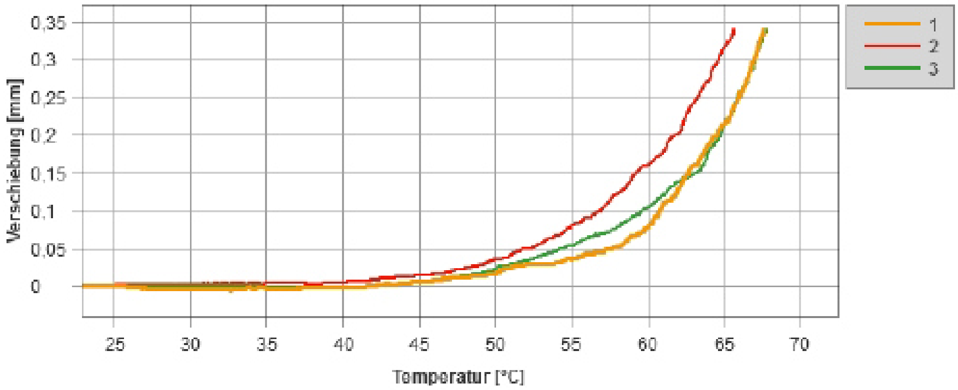

	Endzustand	Endgültige Verschiebung [mm]	Endtemperatur [°C]
1	Getestet	0,340	67,6
2	Getestet	0,340	65,7
3	Getestet	0,340	67,8
Mittelwert		0,340	67,0
Std dev		0,00	1,16
Bereich		0,000	2,1

Test-Erläuterung

Probe-Namen: 25119825 Ch NILS PL 89-29700

Gruppe	1
Material-Code	
Standardtest	HDT ISO 75-2
Standardtestmethode	A (1.8 MPa - 120 °C/h)
Heizrate	120 °C/h
Biegespannung	1,800 [MPa]
Stützweite	64,00 [mm]
Länge	80,00 [mm]
Breite	10,00 [mm]
Stärke	4,00 [mm]
Testende Durchbiegung	0,34 [mm]

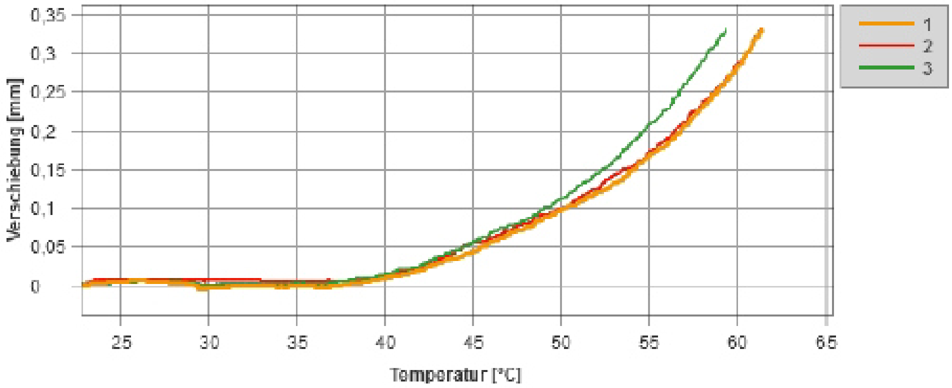

	Endzustand	Endgültige Verschiebung [mm]	Endtemperatur [°C]
1	Getestet	0,330	61,4
2	Getestet	0,330	61,4
3	Getestet	0,330	59,4
Mittelwert		0,330	60,7
Std dev		0,00	1,15
Bereich		0,000	2,0

Test-Erläuterung

Probe-Namen: 25119825 Ch NILS PL 89-29701

Gruppe	1
Material-Code	
Standardtest	HDT ISO 75-2
Standardtestmethode	A (1.8 MPa - 120 °C/h)
Heizrate	120 °C/h
Biegespannung	1,800 [MPa]
Stützweite	64,00 [mm]
Länge	80,00 [mm]
Breite	10,00 [mm]
Stärke	4,00 [mm]
Testende Durchbiegung	0,34 [mm]

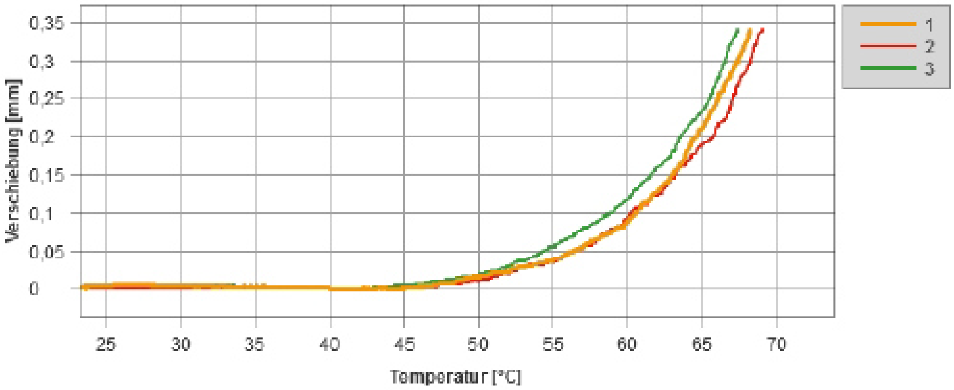

	Endzustand	Endgültige Verschiebung [mm]	Endtemperatur [°C]
1	Getestet	0,340	68,2
2	Getestet	0,340	69,1
3	Getestet	0,340	67,4
Mittelwert		0,340	68,2
Std dev		0,00	0,85
Bereich		0,000	1,7

Test-Erläuterung

Probe-Namen: 25119825 Ch NILS PL 89-29702

Gruppe	1
Material-Code	
Standardtest	HDT ISO 75-2
Standardtestmethode	A (1.8 MPa - 120 °C/h)
Heizrate	120 °C/h
Biegespannung	1,800 [MPa]
Stützweite	64,00 [mm]
Länge	80,00 [mm]
Breite	10,00 [mm]
Stärke	4,00 [mm]
Testende Durchbiegung	0,34 [mm]

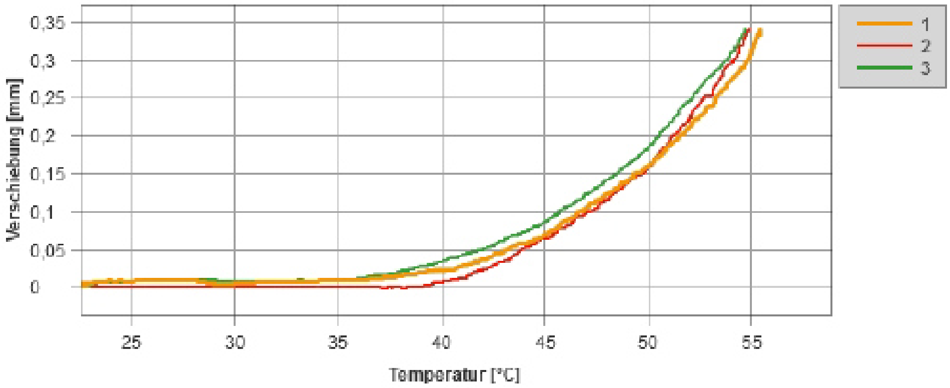

	Endzustand	Endgültige Verschiebung [mm]	Endtemperatur [°C]
1	Getestet	0,340	55,4
2	Getestet	0,340	54,9
3	Getestet	0,340	54,7
Mittelwert		0,340	55,0
Std dev		0,00	0,36
Bereich		0,000	0,7

DSC According to DIN EN ISO 11357-1

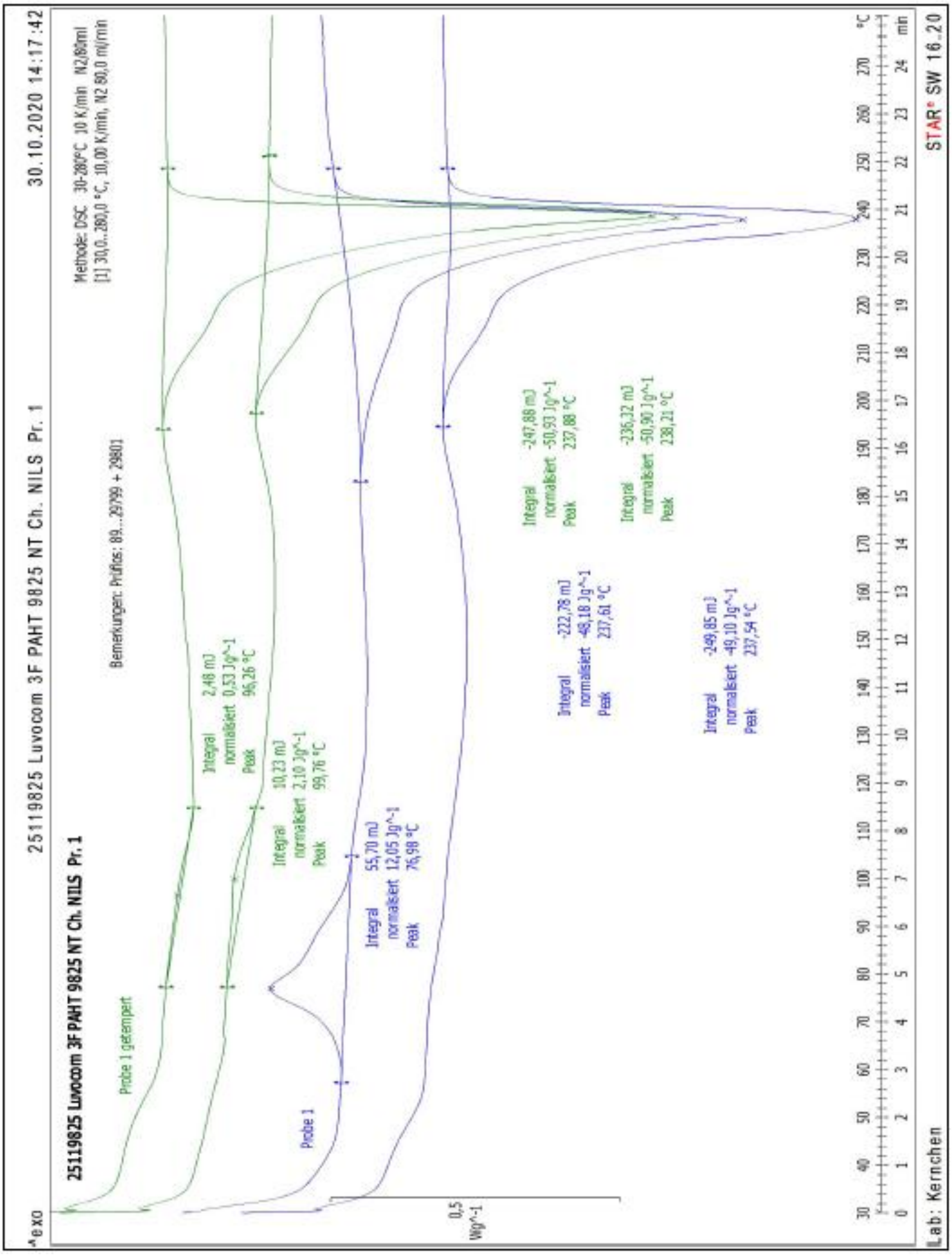

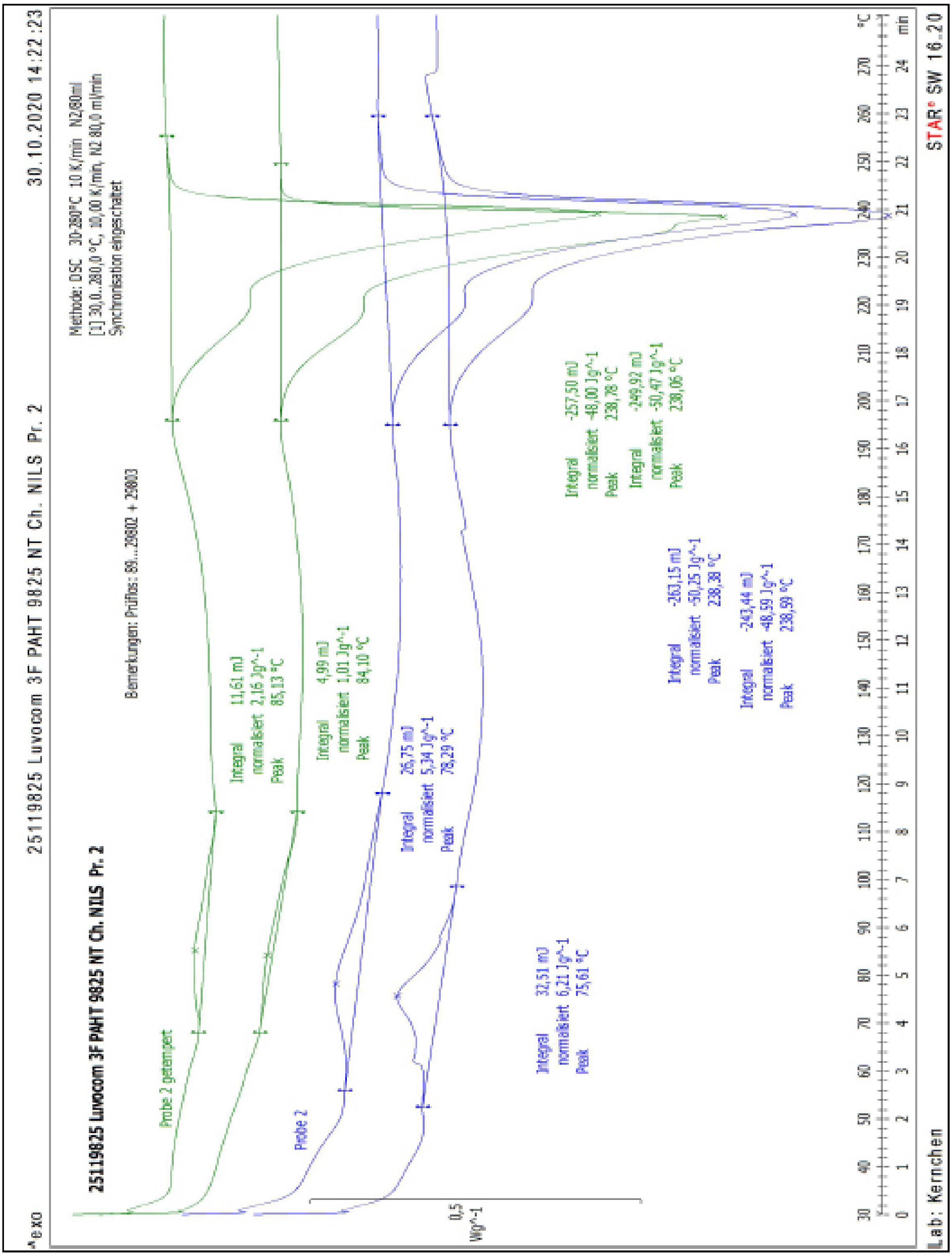
25119825 Luvocom 3F PAHT 9825 NT Ch. NILS Pr. 2
30.10.2020 14:22:23
25119825 Luvocom 3F PAHT 9825 NT Ch. NILS Pr. 2
Methode: DSC 30-280°C 10 K/min N2/80ml
[1] 30,0...280,0 °C, 10,00 K/min, N2 80,0 ml/min
Synchronisation eingeschaltet
Bemerkungen: Prüflos: 89...29802 + 29803
Probe 2 getempert
Probe 2
Integral 11,61 mJ normalisiert 2,16 Jg^-1 Peak 85,13 °C
Integral 4,99 mJ normalisiert 1,01 Jg^-1 Peak 84,10 °C
Integral 26,75 mJ normalisiert 5,34 Jg^-1 Peak 78,29 °C
Integral 32,51 mJ normalisiert 6,21 Jg^-1 Peak 75,61 °C
Integral -257,50 mJ normalisiert -48,00 Jg^-1 Peak 238,78 °C
Integral -249,92 mJ normalisiert -50,47 Jg^-1 Peak 238,06 °C
Integral -263,15 mJ normalisiert -50,25 Jg^-1 Peak 238,38 °C
Integral -243,44 mJ normalisiert -48,59 Jg^-1 Peak 238,59 °C
^exo
0,5 Wg^-1
°C
min
Lab: Kernchen
STAR° SW 16.20

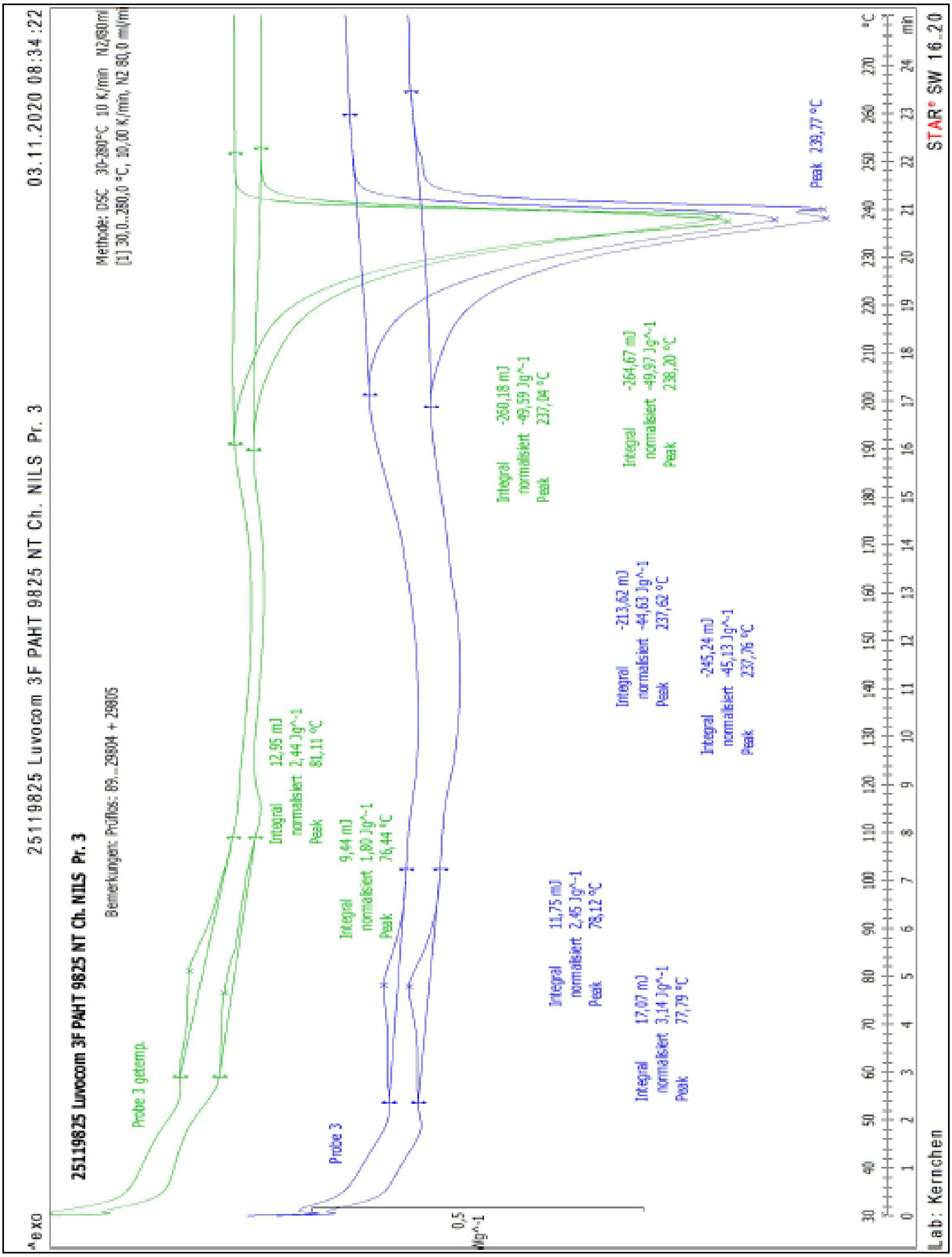
25119825 Luvocom 3F PAHT 9825 NT Ch. NILS Pr. 3
03.11.2020 08:34:22
25119825 Luvocom 3F PAHT 9825 NT Ch. NILS Pr. 3
Bemerkungen: Prüfbs: 89...29804 + 29805
Methode: DSC 30-280°C 10 K/min N2/80ml
[1] 30,0..280,0 °C, 10,00 K/min, N2 80,0 ml/min
Probe 3 getemp.
Probe 3
Integral 12,95 mJ
normalisiert 2,44 Jg^-1
Peak 81,11 °C
Integral 9,44 mJ
normalisiert 1,80 Jg^-1
Peak 76,44 °C
Integral 11,75 mJ
normalisiert 2,45 Jg^-1
Peak 78,12 °C
Integral 17,07 mJ
normalisiert 3,14 Jg^-1
Peak 77,79 °C
Integral -260,18 mJ
normalisiert -49,59 Jg^-1
Peak 237,04 °C
Integral -264,67 mJ
normalisiert -49,97 Jg^-1
Peak 238,20 °C
Integral -213,62 mJ
normalisiert -44,63 Jg^-1
Peak 237,62 °C
Integral -245,24 mJ
normalisiert -45,13 Jg^-1
Peak 237,76 °C
Peak 239,77 °C
^exo
0,5
Wg^-1
Lab: Kernchen
STAR° SW 16.20

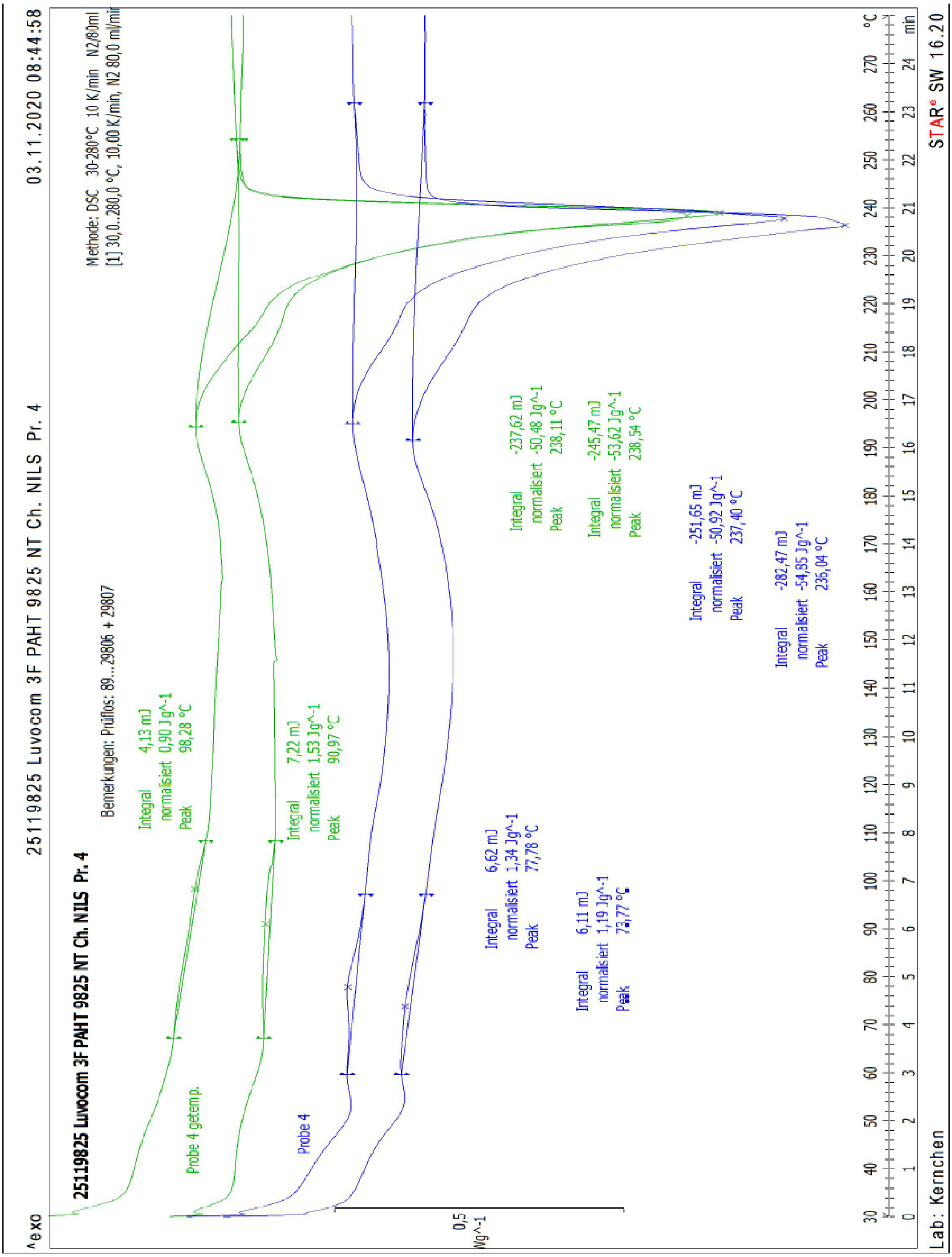
25119825 Luvocom 3F PAHT 9825 NT Ch. NILS Pr. 4
03.11.2020 08:44:58
25119825 Luvocom 3F PAHT 9825 NT Ch. NILS Pr. 4
Bemerkungen: Prüflos: 89....29806 + 29807
Methode: DSC 30-280°C 10 K/min N2/80ml
[1] 30,0..280,0 °C, 10,00 K/min, N2 80,0 ml/min
Probe 4 getemp.
Probe 4
Integral 4,13 mJ normalisiert 0,90 Jg^-1 Peak 98,28 °C
Integral 7,22 mJ normalisiert 1,53 Jg^-1 Peak 90,97 °C
Integral 6,62 mJ normalisiert 1,34 Jg^-1 Peak 77,78 °C
Integral 6,11 mJ normalisiert 1,19 Jg^-1 Peak 73,77 °C
Integral -237,62 mJ normalisiert -50,48 Jg^-1 Peak 238,11 °C
Integral -245,47 mJ normalisiert -53,62 Jg^-1 Peak 238,54 °C
Integral -251,65 mJ normalisiert -50,92 Jg^-1 Peak 237,40 °C
Integral -282,47 mJ normalisiert -54,85 Jg^-1 Peak 236,04 °C
^exo
0,5 Wg^-1
30 40 50 60 70 80 90 100 110 120 130 140 150 160 170 180 190 200 210 220 230 240 250 260 270 °C
0 1 2 3 4 5 6 7 8 9 10 11 12 13 14 15 16 17 18 19 20 21 22 23 24 min
Lab: Kernchen
STAR® SW 16.20

Hochschule für Angewandte Wissenschaften Hamburg
Hamburg University of Applied Sciences

Erklärung zur selbstständigen Bearbeitung einer Abschlussarbeit

Gemäß der Allgemeinen Prüfungs- und Studienordnung ist zusammen mit der Abschlussarbeit eine schriftliche Erklärung abzugeben, in der der Studierende bestätigt, dass die Abschlussarbeit „– bei einer Gruppenarbeit die entsprechend gekennzeichneten Teile der Arbeit [(§ 18 Abs. 1 APSO-TI-BM bzw. § 21 Abs. 1 APSO-INGI)] – ohne fremde Hilfe selbständig verfasst und nur die angegebenen Quellen und Hilfsmittel benutzt wurden. Wörtlich oder dem Sinn nach aus anderen Werken entnommene Stellen sind unter Angabe der Quellen kenntlich zu machen.“

Quelle: § 16 Abs. 5 APSO-TI-BM bzw. § 15 Abs. 6 APSO-INGI

Dieses Blatt, mit der folgenden Erklärung, ist nach Fertigstellung der Abschlussarbeit durch den Studierenden auszufüllen und jeweils mit Originalunterschrift als letztes Blatt in das Prüfungsexemplar der Abschlussarbeit einzubinden.
Eine unrichtig abgegebene Erklärung kann -auch nachträglich- zur Ungültigkeit des Studienabschlusses führen.

Erklärung zur selbstständigen Bearbeitung der Arbeit

Hiermit versichere ich,

Name: Napiwotzki

Vorname: Nils

dass ich die vorliegende Bachelorarbeit bzw. bei einer Gruppenarbeit die entsprechend gekennzeichneten Teile der Arbeit – mit dem Thema:

Influence of different 3D printer designs on the mechanical properties of polyamide compounds in Fused Filament Fabrication

ohne fremde Hilfe selbständig verfasst und nur die angegebenen Quellen und Hilfsmittel benutzt habe. Wörtlich oder dem Sinn nach aus anderen Werken entnommene Stellen sind unter Angabe der Quellen kenntlich gemacht.

- die folgende Aussage ist bei Gruppenarbeiten auszufüllen und entfällt bei Einzelarbeiten -

Die Kennzeichnung der von mir erstellten und verantworteten Teile der Bachelorarbeit ist erfolgt durch:

Hamburg	12.11.2020	[redacted]
Ort	Datum	Unterschrift im Original